

Study on Thermostabilization Mechanisms of
Phosphoenolpyruvate Carboxylase(PEPC) from an Extremely
Thermophilic Bacterium *Rhodothermus obamensis*

Ken Takai

1997

Contents

Chapter 1

Introduction

Chapter 2

Isolation and Characterization of an Extremely Thermophilic Marine Bacterium *Rhodothermus obamensis* OKD7.

1. Introduction
2. Materials and Methods
3. Results
4. Discussion

Chapter 3

Purification and Characterization of an Extremely Thermostable Phosphoenolpyruvate Carboxylase (PEPC) from an Extreme Thermophile *Rhodothermus obamensis* OKD7.

1. Introduction
2. Materials and Methods
3. Results
4. Discussion

Chapter 4

Extrinsic Thermostabilization Factors and Thermodenaturation of Phosphoenolpyruvate Carboxylase (PEPC) from an Extreme Thermophile *Rhodothermus obamensis* OKD7.

1. Introduction
2. Materials and Methods
3. Results
4. Discussion

Chapter 5

Cloning, Sequencing and Overexpression in *Escherichia coli* of Gene for Phosphoenolpyruvate Carboxylase (PEPC) from an Extreme Thermophile *Rhodothermus obamensis* OKD7

1. Introduction
2. Materials and Methods
3. Results
4. Discussion

Chapter 6

- Summary and Conclusion
- Acknowledgement
- References

Chapter 1

Introduction

During the last two decades, an increasing number of extremely thermophilic and hyperthermophilic microorganisms have been discovered from terrestrial hot springs and solfataric fields, shallow and deep sea hydrothermal vent environments [1-4]. They are called "extreme thermophiles", growing up to 80 °C, or "hyperthermophiles", growing up to 90 °C [1, 2]. These extreme thermophiles and hyperthermophiles are phylogenetically diverse of organisms and most of them belong to the domain of Archaea and some are the members of the domain Bacteria [5, 6]. They are also physiologically and biogeographically diverse. Some of them are autotrophic and the others are heterotrophic; most of them are anaerobic but some are aerobic. There are sulfur-reducers, methane generators and hydrogen oxidizers [1-4]. Most of them are discovered from terrestrial or marine hot environments but some are from cold water vents and subsurfaces of sulfur structures in the deep sea [7], and from oil reservoirs under the ground [8, 9]. Despite diverse of interests in extreme thermophiles and hyperthermophiles, the impact they provide us is most from the extraordinary temperature they inhabit.

The extraordinary growth temperature of them leads us to the question, how they can live under such temperature. The system that must be required to sustain them under the extraordinary temperature is the central interest in the study on thermophiles. In fact, the mechanisms for thermostability of biomoleculars in the thermophiles have been extensively studied [1-4, 10-12]. In thermophilic bacteria, the G+C contents of the genomic DNAs are known to be very high [13-16]. The high G+C contents of DNAs are expected to be a possible mechanism for the thermostability of DNA. In hyperthermophilic archaea whose G+C contents are relatively low, the existence of histone-like DNA binding proteins and novel reverse gyrases which generate positively super-coiled DNA can explain the thermostability of DNA to some extent [17-20]. As regards RNA thermostability, it has been suggested that the increasing number of base pairings and the increasing proportions of G:C pairings in the stems of RNA secondary structures significantly contribute the thermostability of RNA. It has been also reported that post-transcriptional methylation of some riboses in tRNA of

Thermus increased the melting point of tRNA [21], and that a variety of post-transcriptional modification help tRNAs to maintain their active structure in thermophilic archaea [22]. Another important biomolecule, lipid has been also studied with respect to the thermostability. Novel lipid components in cell walls have been found in thermophilic archaea [23]. Some components are found to increase with increasing growth temperature and they are thought to be associated with the thermostability of lipids and cell walls [24, 25]. Furthermore, in thermophilic bacteria, temperature-induced alterations in lipid composition are known in thermophilic bacteria *Thermus* species. It has been shown that the carotenoids, phospholipids and glycolipids increased in proportion with growth temperature and suggested that these alterations play an important role to protect membrane fluidity under high temperatures in thermophilic bacteria [26, 27]. Among a number of studies on the thermostability of biomolecules from extreme thermophiles and hyperthermophiles, the thermostability of proteins have been most extensively studied with respect to their novel molecular, biochemical mechanisms of thermostability and their potential for industrial impacts.

All proteins from extreme thermophiles and hyperthermophiles are known to be thermostable under ambient temperatures in which the organisms like to grow and even under supraoptimum temperatures for growth. Hence, the proteins from thermophiles are thought to be intrinsically thermostable. In order to elucidate the mechanisms for the intrinsic thermostability, a number of thermophilic proteins has been studied by the comparison of amino acid sequences between thermophilic and mesophilic homologous proteins [28, 29], the analyses of protein foldings [30], the molecular engineering techniques [31-34], the structural studies of the proteins including the three dimensional structures [35, 36]. However, the mechanisms of intrinsic thermostability have not been resolved yet.

Another approach to the mechanisms for protein thermostability is to explore the extrinsic factors that lie not in the protein itself but out of it, and that might sustain it under high temperature. In fact, there have been discovered possible extrinsic thermostabilization mechanisms in various thermophiles [11, 37-39]. These extrinsic factors contain some metabolites such as cyclic 2,3-diphosphoglycerate [38, 40], cofactors or coenzymes for some enzymes [41, 42], and molecular chaperons which assist in structure formation by counteracting misfolding and misassembly [43, 44]. Although the mechanism and function of extrinsic thermostabilization are largely unknown, it is expected that the system might play an important role *in vivo* to protect the protein from the thermodenaturation on the protein level or the cell level. In addition, the understanding of the mechanisms for the extrinsic thermostabilization at high temperatures can also give new insight into

the understanding of the protein intrinsic thermostability.

On these accounts, it is postulated the thermostability of extremely thermophilic or hyperthermophilic proteins is generally accomplished by both intrinsic and extrinsic thermostabilization systems and by their cooperative function. This implies that understanding of mechanisms for thermostability might require inspections of both intrinsic and extrinsic thermostabilization systems and of their cooperation. In this study, therefore, I sought to investigate thermostability of an enzyme from points of view, intrinsic and extrinsic thermostabilization mechanisms.

A target of enzyme I chose to use in this study was phosphoenolpyruvate carboxylase (PEPC) [EC4.1.1.31]. PEPC catalyzes the reaction that fixes HCO_3^- on phosphoenolpyruvate (PEP) to form oxaloacetate (OAA) and inorganic phosphate using Mg^{2+} as a cofactor [45]. The enzyme is distributed widely in mesophilic bacteria, protozoa, algae and plants, and a large number of the enzymes have been purified, cloned, and sequenced from various sources [46-50]. In these organisms, PEPC primarily plays an anaplerotic role by replenishing C_4 -dicarboxylic acids to the citric acid cycle or a key role in photosynthetic CO_2 assimilation [45]. These regulatory functions are also associated with the allosteric properties of the enzymes [51]. The coworkers and I have purified and characterized PEPCs from hyperthermophilic methanogen *Methanothermobacter sociabilis* and thermoacidophilic archaea *Sulfolobus* species [52, 53, Sako, Y. *et al.* unpublished]. We have shown that these archaeal PEPCs are significantly different from bacterial and eucaryal entities with respect to the molecular and enzymological properties and discussed their physiological roles *in vivo* and the importance of archaeal PEPCs in the comparative biochemistry and the evolution of the enzyme [52, 53]. In addition, the archaeal enzymes were quite thermostable similar to other thermophilic enzymes known to date [52, 53]. However, difficulty in manipulation of the hyperthermophilic archaea and their enzymes, and relatively low growth and enzyme yields have limited biochemical and structural approach to the thermostability of archaeal PEPCs.

For these reasons, another thermophilic PEPC was explored and found in an extremely thermophilic bacterium strain OKD7, that had been isolated from a shallow marine hydrothermal vent at Tachibana Bay, Nagasaki Prefecture, Japan. The preliminary study indicated that PEPC from this organism was extremely thermostable and a possible model for the investigation of thermostability. In chapter 2, the isolation and characterization of the extremely thermophilic bacterium strain OKD7 are described. From detail characterization, this organism was a member of the genus *Rhodothermus*, which was thermophilic genus of bacterium discovered in marine hot environments in Iceland and

Azore [54, 55, 56], and designated "*Rhodothermus obamensis*". In addition, the phylogenetic analysis of 16S rRNA gene indicated that the isolate was a modern lineage of extreme thermophile. The finding suggested that the mechanisms for the thermostability of proteins in this organism were different from those of other ancient lineage of extreme thermophiles and hyperthermophiles [57]. In chapter 3, *R. obamensis* PEPC was purified and characterized with respect to its molecular and enzymological properties. These properties of *R. obamensis* PEPC were compared with those of other thermophilic and mesophilic PEPCs from three domains of living organisms. In the preliminary experiments of its thermostability, *R. obamensis* PEPC was found to be extremely thermostable but the thermostability was strongly enhanced by the substrate, cofactor, salts and allosteric effectors. These substances were likely to be possible extrinsic thermostabilization factors for the enzyme. In chapter 4, the thermostability of *R. obamensis* PEPC was analyzed in detail. In order to determine the extrinsic thermostabilization mechanisms and the relationship between the function and thermodenaturation of the enzyme, the structural change of the enzyme and the effect of extrinsic factors on the change were examined. Not only the phenomenon of thermodenaturation in *R. obamensis* PEPC but also the functions of extrinsic factors during the thermodenaturation were well explained. In chapter 5, the cloning, sequencing and expression in *Escherichia coli* of *R. obamensis* PEPC gene were described. The amino acid sequence of *R. obamensis* PEPC was compared with those of other mesophilic PEPCs to determine some preference or bias for the intrinsic thermostability in the primary structure. The successful overexpression of *R. obamensis*-PEPC was thought to enable the determination of its three dimensional structure. Based on the phylogenetic analysis, the molecular evolution of PEPC was also discussed in this chapter. Finally, the findings in this study were summarized and the possible intrinsic and extrinsic thermostabilization mechanisms of *R. obamensis* PEPC were discussed in final chapter.

Chapter 2

Isolation and Characterization of an Extremely Thermophilic Marine Bacterium *Rhodothermus obamensis* OKD7.

1. Introduction

Over the last ten years, an increasing number of new genera and species of thermophilic organisms have been isolated which are capable of growing up to 80 °C. Most of them belong to the domain Archaea [5] but, only a few genera such as *Thermus*, *Thermotoga*, and *Aquifex*, have been identified within the domain Bacteria [14, 15, 16]. These thermophiles exhibit distinct physiological differences: *Thermus* is a strictly aerobic heterotroph but *Thermotoga* is a strictly anaerobic heterotroph, while *Aquifex* is a microaerobic chemolithoautotroph. On the basis of 16S rRNA analysis, *Thermotoga* and *Aquifex* represent the deepest phylogenetic branches within the domain Bacteria [57, 58]. Moreover, *Thermus* also shows the deep branching in the phylogenetic tree inferred from the 16S rRNA sequence [6]. These results and a phylogenetic study of thermophilic *Hydrogenobacter* reinforce the speculation that bacterial ancestry derives from thermophilic species [57, 59].

The members of the genus *Rhodothermus*, on the other hand, are marine thermophilic bacteria isolated from Iceland and the Azores [54, 55]. *R. marinus* is an aerobic heterotrophic bacterium with an optimum temperature for growth of 65 °C and has been studied for genetic engineering of thermostable enzymes [56]. The 16S rRNA analysis of this organism places the genus *Rhodothermus* close to the root of the *Flexibacter-Cytophaga-Bacteroid* (F-C-B) group with affinities to the green sulfur bacteria, fibrobacteria, and spirochetes [60]. This phylogenetic position of *Rhodothermus* deviates from those of other thermophilic bacteria, and it suggests the existence of thermophilic or extremely thermophilic bacteria distant from the universal root of life and another origin of thermophily within the Bacteria [60].

In this chapter, I describe the isolation and characterization of a new extremely thermophilic species of *Rhodothermus*, which was previously designated strain OKD7, from a shallow marine hydrothermal vent and the importance of its phylogenetic position to the hypothesis of the ancient origin of thermophily within the Bacteria.

2. Materials and Methods

Collection of samples. Effluent waters from hydrothermal vents and sedimentary materials adjacent to vents were collected from Tachibana Bay, Nagasaki Prefecture, Japan, at a depth of 22 m. Hydrothermal vent fluids were at 120-125 °C. Samples were stored aerobically at room temperature for 6 h prior to incubation.

Enrichment and purification. Subsamples taken from effluent waters and sediments were used to inoculate a series of media including Jx medium described below. All tubes of Jx medium with sediments were turbid after one day incubation at 80 °C. To obtain a pure culture, enriched cells were streaked on Jx medium plates and then incubated at 70 °C. Well-defined colonies were picked and streaked onto another plate and incubated at 70 °C and this procedure was repeated at least five times. A pure colony with red color was designated strain OKD7.

Culture medium and condition. The new isolate was routinely cultivated in Jx medium containing per liter: Jamarin S synthetic sea water, powder, 35 g and solution, 5 ml (Jamarin Laboratory, Osaka, Japan); yeast extract (Difco, Detroit, MI) 1 g; Trypticase peptone (BBL, Cockeysville, MD) 1 g; and the pH was adjusted to 6.8-7.2 with H₂SO₄. For growth on plates, 3% (wt/vol) agar GP-700 (Shimizu Shokuhin, Shimizu, Japan) was added to Jx medium. In an attempt to test the effect of NaCl on growth, varying concentrations of NaCl solution (pH 7.0) containing 0.1% (wt/vol) yeast extract and 0.1% (wt/vol) peptone were used instead of the Jx medium. In order to determine the effects of temperature and pH on growth, the new isolate was cultivated in MJ medium containing per liter: NaCl 30.0 g; K₂HPO₄ 0.14 g; CaCl₂ x 2H₂O 0.14 g; NH₄Cl 0.25 g; MgSO₄ x 7H₂O 3.4 g; MgCl₂ x 6H₂O 4.18 g; KCl 0.33 g; NiCl₂ x 6H₂O 0.5 mg; Na₂SeO₃ x 5H₂O 0.5 mg; Fe(NH₄)₂(SO₄)₂ x 6H₂O 0.01 g; Trace mineral solution 10 ml, consisting of (per liter) nitrilotriacetic acid 1.5 g, MgSO₄ x 7H₂O 3.0 g, MnSO₄ x 2H₂O 0.5 g, NaCl 1.0 g, FeSO₄ x 7H₂O 0.1 g, CoSO₄ x 7H₂O 0.18 g, CaCl₂ x 2H₂O 0.1 g, ZnSO₄ x 7H₂O 0.18 g, CuSO₄ x 5H₂O 0.01 g, KAl(SO₄)₂ x 12H₂O 0.02 g, H₃BO₃ 0.01 g, Na₂MoO₄ x 2H₂O 0.01 g, NiCl₂ x 6H₂O 0.025 g, Na₂SeO₃ x 5H₂O

0.3 mg; yeast extract 1 g; Trypticase peptone 1 g; and the pH was adjusted to 6.8-7.2 with H₂SO₄ for the test of growth temperature, and to various values with H₂SO₄ or NaOH for the pH effect. To examine the utilization of carbon-containing substrates, the yeast extract and peptone in MJ medium were replaced with various concentrations of substrates.

Light and electron microscopy. Cells were routinely observed with a differential interference microscope (Nikon). For microscopy at 80 °C, a drop of hot culture was placed on a slide preheated to about 85 °C and observed immediately. Micrographs were taken with a Nikon optishot microscope equipped with Nikon FX-II camera system. For transmission electron microscopy of ultra-thin sections, cells were fixed in Jx medium with 2% (vol/vol) glutaraldehyde and post fixed with 1% OsO₄. The fixed cells were then dehydrated through a series of ethanol precipitations and embedded in Quetol 812 (Nishin EM, Tokyo, Japan) epoxy resin. Thin sections were double contrasted with a JEOL 1200EX II electron microscope operated at 80 kV.

Determination of growth. Growth of the new isolate was determined by measuring turbidity at 660 nm and direct cell count stained with 4',6-diamidino-2-phenylindole (DAPI). Cultures were duplicately grown in 300-ml flask containing 100 ml of medium in the temperature-controlled dry oven (Advantec, Tokyo, Japan) and were shaken at 100 rpm by in all cases. The pH and NaCl growth curves were determined at 75 °C.

Organic substrates for growth. In an attempt to find organic substrates which could support growth of the isolate, experiments were conducted in MJ medium containing potential substrates in place of yeast extract and peptone. Potential substrates were added at concentrations of 0.01%, 0.05%, and 0.1% (wt/vol). Cells were precultured in each medium and inoculated into the same medium. These tests were run in duplicate at 75 °C.

Cellular fatty acid and quinone compositions. Cellular fatty acid and quinone compositions were analyzed from cells of OKD7 cultivated in Jx medium at 75 °C. Cellular fatty acids were determined as described by Kawasumi *et al.* [61], while the major quinones were determined as described by Ishii *et al.* [62].

Isolation and base composition of DNA. DNA was prepared as described by Marmur and Doty [63] and Lauerer *et al.* [64]. The GC content of the DNA was determined by direct analysis of deoxyribonucleotides using high-performance liquid chromatography (HPLC) [65]. A DNA GC Kit (Yamasa, Chiba, Japan) was used as the standard.

Amplification of 16S rRNA gene and sequence determination. The 16S rRNA gene

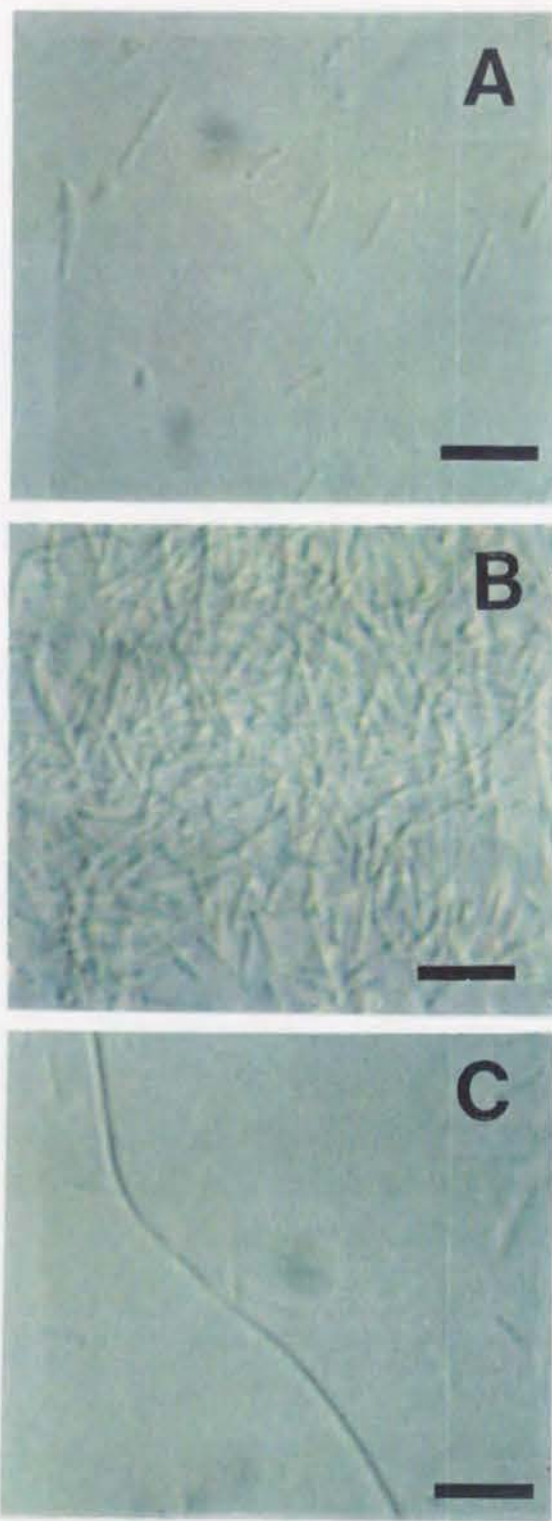


Fig. 1. Differential interference micrographs of *Rhodothermus obamensis* cells. (A) exponentially growing cells; (B) aggregated cells in the stationary phase; (C) filamentous cell in the stationary phase. Bar indicates 5 μ m.



Fig. 2. Transmission electron micrograph of *R. obamensis* cells. Thin sections were double contrasted with a JEOL 1200EX II electron microscope operated at 80 kV. Bar indicates 1 μ m.

was amplified by the polymerase chain reaction (PCR). The primers used for amplification had the sequences 5'-AGAGTTTGATCCTGGCTCAG-3' and 5'-GGTACCTTCCTCCGGCTTA-3', corresponding to positions 8-27 and 1493-1512, respectively in the 16S rRNA sequence of *Escherichia coli* [66]. The 1.5 kb PCR product was directly sequenced by the dideoxynucleotide chain termination method using DNA sequencer Model 373As (Applied Biosystem Inc.). The DNA sequence data were applied to a sequence homology search with other known 16S rRNA sequences by DNASIS ver. 3.6 software (Hitachi Software, Tokyo, Japan).

Data analysis. The almost complete 16S rRNA sequence of OKD7 was aligned and the evolutionary distances (K_{nuc} values) were calculated for 1407 nucleotides from position 29 to 1436 corresponding to *E. coli* 16S rRNA sequence. A software package, ODEN version

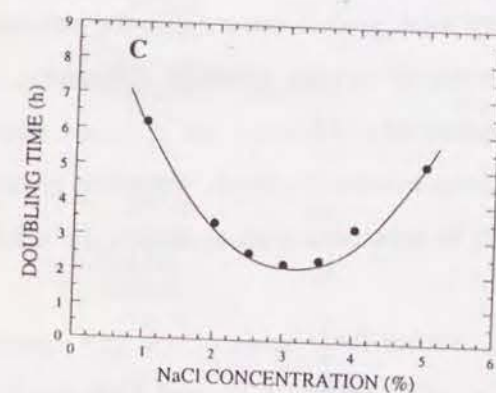
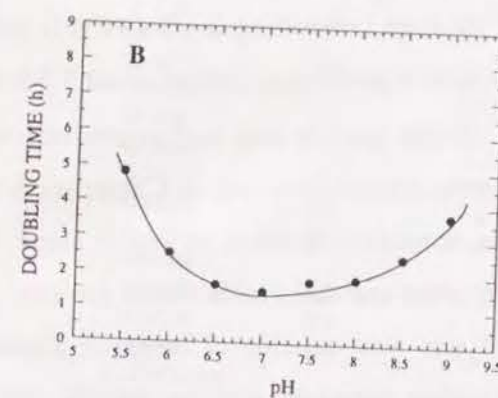
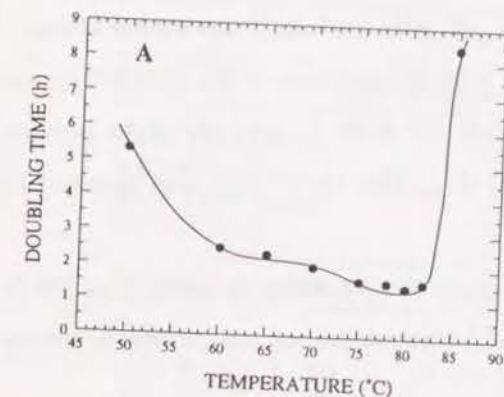


Fig. 3. The effects of temperature, pH and NaCl on the growth of *R. obamensis*. (A) Temperature range for growth of *R. obamensis* in MJ medium at initial pH 6.8-7.2. No growth occurred at temperature below 50 °C and above 85 °C. (B) pH range for growth of *R. obamensis* in MJ medium at 75 °C. The initial pH was adjusted with H₂SO₄ or NaOH at room temperature. (C) Effect of NaCl on growth of *R. obamensis* at 75 °C. For this experiment, solutions containing different concentrations of NaCl, 0.1% (wt/vol) of yeast extract and peptone (pH 7.0) were used.

1.1.1 (National Institute of Genetics, Mishima, Japan) was used for multiple alignment, calculation of the K_{nuc} values and construction of the phylogenetic tree based on the neighbor-joining method [67] and bootstrap examination.

3. Results

Enrichment and purification.

Enrichment took place from sedimentary materials in Jx medium at 80 °C, and a mixed population of coccoid and long, thin, rod-shaped cells were observed after one day incubation. The rod-shaped cells could be successfully purified during the repeated plating procedure at 70 °C. One red colony was used as an inoculum for a liquid culture and was designated strain OKD7 (Japan Collection of Microorganisms, JCM 9785, Wako, Japan). All further experiments were performed with isolate OKD7.

Morphology. Cells of OKD7 were Gram negative rods, which were 4-10 μ m long and 0.5-1.0 μ m wide in the exponential growth phase (Fig. 1A). In the stationary phase, cells tended to occur in aggregates (Fig. 1B) and to become extremely long (Fig. 1C). The transmission electron micrograph of the cells was shown in Fig. 2. The thin sections revealed a typical gram-negative cell envelope profile and a multilayer cell wall (Fig. 2). Isolate OKD7 vigorously grew with shaking and was a typical aerobe.

Temperature range for growth and effects of pH and salt concentration. The isolate grew over a temperature range of about 50-85 °C, with an optimum at 80 °C and a generation time at 80 °C of about 1.5 h (Fig. 3A). No growth was observed at 90 °C. Growth of the new isolate occurred between pH 5.5-9.0, with an optimum about 7.0 (Fig. 3B). No growth was detected below pH 5.5 or above pH 9.0.

Strain OKD7 required NaCl for growth. It grew over in the presence of about 1 to 5% NaCl, with an optimum of around 3% NaCl (Fig. 3C). At NaCl concentrations below 1% or above 5% NaCl, the cells lysed within 2 h.

Nutrition. Strain OKD7 was a heterotroph. In MJ medium containing 0.1% (wt/vol) yeast extract and 0.1% (wt/vol) peptone, OKD7 grew vigorously with a generation time of about 1.5 h and reached a maximum cell density of more than 10⁹ cells/ml. Similar growth rates and somewhat lower maximum cell densities were observed with 0.1% (wt/vol) yeast extract, peptone, or Casamino Acids as a sole energy and carbon source, whereas with sucrose, mannitol, sorbitol, or starch alone, the growth rates and cell yields were quite similar to the growth rates and cell yields with 0.1% (wt/vol) of yeast extract and peptone (Table 1). The new isolate was also capable of utilizing glucose, galactose, maltose, cellobiose, lactate, pyruvate, casein, arginine, aspartate, glycine, alanine, serine, threonine, or proline as a substrate for growth (Table 1). Very weak growth occurred in the presence of isoleucine or valine, and no growth occurred in the presence of xylose, glycerol, glutamine, or leucine (Table 1). In addition, the utilizations of most substrates exhibited the concentration-dependent modulation that high concentrations of carbohydrates inhibited growth, while the growth rates and cell yields increased according to the concentrations of substrates such as carboxylic acids, amino acids, Casamino Acids, and casein (Table 1).

Fatty acid and quinone compositions. The major cellular fatty acids of the new isolate grown at 75 °C consisted of 39% iso-C₁₇, 19% anteiso-C₁₅, 16% anteiso-C₁₇, and 15% iso-C₁₅ acids. The fatty acid composition was similar to those of *Thermus* spp. (Table 2). However, there was a significant difference between the quinone composition of OKD7 and that of *Thermus* spp. Although menaquinone 8 is the major menaquinone component of *Thermus* spp., menaquinone 7 is the major respiratory quinone (83%), and menaquinones 5 and 6 also exist (7 and 10%, respectively), but no menaquinone 8 was observed in OKD7 (Table 2).

DNA base composition. The GC content of OKD7 was 66.6 mol% and similar to those of *Rhodothermus marinus* and *Thermus* spp. (Table 2).

Phylogenetic analyses. The almost complete 16S rRNA sequence of OKD7 was

Table 1. Maximum cell yields and growth rates for *R. obamensis* OKD7 with various carbon-containing substrates. The specific growth rate in the medium containing 0.1% yeast extract and 0.1% peptone was defined as 100%. All preparations were incubated at 75 °C with shaking at 100 rpm and the initial pH of each medium was adjusted to 6.8-7.2 with H₂SO₄ or NaOH.

Substrate	Specific growth rate (SGR) (%)	Max. cell density (MCD) (cells/ml)
0.1% Yeast extract + 0.1% Peptone	100	2 x 10 ⁹
0.1% Yeast extract	89	1 x 10 ⁹
0.1% Peptone	96	1 x 10 ⁹

Substrate	SGR (%)	MCD (cells/ml)	Substrate	SGR (%)	MCD (cells/ml)
Glucose			Casein		
0.01%	64	1 x 10 ⁸	0.01%	25	8 x 10 ⁷
0.05%	22	7 x 10 ⁷	0.05%	49	1 x 10 ⁸
0.1%	7	4 x 10 ⁷	0.1%	65	2 x 10 ⁸
Galactose			Casamino acid		
0.01%	66	2 x 10 ⁸	0.01%	38	8 x 10 ⁷
0.05%	13	5 x 10 ⁷	0.05%	72	3 x 10 ⁸
0.1%	0	-	0.1%	95	7 x 10 ⁸
Maltose			Glycine		
0.01%	45	1 x 10 ⁸	0.01%	12	5 x 10 ⁷
0.05%	27	1 x 10 ⁸	0.05%	31	8 x 10 ⁷
0.1%	10	7 x 10 ⁷	0.1%	44	9 x 10 ⁷
Sucrose			Alanine		
0.01%	86	5 x 10 ⁸	0.01%	16	6 x 10 ⁷
0.05%	77	5 x 10 ⁸	0.05%	38	8 x 10 ⁷
0.1%	59	3 x 10 ⁸	0.1%	52	1 x 10 ⁸
Cellobiose			Leucine		
0.01%	70	2 x 10 ⁸	0.01%	0	-
0.05%	7	4 x 10 ⁷	0.05%	0	-
0.1%	0	-	0.1%	0	-
Mannitol			Serine		
0.01%	77	4 x 10 ⁸	0.01%	0	-
0.05%	52	1 x 10 ⁸	0.05%	14	5 x 10 ⁷
0.1%	38	1 x 10 ⁸	0.1%	33	8 x 10 ⁷
Sorbitol			Threonine		
0.01%	80	2 x 10 ⁸	0.01%	10	4 x 10 ⁷
0.05%	61	1 x 10 ⁸	0.05%	25	9 x 10 ⁷
0.1%	44	1 x 10 ⁸	0.1%	35	9 x 10 ⁷
Xylose			Valine		
0.01%	0	-	0.01%	27	6 x 10 ⁷
0.05%	0	-	0.05%	0	-
0.1%	0	-	0.1%	0	-
Starch			Proline		
0.01%	80	5 x 10 ⁸	0.01%	18	6 x 10 ⁷
0.05%	61	6 x 10 ⁸	0.05%	22	9 x 10 ⁷
0.1%	44	4 x 10 ⁸	0.1%	25	9 x 10 ⁷
Lactate			Arginine		
0.01%	16	6 x 10 ⁷	0.01%	11	4 x 10 ⁷
0.05%	25	8 x 10 ⁷	0.05%	25	6 x 10 ⁷
0.1%	28	8 x 10 ⁷	0.1%	44	8 x 10 ⁷
Pyruvate			Aspartate		
0.01%	5	4 x 10 ⁷	0.01%	17	3 x 10 ⁷
0.05%	44	8 x 10 ⁷	0.05%	39	8 x 10 ⁷
0.1%	72	2 x 10 ⁸	0.1%	48	1 x 10 ⁸
Glycerol			Glutamine		
0.01%	0	-	0.01%	0	-
0.05%	0	-	0.05%	0	-
0.1%	0	-	0.1%	0	-

Table 2. Comparison of some characteristics among *R. obamensis*, *R. marinus*, and the genus *Thermus* and *Thermomicrobium*.

Characteristics	<i>R. obamensis</i>	<i>R. marinus</i> ^{a,b}	<i>Thermus</i> ^{b,c,d}	<i>Thermomicrobium</i> ^{a,e}
Cell length, µm	4-10	2-2.5	5-10	3-6
Colony color	Reddish	Reddish	Yellow/orange/red/transparent	Red
Temp. optimum (°C)	80	65	70-75	70-75
Generation time (min)	90	80	20-60	330
Growth in NaCl:				
0%	-	-	+	+
3%	+	+	-	-
6%	-	+	-	-
Growth on:				
Xylose	-	+	-	n.r.
Sorbitol	+	-	-	n.r.
Casein	+	-	+	+
Casamino acid	+	-	-	n.r.
Glutamine	-	+	Variable	n.r.
Proline	+	-	+	n.r.
Serine	+	-	Variable	n.r.
Oxidase	+	+	+	n.r.
Catalase	+	+	+	n.r.
GC content (mol%)	66.6	65	57-65	n.r.
Major fatty acid(s)	iso-C ₁₅ , iso-C ₁₇ , anteiso-C ₁₅ , anteiso-C ₁₇	n.r.	iso-C ₁₅ , iso-C ₁₇	internally branched 12-methyl-C ₁₈
Major isoprenolog(s)	MK-7, MK-6, MK-5	n.r.	MK-8	n.r.

^aTaken from Alfredsson *et al.* [54], ^bfrom Nunes *et al.* [55], ^{c,d}from Brock *et al.* [13, 14], ^efrom Jacson *et al.* [69].

determined and found to have 95% sequence similarity with the 16S rRNA sequence of *R. marinus* but less than 80% similar to any other sequences known so far. The result suggested that the new isolate belongs to the genus *Rhodothermus*. Therefore, in order to determine the phylogenetic position of the genus *Rhodothermus*, including OKD7, evolutionary distances based on the 16S rRNA gene sequences of several members of Bacteria and Archaea were calculated and a phylogenetic tree was reconstructed by using neighbor-joining method (Fig. 4).

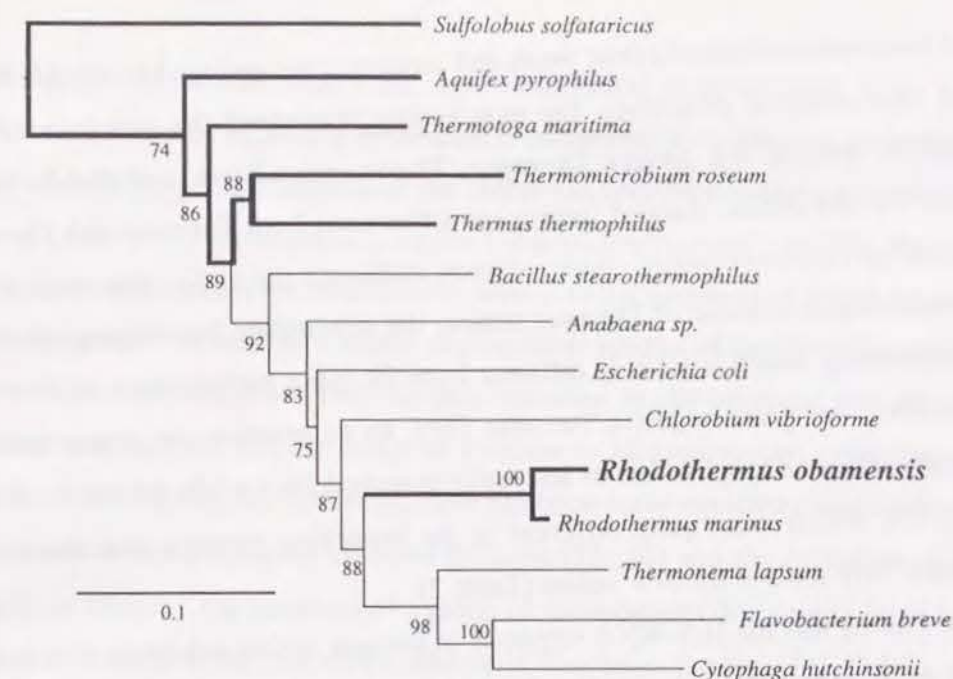


Fig. 4. Phylogenetic tree of representative Bacteria and Archaea inferred from 16S rRNA sequence data. The thick lines indicate hyperthermophilic or extremely thermophilic branches and possible thermophilic origins of life. Each number shows the bootstrap value for the branches (based on 100 replicates). Scale bar indicates substitution per nucleotide. The sequences in this figure are from GenBank under accession numbers: *Sulfolobus solfataricus*, X03235; *Aquifex pyrophilus*, M83548; *Thermotoga maritima*, M21774; *Thermomicrobium roseum*, M34115; *Thermus thermophilus*, X07998; *Bacillus stearothermophilus*, X57309; *Anabaena sp.*, X59559; *Escherichia coli*, V00348; *Chlorobium vibrioforme*, M62791; *Rhodothermus obamensis*, X95071; *Rhodothermus marinus*, X80994; *Thermonema lapsum*, L11703; *Flavobacterium breve*, M59052; *Cytophaga hutchinsonii*, M58768.

On the phylogenetic tree, new isolate OKD7, was located along with *R. marinus* close to the root of the *Flexibacter-Cytophaga-Bacteroid* (F-C-B) group and did not represent a deep branching within the domain Bacteria, in agreement with the previous phylogenetic study of *R. marinus* [60]. The bootstrap confidence data supported the robustness and significance of the placement of OKD7 and *R. marinus*.

The almost complete sequence of OKD7 was deposited in EMBL Nucleotide Sequence Database under accession number X95071.

4. Discussion

The new isolate was a gram negative, rod-shaped, aerobic extreme thermophile and appeared to be a member of the domain Bacteria due to its morphological and physiological similarities to other thermophilic bacteria. Representatives of thermophilic genera belonging to this domain have been

isolated from various hydrothermal vents and terrestrial hot springs [14-16, 54, 62, 68, 69]. On the basis of physiological properties, the new isolate resembled the members of three extremely thermophilic genera, the genera *Thermus*, *Thermomicrobium*, and *Rhodothermus* (Table 2). However, the new isolate showed significant differences from *Thermus* and *Thermomicrobium*, as determined by chemotaxonomic characteristics. Although the major fatty acid components of the isolate were similar to those of *Thermus* strains, the new isolate had menaquinone 7 (MK-7) as the major isoprenolog, which is not only different from the major menaquinone of *Thermus* (Table 2) but is rare among the gram-negative bacteria [70]. In comparison of major cellular fatty acids, *Thermomicrobium* had high levels of internally branched fatty acids, primarily 12-methyl C₁₈ fatty acid [13, 69], which were quite different in the branching patterns and chain lengths from the predominant fatty acids of the new isolate (Table 2).

The finding that the 16S rRNA sequence of the new isolate exhibited 95% homology with the sequence of *R. marinus* suggests that the new isolate belongs to the genus *Rhodothermus*. The members of *Rhodothermus* are aerobic, heterotrophic thermophiles that have been recently isolated from sites in Iceland and the Azores [54, 55]. *R. marinus* is a marine thermophile which grows at temperature between 54 and 77 °C (optimum temperature, 65 °C), and utilizes a variety of sugars and carboxylic acids as sole carbon and energy sources [54, 55]. In contrast, the new isolate is an extreme thermophile that grows at temperature up to 85 °C, has an optimum temperature of 80 °C (Fig. 3A) and utilizes different carbon-containing substrates for growth (Table 2). Contrary to *R. marinus*, the new isolate can utilize sorbitol, casein, Casamino Acids, proline, and serine and does not utilize xylose or glutamine as a sole carbon and energy source (Table 2). Moreover, the morphology and salt tolerance of OKD7 and *R. marinus* are different and the evolutionary distance between these taxa based on the 16S rRNA sequence data is equivalent to the distance used to distinguish species within the domain Bacteria. On the basis of the results, I propose that the new isolate is a member of a new species of the genus *Rhodothermus*, *Rhodothermus obamensis*. The type strain of *R. obamensis* is OKD7.

On the basis of its optimal growth in the presence of 3% NaCl, *R. obamensis* is a typical marine organism similar to *R. marinus*. Previously, it was thought that members of the genus *Thermus* are the most common heterotrophs in submarine hot springs, as well as in terrestrial ones [71, 72]. However, members of at least two heterotrophic genera in the Bacteria, the genera *Thermotoga* and *Rhodothermus*, have been isolated from submarine hydrothermal environments [54, 55, 68], and it has also been suggested that there are unculturable heterotrophic thermophiles [73]. The isolation of a

member of the genus *Rhodothermus* from Japan submarine hydrothermal vents leads to the speculation that this genus may be widely distributed in submarine hydrothermal environments.

The results of the phylogenetic analysis of the 16S rRNA sequence demonstrated the significance of the phylogeny of the genus *Rhodothermus* on the bacterial phylogenetic tree (Fig. 4). Interestingly, both of the *Rhodothermus* species are most closely related to the members of *Flexibacter-Cytophaga-Bacteroid* (F-C-B) group. The results of recent phylogenetic studies of thermophilic members of the Bacteria and Archaea have suggested that the deep branches on the universal tree are occupied by thermophiles and have implied that the common ancestor to all present-day organisms might be a thermophile [16, 57-59, 74, 75]. Nevertheless, there has been some evidences against this hypothesis that has been based on the phylogeny of other proteins [15, 76] and the evolution of the reverse gyrase gene [19]. In addition, the members of a group of thermophiles (the genera *Rhodothermus* and *Thermonema*) placed close to the root of *Flexibacter-Cytophaga-Bacteroid* (F-C-B) group are not deep branches [60, this work], and there are diverse thermophilic members of Bacteria that are only distantly related to the universal root [13]. The discovery of the extreme thermophile *R. obamensis*, whose lineage is apparently modern, suggests that extreme thermophily is not necessarily an ancient characteristic but may have a second, modern origin within the Bacteria.

Chapter 3

Purification and Characterization of an Extremely Thermostable Phosphoenolpyruvate Carboxylase (PEPC) from an Extreme Thermophile *Rhodothermus obamensis* OKD7.

1. Introduction

Recently, there has been increasing interest in thermophilic organisms due to their novel biochemical machinery that must be required to sustain them under extraordinary temperature [2, 3]. A number of thermophilic enzymes have been isolated from various thermophiles, and the enzymes from a few representative thermophiles such as *Thermus*, *Thermotoga*, *Sulfolobus*, and *Pyrococcus* have been well studied and focused on [2-4, 77]. However, the mechanisms of thermostability are largely unknown.

The first step of elucidating the mechanisms is to accumulate the knowledge of thermophilic enzymes and to compare the properties with those of other thermophilic and mesophilic counterparts. In addition, different types of enzymes from various thermophilic sources should be taken in further consideration. For this purpose, the coworkers and I isolated and characterized phosphoenolpyruvate carboxylases (PEPCs) [EC4.1.1.31] from hyperthermophilic methanogen, *Methanothermobacter sociabilis*, and thermoacidophilic archaea *Sulfolobus* species, and compared them with other thermophilic and mesophilic homologs [52, 53, Sako, Y. *et al.* unpublished].

As described in Chapter 1, PEPC catalyzes the reaction that fixes HCO_3^- on phosphoenolpyruvate (PEP) to form oxaloacetate (OAA) and inorganic phosphate using Mg^{2+} as the cofactor [45]. The enzyme is distributed widely in bacteria, protozoa, algae, and plants, and a large number of the enzymes have been purified, cloned, and sequenced from various sources, including *Escherichia coli* [46], *Zea mays* [50], and *Thermus* sp. [47]. In the previous studies, we purified PEPCs from the domain of Archaea and reported that the enzymes from the hyperthermophilic archaea were quite different from the counterparts of the other domains, Bacteria and Eucarya, with respect to the molecular size and allosteric properties [52, 53]. Moreover, the archaeal PEPCs were

quite thermostable similar to all known hyperthermophilic enzymes. However, difficulty in manipulation of the hyperthermophilic archaea and their enzymes, and relatively low growth and enzyme yields have limited biochemical and structural approach to the thermostability of archaeal PEPCs.

Therefore, we sought to explore another thermophilic PEPC from an extremely thermophilic bacterium *Rhodothermus obamensis*, which was isolated from a shallow hydrothermal vent environment in Japan and characterized in Chapter 2. *R. obamensis* was an aerobic heterotroph, capable of growing up to 85 °C and suitable for biochemical and biotechnological investigation of thermophilic proteins in advantage of the easy cultivation and high growth yield. In this chapter, I present the purification and characterization of PEPC from extreme thermophile *R. obamensis*. The enzymological properties were compared with those of thermophilic and mesophilic entities. In addition, the effect of the substances associated with the enzyme on the thermostability was examined as extrinsic thermostabilization factors.

2. Materials and Methods

Bacterial strains and growth conditions. The bacterial strain used was *Rhodothermus obamensis* OKD7 (JCM 9785) which was isolated by Sako, Y. *et al.* from a shallow marine hydrothermal vent at Tachibana Bay, Nagasaki Prefecture, Japan [78, Chapter 2]. For cultivation of *R. obamensis*, Jx medium was used [78, Chapter 2]. *R. obamensis* was grown at 76 °C and harvested at the late exponential growth phase by centrifugation and washed three times with 50 mM Tris-HCl (pH 7.5). The cell pellet was frozen at -90 °C prior to enzyme purification.

Enzyme assays. PEPC activity was routinely coupled to the malate dehydrogenase (MDH) reaction and assayed in duplicate by the previously described method [52, 53]. For measurement of the activity, a heat-stable MDH from *Thermus flavus* (SIGMA) was used as a coupling enzyme. All assays were initiated by addition of enzyme preparation to the preheated reaction mixture containing 50 mM Tris- H_2SO_4 (pH 8.0), 10 mM NaHCO_3 , 5 mM PEP, 10 mM MgSO_4 , 0.15 mM NADH, and 2U *T. flavus* MDH in a final volume of 1.0 ml unless otherwise noted (standard assay condition). In an attempt to examine the effect of pH on enzyme activity, 50 mM Tris- H_2SO_4 was used at a range of pH 7.0-9.5 and 50 mM KH_2PO_4 - Na_2HPO_4 (phosphate buffer) was used at a range of pH 5.5-7.0, as a buffer of the reaction mixture. In order to test the requirement of divalent cations for PEPC activity,

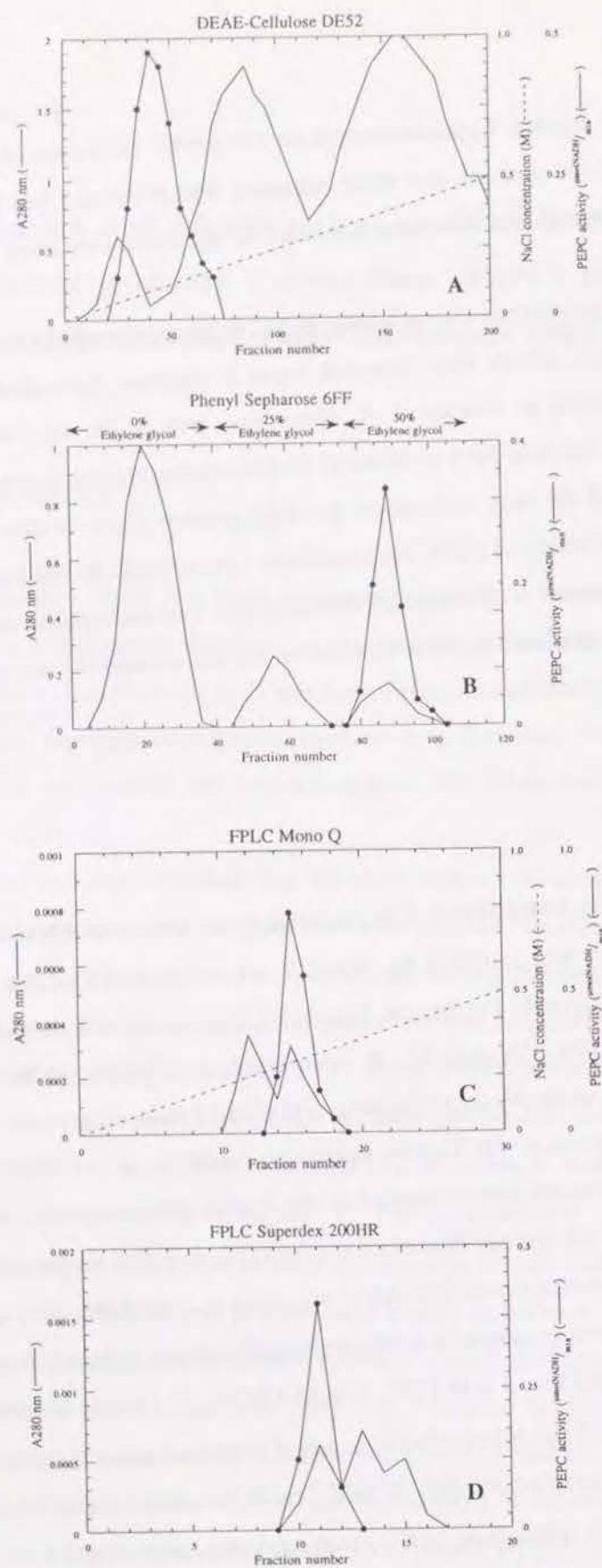


Fig. 5. The elution profiles of PEP carboxylase in the purification steps. (A) The elution profile in the column of DEAE-Cellulose. The bulk of active fractions were eluted with the buffer between 0.05 and 0.15 M NaCl. (B) The elution profile in the column of Phenyl-Sepharose 6FF. The enzyme was stepwisely eluted with 300 ml of 10 mM Tris-HCl (pH 8.0) buffers containing 25, 50, and 75% (vol/vol) of ethylene glycol, respectively. The active fractions were eluted with the buffer containing 50% of ethylene glycol. (C) The profile in the column of Mono Q. The active fractions were eluted with 10 ml of a linear gradient of NaCl (0-0.5 M) using FPLC system (Pharmacia). (D) The elution profile in the column of Superdex 200 HR. The gel filtration column was not only for the final purification step but for determining the molecular mass of the enzyme. From the elution pattern, the molecular mass of the enzyme was found to be 400 kDa. As standards of molecular weight, HMW gel filtration calibration kit was used (Pharmacia).

Table 3. Purification of PEPC from *R. obamensis*.

Preparation	Volume (ml)	Total protein (mg)	Total activity ($\mu\text{molNADH}/\text{min}$)	Yield (%)	Specific activity ($\mu\text{molNADH}/\text{min}/\text{mg}$)	Purification fold
Crude extract	400	10470				
35-80% $(\text{NH}_4)_2\text{SO}_4$	185	5790	370	100	0.064	1
DEAE-Cellulose DE-52	175	723	284	76.8	0.393	6
Phenyl-Sepharose 6-FF	72.0	23.4	162	43.8	6.92	108
FPLC Mono Q	13.1	1.83	160	43.2	87.4	1366
FPLC Superdex 200 HR	16.0	0.64	64	17.3	100	1563

various concentrations of MgSO_4 or MnSO_4 were added to the reaction mixture instead of 10 mM MgSO_4 . To test the effect of metabolites on the activity, various concentrations of acetyl-CoA, fructose 1,6-bisphosphate, L-aspartate, and L-malate were added to the reaction mixture. One unit of PEPC activity was defined as the amount of enzyme that catalyzed the oxidation of 1 μmol of NADH per min.

Purification. All procedures were carried out at 0 to 4 °C. Thawed cell paste of *R. obamensis* (150 g) was suspended in 300 ml of 50 mM Tris-HCl (pH 7.5). The cells were disrupted by seven passages through a French Press 5501-N (Ohtake Seisakusho, Tokyo, Japan) at 1,500 kg/cm^2 and centrifuged at 24,000 $\times g$ for 20 min. The supernatant was used as the crude extract. Solid ammonium sulfate was added slowly to the crude extract to reach 35% saturation. After stirring for 30 min, the extract was centrifuged at 24,000 $\times g$ for 20 min. The supernatant was brought to 80% saturation of ammonium sulfate. After centrifugation, the pellet was dissolved in 150 ml of 50 mM Tris-HCl (pH 7.5) buffer and dialyzed against 100-fold volume of the same buffer twice. PEPC activity recovered with ammonium sulfate fractionation was applied to the next purification step.

The active fraction was loaded on to DEAE-cellulose DE-52 (Whatman, Kent, UK) column (2.5 \times 30 cm) equilibrated with 50 mM Tris-HCl (pH 7.5), and then washed with the same buffer. The enzyme was eluted with 1200 ml of a linear gradient of NaCl (0-0.5 M) in the buffer. The bulk of

active fractions eluted with the buffer between 0.05 and 0.15 M NaCl were pooled and dialyzed twice against 100-fold volume of 10 mM Tris-HCl (pH 8.0) (Fig. 5A).

The dialyzed enzyme solution was put on a column of Phenyl-Sepharose 6FF (Pharmacia) (1.5x30 cm) equilibrated with the same buffer for the dialysis. The enzyme was stepwisely eluted with 300 ml of 10 mM Tris-HCl (pH 8.0) buffers containing 25, 50, and 75% (vol/vol) of ethylene glycol, respectively. The active fraction eluted with the buffer containing 50% of ethylene glycol was dialyzed twice against 100-fold volume of 50 mM Tris-HCl (pH 7.5) (Fig. 5B).

The dialyzed enzyme solution was put on to a column of MonoQ (Pharmacia) (bed volume 1 ml) equilibrated with 50 mM Tris-HCl (pH 7.5) and eluted with 10 ml of a linear gradient of NaCl (0-0.5 M) using FPLC system (Pharmacia) (Fig. 5C). The pooled active fractions were concentrated 5-fold with the Amicon ultrafiltration apparatus with a YM-30 ultrafilter (Amicon). The concentrated enzyme solution was applied to the final step, the column of Superdex 200HR (Pharmacia) (bed volume 8 ml) in the FPLC system equilibrated with 200 mM Tris-HCl (pH 7.5) (Fig. 5D).

The gel filtration column was not only for the final purification step but for determining the molecular mass of the enzyme. As standards of molecular weight, HMW gel filtration calibration kit was used (Pharmacia). The purified enzyme was dialyzed twice against 100-fold volume of 50 mM Tris-HCl (pH 7.5) and then stored at -90 °C. The frozen enzyme solution was stable and had the same properties at least for a year.

Other methods. Polyacrylamide gel electrophoresis (PAGE) of the purified enzyme was performed with 7.5% (wt/vol) polyacrylamide gel in the absence of sodium dodecylsulfate (SDS) for confirming the enzyme purity, and with 10% (wt/vol) polyacrylamide gel in the presence of SDS for determining the molecular mass of the subunit by the method of Laemmli [79]. Molecular weight markers for SDS-PAGE were from Bio-Rad. Protein concentrations were routinely estimated by Bradford [80] with bovine serum albumin as the standard.

Thermostability studies. For the measurement of thermostability, the enzyme was usually incubated at various temperatures in 50 mM Tris-HCl (pH 8.0) containing 10% (vol/vol) of glycerol at a concentration of 9 µg PEPC/ml for different periods of time, unless otherwise noted. Then, the thermoinactivation was stopped by cooling the aliquots on ice and the residual PEPC activity was measured at 75 °C under standard assay condition. The effects of pH, salts and enzyme concentration on thermostability were also examined. In these experiments, thermoinactivations were run with various pH of 50 mM Tris-HCl (pH 7.0-9.0), with 50 mM Tris-HCl (pH 8.0) containing a variety of salts, or at different enzyme concentrations (9 µg, 18 µg, or 36 µg PEPC/ml). To examine the effects

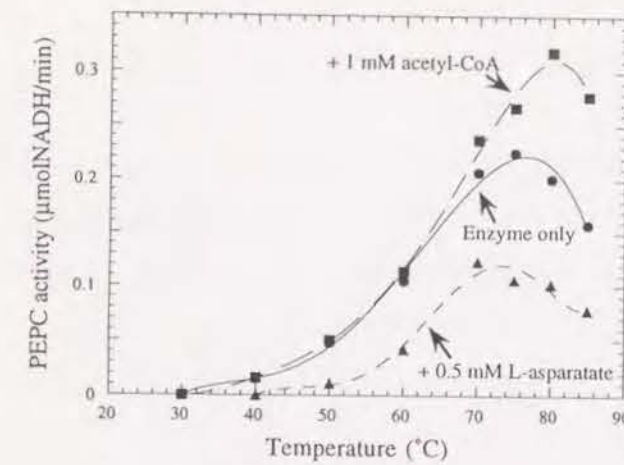


Fig. 7. The effect of temperature on the activity of *R. obamensis* PEPC. The activity was measured at various temperature at a enzyme concentration of 3.6 µg PEPC/ml under standard assay condition in the absence or presence of allosteric effectors. With allosteric effectors, the optimum temperature for activity was shifted from 75 °C to 80 °C for a positive effector of acetyl-CoA, or to 70 °C for negative effector of L-aspartate.

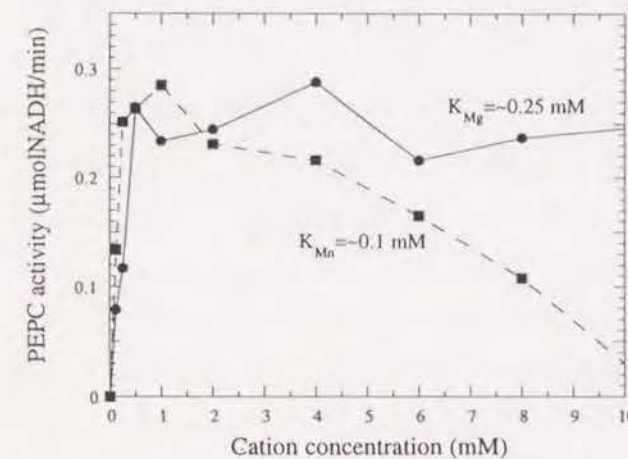


Fig. 8. The effect of divalent cations on the activity of *R. obamensis* PEPC. The activity was measured at 75 °C and pH 8.0 at a concentration of 3.6 µg PEPC/ml. K_{Mg} or K_{Mn} indicates the concentration of Mg^{2+} or Mn^{2+} that results in the half of the maximum activity.

(Fig. 5B). This extreme hydrophobicity caused the enzyme to be successfully separated in the preparation (Table 3).

Molecular properties of PEPC. The molecular mass of PEPC from *R. obamensis* was estimated by gel filtration to be 400 kDa. In SDS-PAGE, the purified enzyme gave rise to a single protein band with a molecular mass of 100 kDa (Fig. 6). These results suggested that the enzyme was a 400 kDa of homotetramer consisting of 100 kDa of subunits. On the basis of the molecular mass, the *R. obamensis* PEPC was similar in size to other known PEPCs from Bacteria and Eucarya.

The effect of temperature, pH, and cations on PEPC. The effect of temperature on the enzyme activity is shown in Fig. 7. The enzyme indicated the highest activity at ambient temperature for growth of 75 °C. The optimum pH value for activity was approximately 8.0. The enzyme absolutely required Mg^{2+} or Mn^{2+} for the activity (Fig. 8). It utilized not only Mg^{2+} which is the most common co-factor for PEPC, but a low concentration of Mn^{2+} instead of Mg^{2+} . The concentrations which resulted in the half of maximum enzyme activity were 0.25 mM for Mg^{2+} and 0.1 mM for Mn^{2+} . With the concentrations of both cations increased, however, the enzyme activity was gradually decreased and completely inhibited by 15 mM of Mn^{2+} or 100 mM of Mg^{2+} . Michaelis constant for PEP was

of the substrate, co-factors and metabolites on the thermostability, each substance (5 mM of PEP, 0.5 mM of $MgSO_4$, 0.5 mM of $MnSO_4$, 1 mM of acetyl-CoA, 10 mM of fructose 1,6-bisphosphate, 0.5 mM of L-aspartate, or 0.5 mM of L-malate) was added to the incubation buffer described above. Residual activity after thermoinactivation was exhibited as relative to the enzyme activity in the same condition without the thermoinactivation. Thermoinactivation rate (I) was calculated by $(I) = \ln dR/dT$, dR ; change of residual activity (%), dT ; change of time (min), and thermostabilization effect was exhibited as (thermoinactivation rate without a factor at a temperature)/(thermoinactivation rate with a factor at the same temperature).

3. Results

Purification of PEPC from *Rhodothermus obamensis*. As shown in Table 3, PEPC of *R. obamensis* was purified 1563-fold with a final specific activity of 100 $\mu\text{molNADH}/\text{min}/\text{mg}$ and an overall yield of about 17.3%. The purity of the purified enzyme was confirmed by native PAGE and SDS-PAGE. The sample after the gel filtration column of Superdex 200HR showed a single protein band both in native PAGE and SDS-PAGE (Fig. 6) and the band position in the native PAGE corresponded to an active fraction of the gel fractions sliced every 3 mm from top to bottom. Therefore, the purification of the enzyme was completed by the column of Superdex 200HR (Fig. 6 and Table 3). The most notable property observed in the course of purification was that the enzyme strongly bound hydrophobic interaction chromatography. The enzyme was eluted with 10 mM Tris-HCl (pH 8.0) containing 75% (vol/vol) ethylene glycol

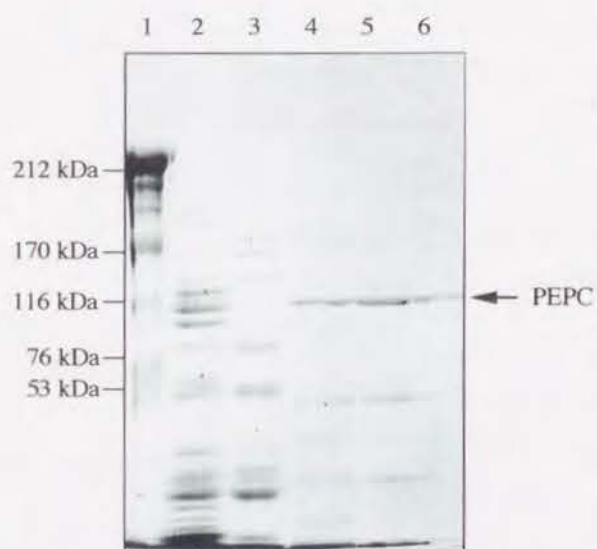


Fig. 6. SDS-polyacrylamide gel electrophoresis of the purified *R. obamensis* PEPC. Approximately 10 μg of protein was applied to each lane. After electrophoresis, the gel was stained by 40% (vol/vol) methanol-10% (vol/vol) acetate containing 0.2% (wt/vol) coomassie brilliant blue (CBB) R250. Lane 1 contains the molecular weight marker, lane 2; 35-80% saturation of $(\text{NH}_4)_2\text{SO}_4$ fraction, lane 3; active fraction through DEAE-cellulose, lane 4; Phenyl-Sepharose 6 FF, lane 5; FPLC Mono Q, lane 6; FPLC Superdex 200 HR.

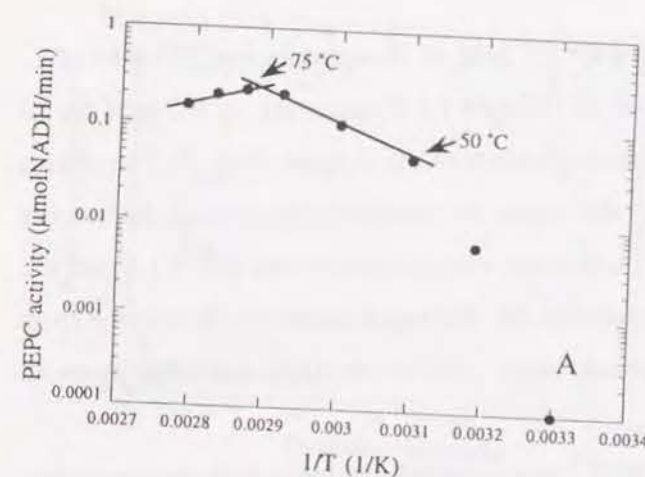
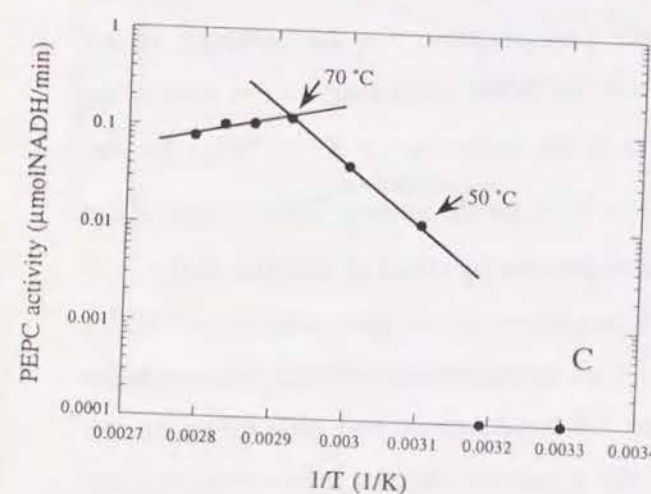
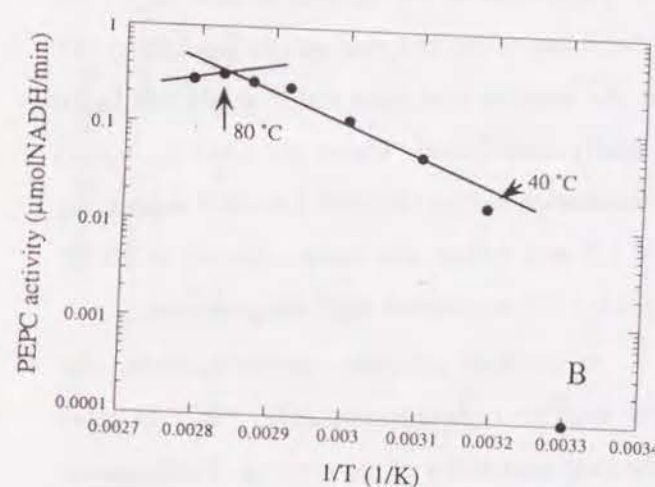


Fig. 9. The Arrhenius plot for the activity of *R. obamensis* PEPC. The data were taken from Fig. 7. (A) indicates the plot without allosteric effectors. (B) or (C) indicates the plot with 1 mM acetyl-CoA or 0.5 mM L-aspartate, respectively. The arrows show the upper and lower temperatures of the Arrhenius range for activity.



calculated in the range of PEP concentration between 0.1 mM to 100 mM to be 20.9 ± 1.2 mM.

The effect of metabolites on PEPC.

The effect of several metabolites which are major positive or negative effectors for the mesophilic PEPCs were investigated. The relative activities with various concentrations of metabolites were 143.2% (1 mM), 155.8% (2 mM), 157.1% (5 mM) with acetyl-CoA, and 126.6% (2 mM), 141.8% (5 mM), 143.7% (10 mM) with fructose 1,6-bisphosphate, and 72.4% (0.5 mM), 23.7% (1 mM), 9.1% (2 mM), 0% (2.5 mM) with L-aspartate, and 22.3% (0.5 mM), 9.5% (1 mM), 0% (2 mM) with L-malate, respectively. For the part of positive effectors, acetyl-CoA and fructose 1,6-bisphosphate significantly enhanced the enzyme activity (maximally 157 and 144%, respectively). The concentration of each effector which resulted in the half of the maximum effectiveness was 0.35 mM for acetyl-CoA or 1.2 mM for fructose 1,6-bisphosphate. On the other

hand, the enzyme activity was completely inhibited by 2.5 mM of L-aspartate and 2.0 mM of L-malate. A 50% of inhibition required a concentration of 0.7 mM for L-aspartate, or 0.3 mM for L-malate. In addition, these metabolites affected the thermophilicity of the enzyme (Fig. 7). The effects of them were strengthened at high temperature range and hence, the optimum temperature for activity was shifted to higher with a positive effector (80 °C) and lower with a negative one (70 °C). From the Arrhenius plot of the result, the positive effectors extended the Arrhenius range of the enzyme from 50-75 °C to 40-80 °C and the negative effectors decreased upper point of the Arrhenius range from 75 °C to 70 °C (Fig. 9).

Thermostability of PEPC. *R. obamensis* PEPC was extremely stable at high temperatures. No loss of activity was observed after the incubation for 2 h at 85 °C (Fig. 10A). The times required for 50% loss of activity were about 240 min at 90 °C, 60 min at 91 °C and 10 min at 93 °C, respectively (Fig. 10A). Moreover, the extreme thermostability of the enzyme was influenced by pH, salts, and enzyme concentration. As shown in Fig. 9B, the enzyme was most stable at pH 8.0. In the buffer whose pH was 7.0 or 9.0, the enzyme was rapidly inactivated. These pH were the values adjusted at 25 °C. Around 90 °C, the pH value of the incubation buffer (50 mM Tris-HCl containing 10% glycerol) was found to decrease to the extent of 1.3 or 1.4 from the value adjusted at 25 °C. Therefore, the enzyme was likely to be stable around pH 6.5-7.0 at ambient high temperatures.

When the enzyme was incubated at 93 °C at several protein concentrations, the thermoinactivation rate decreased in proportion to the enzyme concentration (Fig. 10C). In other words, the elevated enzyme concentration enhanced the thermostability of the enzyme. Furthermore, the effects of salts on the thermostability were investigated (Table 4). In the divalent cations including co-factors of the enzyme, the thermostabilization effect (i.e., the protective ability to reduce the thermoinactivation rates) decreased in proportion to the concentration. On the contrary, in the monovalent cations and anions, the stabilization effect increased according to the increasing concentrations. In addition, the stabilization effect was in the order $\text{Na}^+ > \text{K}^+ > \text{NH}_4^+$ for the monovalent cations, or in the order $\text{SO}_4^{2-} > \text{HPO}_4^{2-} > \text{Cl}^- > \text{NO}_3^-$ for the anions. These orders of the stabilizing PEPC were consistent with the order of the water structuring effect of ions [81, 82].

Not only salts but a substrate and allosteric effectors had effects on the thermostability of PEPC (Fig. 11). The substrate, PEP and positive effector, acetyl-CoA strongly enhanced the thermostability of the enzyme, while another positive effector, fructose 1,6-bisphosphate had little effect on the enzyme thermostability (Fig. 11A). On the other hand, the negative effectors reduced the enzyme thermostability and the effectiveness was consistent with the inhibitory effectiveness of the effectors

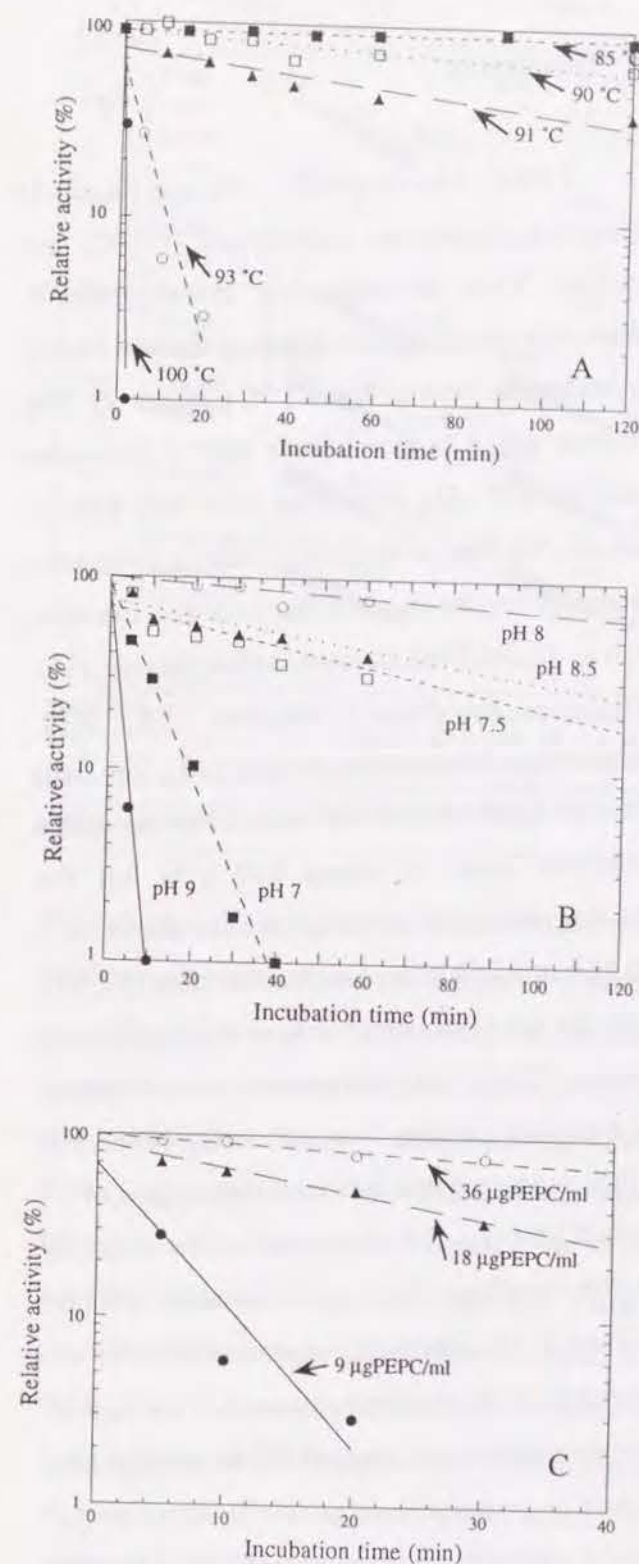


Fig. 10. The effects of temperature, pH and enzyme concentration on thermostability. (A) The thermoinactivation of *R. obamensis* PEPC at various temperatures. The enzyme was incubated at a concentration of 9 µg PEPC/ml in the incubation buffer (50 mM Tris-HCl containing 10% glycerol, pH 8.0) for different periods of time. The thermoinactivation was terminated by cooling the aliquots on ice and the residual activity was measured at 75 °C at pH 8.0. The activity before the thermoinactivation was set to 100%. (B) The effect of pH on the thermostability of *R. obamensis* PEPC. The enzyme was incubated at 91 °C and a concentration of 9 µg PEPC/ml. The pH of the incubation buffer indicated in this figure was the value adjusted at 25 °C and the value was found to decrease to the extent of 1.3 at 91 °C. The activity at each pH value before the thermoinactivation was set to 100%. (C) The effect of enzyme concentration on the thermostability of *R. obamensis* PEPC. The enzyme was incubated at 93 °C and pH 8.0 at 9, 18 or 36 µg PEPC/ml. In this experiment, the total protein concentration was standardized to a concentration of 72 µg/ml in all cases by the compensation of bovine serum albumin (BSA). The activity at each enzyme concentration before the thermoinactivation was set to 100%.

on enzyme activity (Fig. 11B). In addition, the combined effects of the substrate, co-factor, allosteric effector, and salt on the thermostability were examined (Table 5). The thermostabilization effect of each factor in the course of thermoinactivation at 95 °C was 3.14 for PEP, 4.37 for MgSO_4 , 5.58 for Na_2SO_4 and 8.81 for acetyl-CoA. The thermostabilization effect was in the order acetyl-CoA > Na_2SO_4 > MgSO_4 > PEP at all temperatures tested. When the enzyme was incubated with the combinations of these factors, the thermostabilization effects were additive and significantly higher than when with each factor (Table 5).

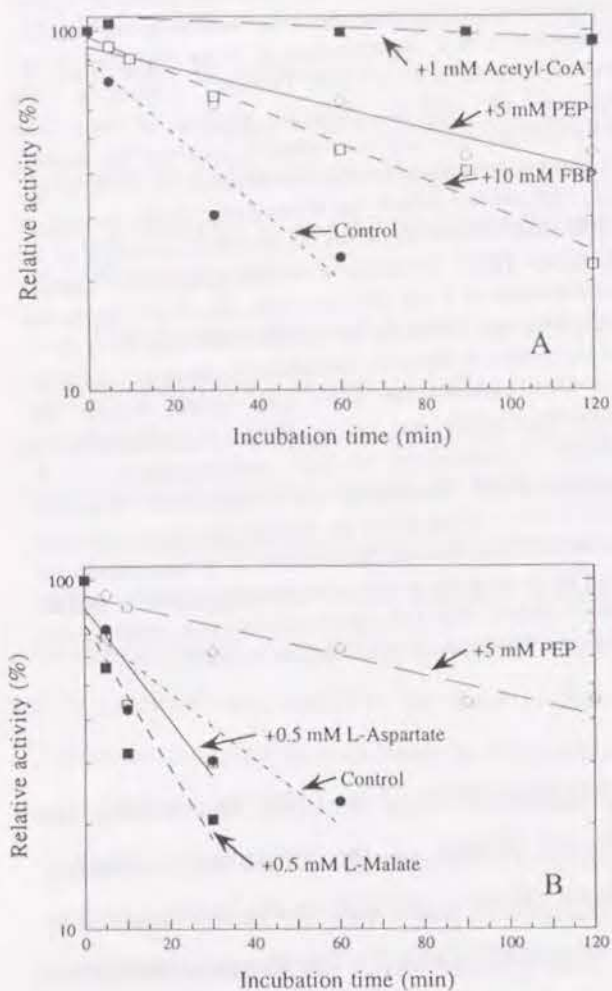


Fig. 11. The effect of substrate or allosteric effectors on the thermostability of *R. obamensis* PEPC. The enzyme was incubated at 93 °C and pH 8.0 at a concentration of 18 μg PEPC/ml in the absence or presence of each substance. (A) indicates the thermoinactivation rates with the substrate and positive effectors. (B) indicates those with the substrate and negative effectors. No change of pH was observed in the incubation buffer in the presence of each substance and the activity with each substance before the thermoinactivation was set to 100%.

4. Discussion

The extremely thermostable phosphoenolpyruvate carboxylase (PEPC) was purified from an extremely thermophile *R. obamensis* recently isolated from a shallow marine hydrothermal vent in Japan [78, Chapter 2]. The enzyme was a homotetramer with a molecular mass of 400 kDa consisting of a 100 kDa of subunit. To date, a number of PEPCs have been purified from the domain Bacteria and Eucarya, such as *E. coli* [46], *Brevibacterium flavum* [83], *Thermus* sp. [47], *Anabaena* sp. [48], *Mesembryanthemum crystallinum* [49], *Zea mays* [50, 84]. Most of them are homotetramers with a molecular mass of about 400 kDa but the homologs from the domain Archaea displayed a 240 kDa or a 260 kDa of molecular mass [52, 53]. From the comparison of amino acid sequences between PEPCs from *Escherichia coli* (allosteric) and *Anacystis nidulans* (non-allosteric), Ishijima *et al.* [85] suggested that the conserved region of C-terminal half was the active core of the enzymes and the variable region of N-terminal half be involved in the allosteric regulation. Hence, we speculated in the previous studies that the lack of N-terminal half might account for the smaller size and non or incomplete-allosteric property in the archaeal enzymes to large extent [52, 53]. The allosteric property and the full size of molecular mass (400 kDa) in *R. obamensis* PEPC were

Table 4. The effect of various cofactors and salts on the thermostability of *R. obamensis* PEPC.

Cations	Anions	SO ₄ ²⁻			HPO ₄ ²⁻			Cl ⁻			NO ₃ ⁻		
		50 mM	5 mM	0.5 mM	50 mM	5 mM	0.5 mM	100(50) mM	10(5) mM	1(0.5) mM	100(50) mM	10(5) mM	1(0.5) mM
Mg ²⁺	50 mM	4.45			N.D.			2.28			N.D.		
	5 mM		4.32			N.D.			1.95			N.D.	
	0.5 mM			5.51		N.D.				3.02			N.D.
Ca ²⁺	50 mM	N.D.			N.D.			0.772			0.639		
	5 mM		N.D.			N.D.			1.08			1.68	
	0.5 mM			N.D.		N.D.				3.25			2.81
Mn ²⁺	50 mM	0			N.D.			0			N.D.		
	5 mM		0.587			N.D.			0.786			N.D.	
	0.5 mM			5.72		N.D.				4.32			N.D.
Na ⁺	100(50) mM	6.81			4.40			4.11			2.60		
	10(5) mM		4.36			4.11			3.36			2.32	
	1(0.5) mM			4.66		1.58				2.38			2.19
K ⁺	100(50) mM	4.19			3.89			2.98			3.34		
	10(5) mM		4.11			3.25			1.22			1.67	
	1(0.5) mM			3.77		2.91				0.867			0.907
NH ₄ ⁺	100(50) mM	3.62			5.17			2.13			2.70		
	10(5) mM		3.62			2.49			1.67			1.78	
	1(0.5) mM			2.49		2.28				0.923			0.789

The enzyme was incubated at 93 °C and pH 8.0 at a concentration of 9 μg PEPC/ml in presence of various concentrations of cofactors and salts. Each value indicates a thermostabilization effect as described in Materials and Methods and bold numbers imply the positive effects. The arrows on the top or left shows the water-structuring effectiveness of the ions. Since each ion was supplied as a salt to the incubation buffer, the concentrations of monovalent ions in the buffer were doubled as coupled to divalent ions. The numbers in () exhibit the concentrations as coupled to monovalent ions. The pH in the incubation buffer was readjusted to 8.0 when the presence of some salts led to significant shift of pH in the buffer.

consistent with the speculation that the considerable part of the 400 kDa might be involved in the binding with effectors and the regulation of enzyme activity.

On the basis of the enzymological characteristics, *R. obamensis* PEPC was closely related with bacterial counterparts [Table 6]. Although the optimum temperature for enzyme activity was 75 °C and much higher than any other bacterial PEPC, the optimum pH for activity, the requirement for divalent cations, and the allosteric regulation by metabolites involved in the glycolytic and tricarboxylic acid metabolisms were quite similar to those of the bacterial PEPCs. Furthermore, the enzyme exhibited relatively high K_m value to PEP (20.9 ± 1.2 mM) and V_{max} (378 ± 22 $\mu\text{molNADH}/\text{min}/\text{mg}$). It has been accepted that the bacterial PEPCs have higher K_m and V_{max} values than the eucaryotic ones and the K_m and V_{max} values of the bacterial PEPCs are the same level as those of *R. obamensis* PEPC [86]. These enzymological and kinetic properties indicated that *R. obamensis* PEPC was a typical bacterial PEPC and an extremely thermophilic version of the enzyme [Table 6].

R. obamensis PEPC was extremely thermostable. The enzyme remained active even after it was exposed to high temperatures that were above the upper limit of growth for a few hours. As compared to other thermophilic PEPCs [47, 52, 53], *R. obamensis* PEPC was the most thermostable

Table 5. The combined effects of extrinsic thermostabilization factors.

Factor	Thermostabilization effect multiplications indicate the calculated values
(1) +5 mM PEP	3.14
(2) +0.5 mM MgSO ₄	4.37
(3) +50 mM Na ₂ SO ₄	5.58
(4) +1 mM Acetyl-CoA	8.81

(5) +5 mM PEP, 0.5 mM MgSO ₄	16.1 (1)x(2)=13.7
(6) +50 mM Na ₂ SO ₄ 1 mM Acetyl-CoA	39.9 (3)x(4)=49.2
(7) +5 mM PEP, 0.5 mM MgSO ₄ , 50 mM Na ₂ SO ₄	50.6 (1)x(2)x(3)=76.6 (3)x(5)=89.8
(8) +5 mM PEP, 0.5 mM MgSO ₄ , 1 mM Acetyl-CoA	106.4 (1)x(2)x(4)=121 (4)x(5)=141.8
(9) +5 mM PEP, 0.5 mM MgSO ₄ , 50 mM Na ₂ SO ₄ , 1 mM Acetyl-CoA	106.3 (1)x(2)x(3)x(4)=673.5 (3)x(4)x(5)=791.4 (1)x(2)x(6)=547.5 (3)x(8)=593.7 (4)x(7)=445.8

The enzyme was incubated at 95 °C and pH 8.0 at a concentration of 9 µg PEPC/ml. The thermostabilization effects were taken as described in Materials and Methods.

PEPC reported to date. Moreover, the thermostability of the enzyme was increased in proportion to the enzyme concentration (Fig. 10C). It has been shown and postulated that the protein concentration influenced the enzyme activity and the interconversion of quaternary structure of PEPC in the C₄ and CAM (crassulacean acid metabolism) plants, and that the high concentration of the enzyme induced the formation and maintenance of more active tetrameric structure while the dilution induced the less active dimeric formation in these plants [87-89]. The elevated thermostability at higher concentration of *R. obamensis* PEPC may be caused by the interconversion of the quaternary structure and suggested that the intrinsic thermostability of the enzyme strongly depended on the formation and maintenance of the tetrameric structure.

Recently, there has been increasing interest in thermophilic organisms and their thermostable biochemical molecules associated with the findings of their extraordinary habitats [2, 3, 8, 9]. Accordingly, an increasing number of thermophilic enzymes have been studied by the comparison of amino acid sequences between thermophilic and mesophilic homologous proteins [28, 29], the analyses of protein foldings [30], and the structural studies of the proteins including the three dimensional structures [35, 36]. Another approach to the mechanism of protein thermostability is to explore the extrinsic factors that lie not in the protein itself but out of it, and might sustain it under high temperature. In fact, there have been discovered possible extrinsic thermostabilization mechanisms in various thermophiles [37-39]. The thermostabilization of the allosteric enzymes by the positive effectors is likely to be one of such mechanisms [90]. Taguchi *et al.* reported that fructose 1,6-bisphosphate stabilized L-lactate dehydrogenase (LDH) of *Thermus caldophilus* GK24 toward heat and that the stabilization might reflect the stabilization of the tetrameric form [90]. Likewise, in this study, PEPC of *R. obamensis* was strongly stabilized by the positive effector of acetyl-CoA (Fig. 11). However, the enzyme was not remarkably stabilized by fructose 1,6-bisphosphate which is another positive effector and destabilized by the negative effectors (Fig. 11). These results suggested that the allosteric effectors with affinities to the enzyme had effects not only on the enzyme activity but on the enzyme stability. In the case of the LDH of *T. caldophilus* GK24, it has been suggested that the binding of fructose 1,6-bisphosphate enlarges the substrate binding pocket and strengthened the subunit-subunit hydrophobic interaction [91]. Although *T. caldophilus* LDH is smaller than *R. obamensis* PEPC, both enzymes are similar in many points; allosteric property, homotetrameric structure, and enhanced thermostability by positive effector [90]. Hence, one of the possible explanations of the enhanced thermostability of *R. obamensis* PEPC may be the enhanced subunit-subunit hydrophobic interaction by the binding of acetyl-CoA to the enzyme.

Table 6. The comparison of enzymological properties in various PEPCs from the three domains of organisms

STRAIN	Bacteria	Archaea	Archaea	Bacteria	Eucarya
PROPERTIES	<i>R. obamensis</i>	<i>S. acidocaldarius</i>	<i>M. sociabilis</i>	<i>E. coli</i>	<i>Z. mays</i>
Molecular mass	400kDa	260kDa	240kDa	360kDa	400kDa
Subunit	Homotetramer	Homotetramer	Homotetramer	Homotetramer	Homotetramer
Optimum temp. for activity	75°C	90°C	85°C	35-38°C	40°C
Optimum pH for activity	8.0	8.0	8.5	7.5	7.5-8.0
K _{PEP} value	~20mM	~0.1mM	1.3mM	~20mM	~0.1mM
Positive effectors	Acetyl-CoA, Fructose 1,6-bisphosphate	-	-	Acetyl-CoA, Fructose 1,6-bisphosphate, Fatty acids, etc.	Glucose 6-phosphate
Negative effectors	L-Asparatate, L-Malate	L-Asparatate, L-Malate	-	L-Asparatate, L-Malate	L-Malate

R. obamensis PEPC was also stabilized by the substrate, cofactor and various salts (Table 4 and Fig. 11A). The presence of PEP or MgSO₄ significantly decreased the thermoinactivation rates of the enzyme. This implied that the substrate and cofactor as well as the allosteric effectors were possible thermostabilization factors of the enzyme. It was acceptable that the binding of the substrate and cofactor altered the enzyme conformation to the active state and the active conformation was more stable than the native one. Moreover, the thermostabilization by various salts and the variation of the effectiveness led us not only to recognize the contribution of salts as a important thermostabilization factor, but to expect a part of mechanism for the intrinsic thermostability of *R. obamensis* PEPC. As seen in Table 4, the thermostabilization effects increased in proportion to the concentrations for the monovalent cations and anions. In contrast, the effects decreased in proportion to the concentrations for divalent cations. As regards the divalent cations, Mg²⁺ or Mn²⁺ was the cofactor of the enzyme and necessary for the enzyme activity, nevertheless it was shown that the excess amount of these ions inhibited the enzyme activity (Fig. 8). Therefore, the excess amount of the divalent cations were expected to cause some harmful problems on the enzyme activity and stability. On the other hand, the

thermostabilization by the monovalent cations and anions were thought to result from a different interaction from that by the divalent cations. In the stability study on maize leaf PEPC, Jansen *et al.* reported that the enzyme was stabilized by kosmotropic (water structuring) anions such as HPO₄²⁻ and SO₄²⁻, and suggested that the stabilization effect was attributed to the promotion of the intersubunit hydrophobic interaction due to solvent-mediated effects of these anions [92]. This suggestion was conducted by the concept of the solvophobic theory that the water-structuring effectiveness of these anions with high charge densities elevates the surface tension of the solvent, which subsequently increases the free energy of cavity formation in the protein surface area, and as the result, the increment of the cavity free energy will induce stronger intersubunit hydrophobic interactions [93-95]. However no apparent correlation with the theory was found between the stabilization of the maize PEPC and the water-structuring series of cations[92]. In *R. obamensis* PEPC, the thermostabilization effect was in the order Na⁺ > K⁺ > NH₄⁺ for the monovalent cations, or in the order SO₄²⁻ > HPO₄²⁻ > Cl⁻ > NO₃⁻ for the anions, which were in good agreement with the order of water-structuring effectiveness [81, 82]. Moreover, the thermostabilization effectiveness were consistent with the increased concentrations of these ions. These results indicated that the ions with high water-structuring effectiveness and the increased concentrations of such ions had stronger effect in enhancing the enzyme thermostability and suggested that the enhanced thermostability by the salts of monovalent cations and anions was from the stronger intersubunit hydrophobic interactions induced by the surface tension of the solvent and the cavity free energy of protein surface, resulting in the maintenance of the tetrameric structure of the enzyme.

On the basis of the results presented herein, I propose that the substrate (PEP), cofactor (Mg²⁺), allosteric effector (acetyl-CoA), and salts (e.g. Na₂SO₄) are possible extrinsic thermostabilization factors. In general, these substances are constitutional components of bacterial cells, and PEP, Mg²⁺, and acetyl-CoA are essential to PEPC activity or its regulation. In this study, *R. obamensis* PEPC was shown to be extremely thermostable in itself (Fig. 10), but it was also shown that the thermostability of the enzyme was considerably increased by these substances. Therefore, I came to a conclusion that the thermostability of *R. obamensis* PEPC *in vivo* might be sustained due to the extrinsic mechanisms in addition to the intrinsic thermostability. In order to determine the function and interaction of these factors, the combined effect of the extrinsic thermostabilization factors was investigated at high temperatures where the enzyme was rapidly inactivated (Table 5).

When the *R. obamensis* PEPC was incubated with each of the extrinsic thermostabilization factors at 95 °C, the thermo-stabilization effect was in the order acetyl-CoA > Na₂SO₄ > MgSO₄ > PEP (Table 5). The order of effectiveness was the same at all temperatures tested and acetyl-CoA appeared to be the most effective factor for the enzyme thermo-stabilization. Furthermore, when the various combinations of the factors were added to the enzyme solution, the effects were significantly increased and additive of the individual effects. These results strongly suggested that each of the factors noncompetitively interacted with the enzyme and enhanced the thermostability of PEPC without interference among themselves on the thermostabilization of the enzyme. The combined thermostabilization effect by these factors was quite strong and dominant at high temperatures above the optimum range for activity. The extrinsic thermostabilization mechanism proposed in this study can give new insight into elucidating the thermostability of the proteins from thermophiles. In addition, it was suggested through this study that the thermostability of *R. obamensis* PEPC and the thermostabilization effect were strongly associated with the maintenance of the tetrameric form of PEPC. In order to determine how the intrinsic thermostability of the enzyme is established and how the extrinsic thermostabilization mechanism work on, the structural approach for the thermostability and the molecular basis of the extrinsic thermostabilization mechanism are essential. The study of the folding or conformation in the enzyme in relation to the extrinsic thermostabilization factors and the gene cloning and expression for the three dimensional structure of the enzyme are described in following chapters. These attempts might shed light on the understanding of both intrinsic and extrinsic thermostabilization mechanisms in *R. obamensis* PEPC.

Chapter 4

Extrinsic Thermostabilization Factors and Thermodenaturation of Phosphoenolpyruvate Carboxylase (PEPC) from an Extreme Thermophile *Rhodothermus obamensis* OKD7.

1. Introduction

In Chapter 3, I mentioned the purification and characterization of an extremely thermostable PEPC from the newly isolated extreme thermophile *Rhodothermus obamensis* [78, Chapter 2] and found that the molecular and enzymological characteristics of the enzyme were similar to those of bacterial entities. I also found the enhanced thermostability of the enzyme by the substrate, cofactor, salts and positive allosteric effectors, and concluded that these substances might play an important role *in vivo* as extrinsic thermostabilization factors to protect the denaturation of the enzyme in addition to the intrinsic thermostabilization [96, Chapter 3].

In several studies of plant PEPCs, it has been shown and suggested that the stability of the enzymes is strongly associated with the maintenance of the multimeric structure and that the dissociated monomeric or dimeric structure tends to lose the enzyme activity and form the aggregated structure [87-89]. Therefore, it was expected that the dissociation of the quaternary structure was strongly involved in the thermostability of *R. obamensis* PEPC. Based on the effectiveness of enzyme concentration and various kinds of salts on the thermostability, it was speculated that the thermostability of the enzyme was to large extent dependent on the maintenance of tetrameric form [96, Chapter 3]. However, I could not have evidence enough to prove the speculation and exclude another aspect. In addition, the subsequent thermodenaturation to the dissociation of the multimeric structure and the interaction of the extrinsic thermostabilization factors to the structural change remain unknown.

In this chapter, therefore, I sought to determine the thermodenaturation of *R. obamensis* PEPC with focus on the structural transition. I examined the enzyme activity, the electrophoretical pattern, the UV-visible absorption spectra, Trp fluorescence emission spectra and 1-anilinonaphthalene-8-

sulfonate (ANS) bindings to the enzyme during the denaturation at different temperatures. I also examined the renaturation capability of the enzyme from the different states of denaturation and the effect of the extrinsic thermostabilization factors on the thermodenaturation. The understanding of the thermodenaturation is expected to give an important clue to elucidate the mechanisms of the thermostability. The function and interaction of the extrinsic factors to the enzyme thermostability are also discussed.

2. Materials and Methods

Bacterial strains and growth conditions. The bacterial strain used in this study was *Rhodothermus obamensis* OKD7 (JCM 9785) isolated from a shallow marine hydrothermal vent at Tachibana Bay, Nagasaki Prefecture, Japan [78, Chapter 2]. For cultivation of *R. obamensis*, the Jx medium was used [78, Chapter 2]. *R. obamensis* was grown at 76 °C and harvested in the late exponential growth phase. Cell pellet was freeze-dried at -90 °C prior to enzyme purification.

Enzyme assays. PEPC activity was routinely coupled to the malate dehydrogenase (MDH) reaction and dually assayed as described in Chapter 3. In an attempt to examine the thermostability of the enzyme, a concentration of enzyme solution (9 µgPEPC/ml) containing 50 mM Tris-HCl (pH 8.0) and 10% (vol/vol) of glycerol was usually incubated at various temperatures (80, 93 or 100 °C) for different periods of time. Then, the thermoinactivation was stopped by cooling the aliquots on ice and the residual PEPC activity was measured at 75 °C under standard assay condition [78, Chapter 3]. The effects of the extrinsic factors on thermostability were also examined. In these experiments, thermoinactivations were performed with the incubation buffer (50 mM Tris-HCl, pH 8.0 and 10% of glycerol) containing a concentration of factor each (5 mM for phosphoenolpyruvate; PEP, 0.5 mM for MgSO₄, 50 mM for Na₂SO₄, 1 mM for acetyl-CoA) or combined. In all cases, residual activity after thermoinactivation was exhibited as relative to the enzyme activity in the same condition before the thermoinactivation. Thermoinactivation rate (I) was calculated by $I = \ln dR/dT$, dR ; change of residual activity (%), dT ; change of time (min), and thermostabilization effect was exhibited as (thermoinactivation rate without a factor at a temperature) / (thermoinactivation rate with a factor at the same temperature).

Preparation of the purified enzyme. The purification of *R. obamensis* PEPC was completed by following steps of columns, DEAE-cellulose DE 52 (Whatman, Kent, UK), Phenyl-Sepharose 6FF (Pharmacia), FPLC-MonoQ (Pharmacia) and FPLC-Superdex 200HR (Pharmacia) as

described in Chapter 3. The purified enzyme to electrophoretic homogeneity was dialyzed with 50 mM Tris-HCl containing 10% (vol/vol) glycerol and stored in the liquid nitrogen prior to the experiments.

Electrophoretic analysis. The polyacrylamide gel electrophoresis of the non-denatured enzyme or the different stages of enzymes during the thermodenaturation were performed with 7.5% (wt/vol) polyacrylamide gel in the absence of sodium dodecylsulfate (SDS) to examine the change of quaternary structure or with 10% (wt/vol) polyacrylamide gel in the presence of SDS in order to check the covalent changes such as hydrolysis of the subunit by the method of Laemmli [79]. In addition, another possible covalent changes such as deamidation of Asn or Gln residue were examined by the urea-denatured isoelectrofocusing (IEF) electrophoresis using immobilized IEF-PAGE plate (pH range 3-10.5) (Pharmacia). The detail procedure of IEF-PAGE was described in the manufacturer's manual (Pharmacia). The proteins after electrophoresis were stained by Coomassie Brilliant Blue (CBB) R-250 or silver stain kit (Bio-Rad). In the SDS-PAGE, the intensity of each monomeric subunit stained by CBB was measured using the UltroScan XL laser densitometer (Pharmacia) and expressed as the integral optical density (IOD). Molecular weight markers for SDS-PAGE was from Bio-Rad. Protein concentrations were routinely estimated by Bradford [80] with bovine serum albumin as the standard.

The measurement of UV-visible absorption spectra. The samples for the measurement of UV-visible absorption spectra were prepared in the same way as the samples for the measurement of enzyme activity during the thermodenaturation described above. The enzyme (9 µgPEPC/ml) in the incubation buffer (50 mM Tris-HCl, pH 8.0 containing 10% of glycerol) was treated at 80, 93 or 100 °C for the different periods of time and cooled on ice, and then concentrated 4-fold by the centrifugal filtration using ULTRAFREE-MC 10,000 NMWL filter (Millipore, Bedford, MA). The UV-visible absorption spectrum of each concentrated sample was recorded at room temperature with Shimadzu UV 160A UV-visible recording spectrophotometer. The spectra were usually obtained with a 1 cm quartz cuvette at a concentration of 36 µgPEPC/ml in the incubation buffer but when appropriate, in the incubation buffer containing 5 mM PEP, 0.5 mM MgSO₄, 50 mM Na₂SO₄ or 1 mM acetyl-CoA.

The measurement of Trp fluorescence emission spectra. The samples for this experiment were prepared in the same way as the samples for the measurement of UV-visible absorption spectra except for no concentration step of the incubated enzyme. Trp fluorescence emission spectrum of each sample was recorded at room temperature with Shimadzu RF-1500

recording spectrofluorophotometer. The sample was excited at 280 nm and the emission spectrum was measured in the range of between 300 and 400 nm. The spectra were usually obtained with 1 cm quartz cuvette at a concentration of 9 $\mu\text{gPEPC/ml}$ in the incubation buffer but when appropriate, in the incubation buffer containing 5 mM PEP, 0.5 mM MgSO_4 , 50 mM Na_2SO_4 or 1 mM acetyl-CoA.

The measurement of ANS emission spectra. The enzyme (9 $\mu\text{gPEPC/ml}$) in the incubation buffer (50 mM Tris-HCl, pH 8.0 containing 10% of glycerol) was treated at 80, 93 or 100 °C for the different periods of time and cooled on ice. Immediately, ANS solution (2 μM of ANS in the incubation buffer) was added to the aliquots at a final concentration of 1 μM ANS. After the incubation of the sample at 4 °C for 5 h, the ANS emission of each sample was recorded at room temperature with Shimadzu RF-1500 recording spectrofluorophotometer. The excitation wavelength for the ANS emission spectrum was 350 nm and the emission spectrum was measured between 400 and 600 nm. The spectra were usually measured with 1 cm quartz cuvette at a concentration of 4.5 $\mu\text{gPEPC/ml}$ in the 1 μM of ANS solution but when appropriate, in the solution containing 5 mM PEP, 0.5 mM MgSO_4 , 50 mM Na_2SO_4 or 1 mM acetyl-CoA.

The renaturation analysis. The thermodenaturation was performed at 80, 93 or 100 °C for different periods of time in the incubation buffer (50 mM Tris-HCl, pH 8.0 containing 10% of glycerol) at a concentration of 9 $\mu\text{gPEPC/ml}$. The denaturation was stopped by cooling the aliquots on ice and the aliquots were incubated on ice for 30 min. The renaturation was initiated by transferring the aliquots from ice to water bath at 45 °C and periodically monitored by the enzyme activity. In an attempt to examine the effect of the extrinsic thermostabilization factors on the renaturation of the enzyme, the renaturation was performed in the absence or presence of 5 mM PEP, 0.5 mM MgSO_4 , 50 mM Na_2SO_4 , 1 mM acetyl-CoA, respectively or all.

3. Results

Thermostability of *R. obamensis* PEPC. PEPC purified from extreme thermophile *R. obamensis* was extremely thermostable as shown in Fig. 10A. No loss of activity was observed after the incubation for 2 h at 85 °C (Fig. 10A). The times required for 50% loss of activity were about 26 h at 80 °C, 11 h at 85 °C, 240 min at 90 °C, 60 min at 91 °C and 10 min at 93 °C, respectively (Fig. 10A). In comparison of short-time thermoinactivation at different temperatures, there were observed sharp changes around 90 °C in the residual activity after the thermodenaturation for 30 min and the

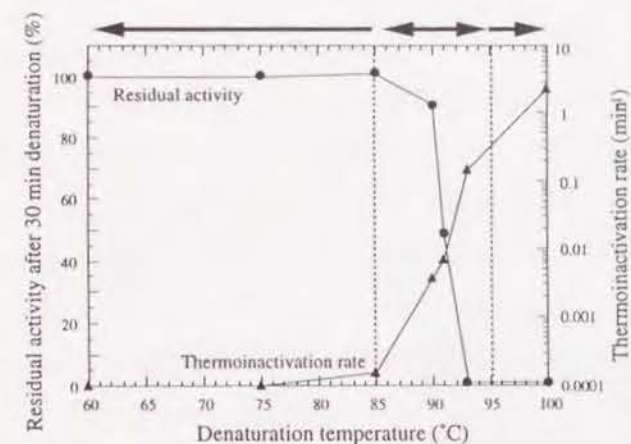


Fig. 12. The effect of the temperatures on the thermodenaturation of *R. obamensis* PEPC. The residual activity was measured after the incubation for 30 min at various temperatures and the thermoinactivation rates were calculated as describe in Materials and Methods. The bold arrows indicated the three temperature ranges in which the enzyme might be denatured in different manners.

thermoinactivation rate (Fig. 12). These results suggested that the different incubation temperatures led the enzyme to the temperature-dependent thermodenaturation and that there might exist at least three distinct patterns (below 85 °C, around 90 °C and above 95 °C) in the thermodenaturation of this enzyme. Therefore, all further experiments on the thermodenaturation are performed at three different denaturation temperatures at 80, 93 or 100 °C.

The effects of thermostabilization factors on the thermostability were also examined. The thermostabilization effect of each factor at 95 °C was shown in Table 5. As described in Chapter 3, the effectiveness of the factors was in the order acetyl-CoA > Na_2SO_4 > MgSO_4 > PEP and the effect was additive when the factors were combined (Table 5).

Electrophoretical analyses. The structural and covalent changes of the enzyme during the thermodenaturation were determined by the native polyacrylamide gel electrophoresis (native-PAGE), sodium dodecylsulfate-PAGE (SDS-PAGE) and denatured isoelectrofocusing-PAGE (IEF-PAGE). In the native-PAGE, the non-denature enzyme exhibited three major bands (Fig. 13). The upper major band and the middle one appeared to correspond a tetrameric form and dimeric form since the enzyme activity was found in those positions from the gel slice cut every 1 mm (Fig. 13). The lower band was not identified by the enzyme activity but likely to be a monomeric form because the sample was highly purified and showed a single band in SDS-PAGE (Fig. 14A). During the denaturation at 80 °C, although the putative monomeric form decreased in the native-PAGE, no apparent change of other structures was seen after 30 h incubation in all electrophoresis (Figs. 13, 14A). However, under the denaturation at higher temperatures, the tetrameric and dimeric forms decreased according to the incubation time and disappeared after 5 min incubation at 100 °C in the native-PAGE (Fig. 13). In addition, the covalent change of the monomeric subunit was found in the SDS-PAGE under severe denaturation. The enzyme consistently exhibited a 100 kDa of single band during the denaturation but

the amount of the subunit was reduced in proportion to the incubation time from the integrated optical density (IOD) of each band (Fig. 14A, B).

The extrinsic thermostabilization factors had effects on the maintenance of quaternary structure and monomeric form toward the structural and covalently change during the denaturation at 93 °C for 30 min (Figs. 13, 14A, B). In the presence of the factors, the electrophoretic patterns before the denaturation and after 30 min denaturation at 93 °C were almost identical. Of these factors, the presence of PEP strongly sustained the tetrameric and dimeric structure of the enzyme (Fig. 13). In the urea-denatured IEF-PAGE, all sample showed a single band of the subunit at pI 6.7 and no significant change of electrophoretic pattern was found regardless of the denaturation temperatures or the presence of factors.

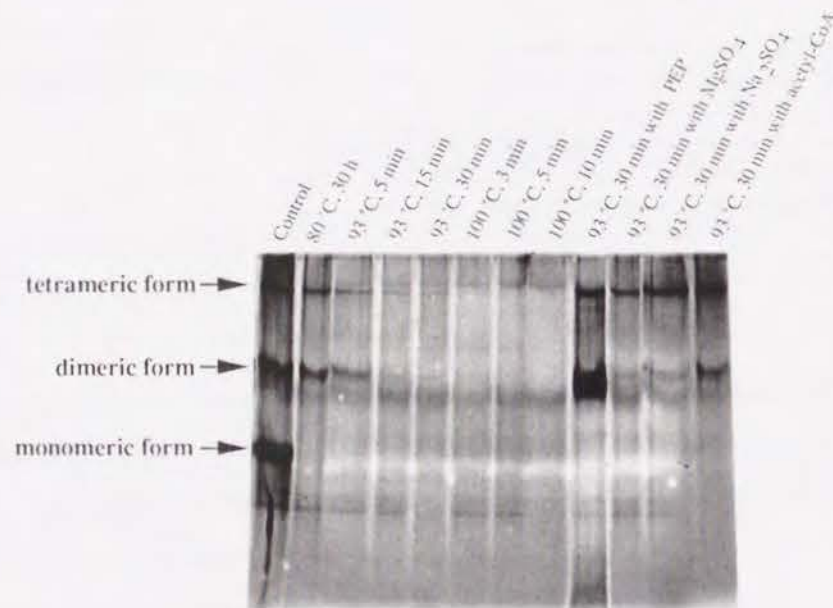


Fig. 13. Native-PAGE analysis of the enzyme during the thermodenaturation. The same amount of enzyme (1 µg) incubated at various temperatures for several periods of time was loaded on 7.5% (wt/vol) PAGE and then silver-stained. In order to check the different forms of PEPC, the non-denatured enzyme was loaded in two lanes. The one was silver-stained and the other was sliced every 1 mm from top to bottom. The enzyme activity was measured with respect to each fraction electrophoretically eluted from the gel. The active fractions were thought to correspond to the tetrameric and dimeric form. The monomeric forms was expected from the relative molecular size. The reproductivity of the electrophoretic patterns was confirmed at least three times.

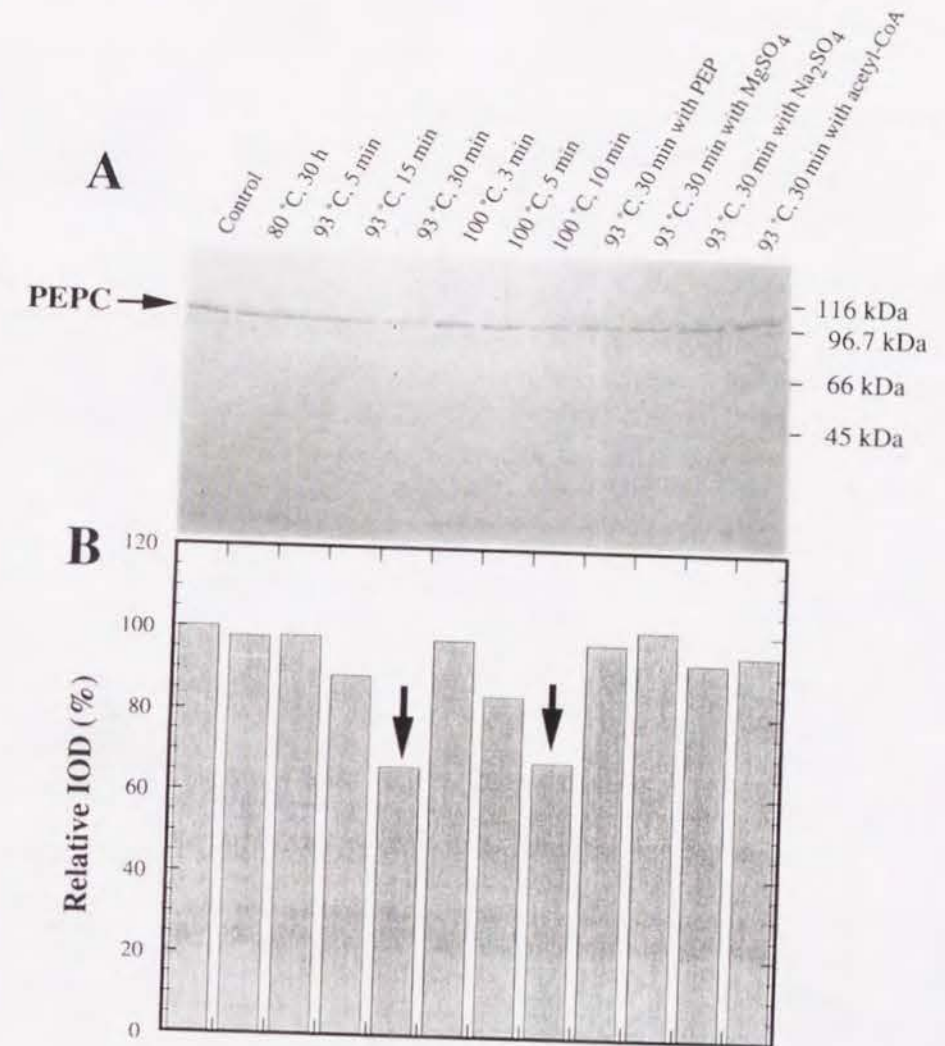


Fig. 14. SDS-PAGE analysis of the enzyme during the thermodenaturation and the integral optical density (IOD) of the stained gel. (A) the same amount of enzyme (2 µg) incubated at various temperatures for several periods of time was loaded on 10% (wt/vol) SDS-PAGE and then stained by Coomassie brilliant blue (CBB) R-250. Each lane exhibited the single band at 100 kDa of molecular mass. (B) the stained gel was dried with cellophane sheets and the IOD of the gel was measured using the UltroScan XL laser densitometer (Pharmacia). The IOD of the non-denatured enzyme was set to 100. The reproductivity was confirmed at least three times.

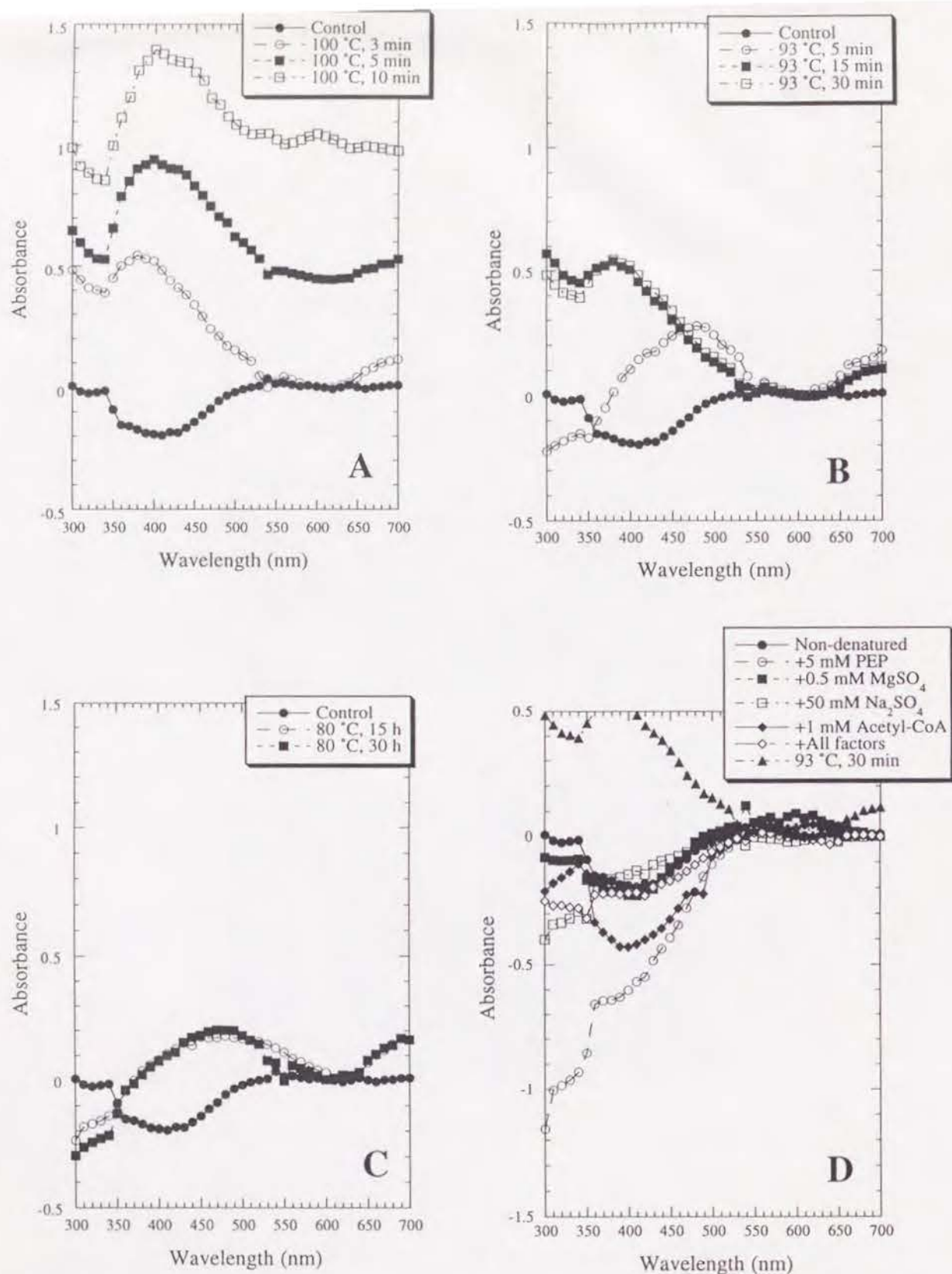


Fig. 15. The UV-visible absorption spectra of the enzyme denatured at 100 °C (A), 93 °C (B) and 80 °C (C). The enzyme (9 µgPEPC/ml) in the Tris-HCl (pH 8.0) containing 10% (wt/vol) glycerol was incubated for several periods of time at each temperature and cooled on ice, and then concentrated 4-fold by the centrifugal filtration. Then the spectrum of the concentrated sample was measured at room temperature with the spectrophotometer. In an attempt to examine the effect of the extrinsic thermostabilization factors, the spectra were measured under the denaturation at 93 °C for 30 min in the presence or absence of the factors (D). No apparent change was found in the spectra with the factors between before and after the thermodenaturation. All the spectra were contracted with the spectra of the incubation solution without the enzyme.

UV-visible absorption. The UV-visible absorption spectra of *R. obamensis* PEPC were measured under different thermodenaturation temperatures (Fig. 15). At a temperature of 100 °C, the spectra changed largely and rapidly (Fig. 15A). During the denaturation at 100 °C, the values both in the UV and visible range of wavelength increased and especially the absorption signal at 420 nm was strongly enhanced (Fig. 15A). The similar change was observed in the denaturation at 93 °C and the spectra after the denaturation at 93 °C for 15 and 30 min were quite similar to that after the denaturation at 100 °C for 2 min (Fig. 15B). At 80 °C, there were observed the smaller changes of the spectra after 30 h denaturation that were equivalent to the change of 5 min denaturation at 93 °C (Fig. 15C). These spectra observed in this experiment were generally classified into three representative patterns; the spectra showing high absorption in both the UV and visible range (e.g. that of 100 °C, 5 or 10 min), the spectra showing elevated absorption in the UV range (e.g. that of 93 °C, 15 or 30 min) and the spectra with small change in the range between 350 and 550 nm (e.g. that of 80 °C, 15 or 30 h).

All the extrinsic thermostabilization factors had ability to protect the change of the UV-visible absorption spectra during the denaturation at 93 °C (Fig. 15D). There was no significant change between the spectra before the denaturation and after 30 min denaturation at 93 °C with factors (Fig. 15D). The way for the protection were different among the factors. MgSO₄ and Na₂SO₄ maintained the spectrum of non-denatured enzyme even after 30 min, while PEP and acetyl-CoA resulted in the different spectra from that of native enzyme (Fig. 15D).

Trp fluorescence emission. The Trp fluorescence emission spectra of *R. obamensis* PEPC were measured during the thermodenaturation at different temperatures. At all denaturation temperatures tested, the enzyme demonstrated a transition of the spectra during the denaturation that the peak signal at 335 nm increased in the early phase of the denaturation and then decreased according to the incubation time (Fig. 16A, B, C). When the further denaturation occurred, the signal was weakened below the level of the non-denatured enzyme (Fig. 16A, B, C). These changes of the Trp fluorescence emission spectra were likely dependent of the incubation time rather than the incubation temperature and hardly associated with the changes of UV-visible absorption spectra.

In the presence of some extrinsic thermostabilization factors such as MgSO₄ or Na₂SO₄, the enzyme exhibited different curve of spectra (Fig. 16D). Although there was no significant change between the spectra before the denaturation and after 30 min denaturation at 93 °C with factors, the signal around 300 nm was enhanced with MgSO₄ or Na₂SO₄ (Fig. 16D). When the enzyme was incubated with all factors, the Trp fluorescence emission spectrum was significantly altered and

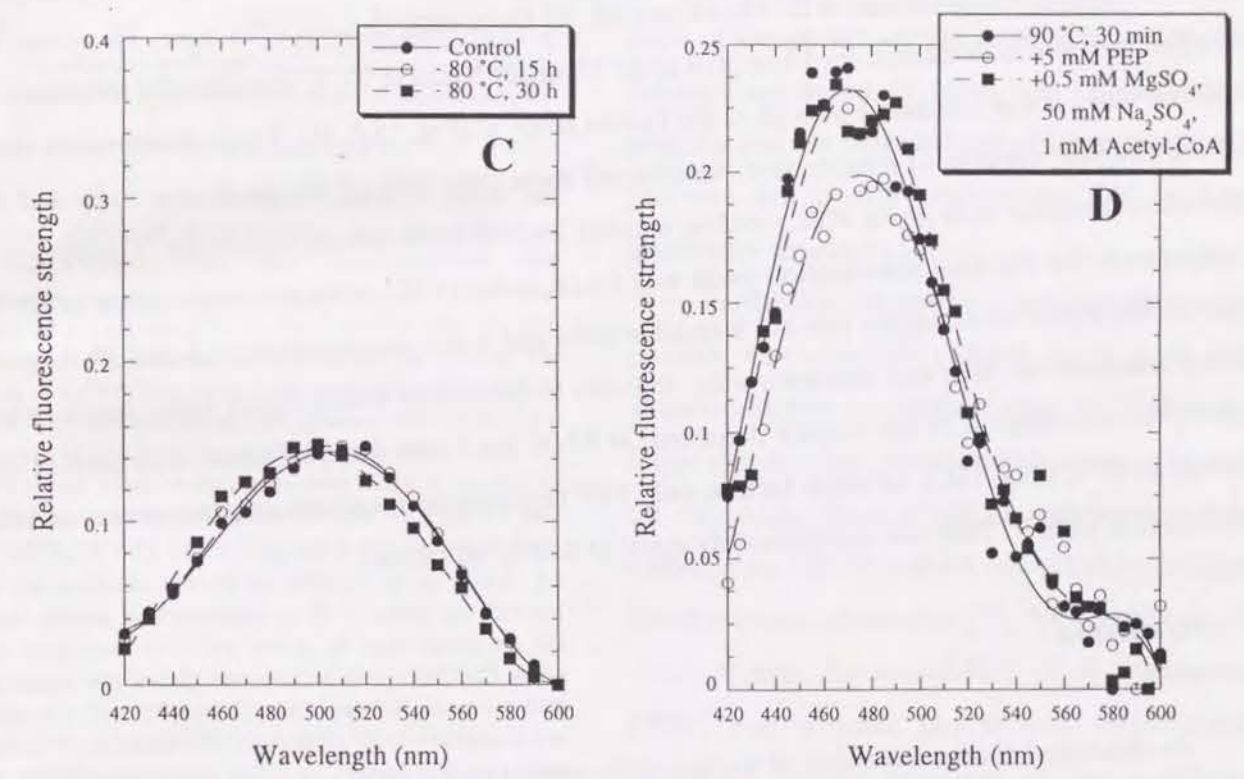
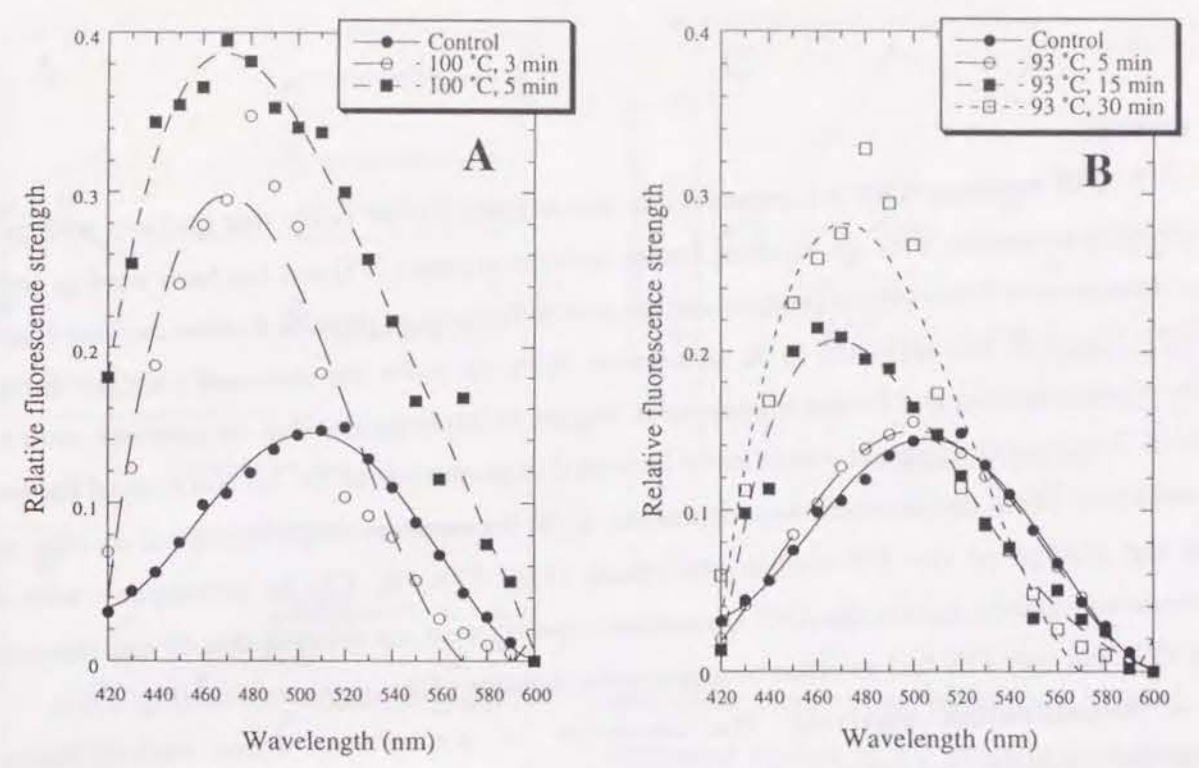
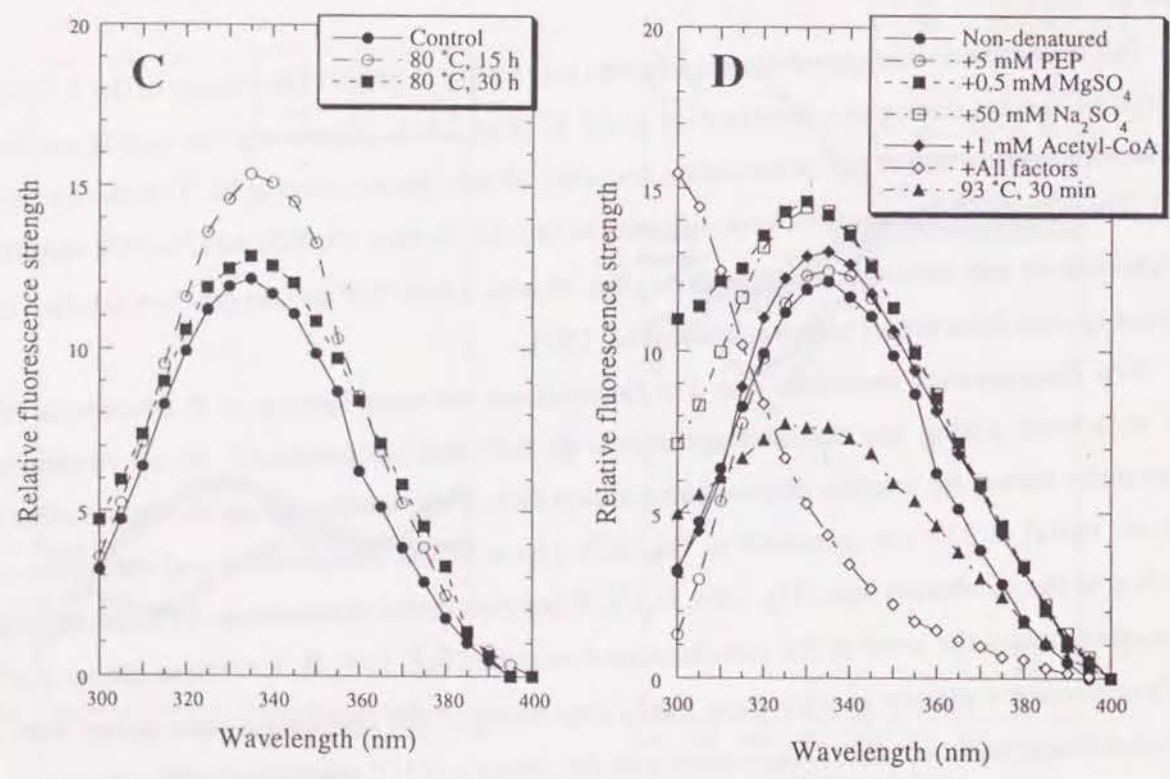
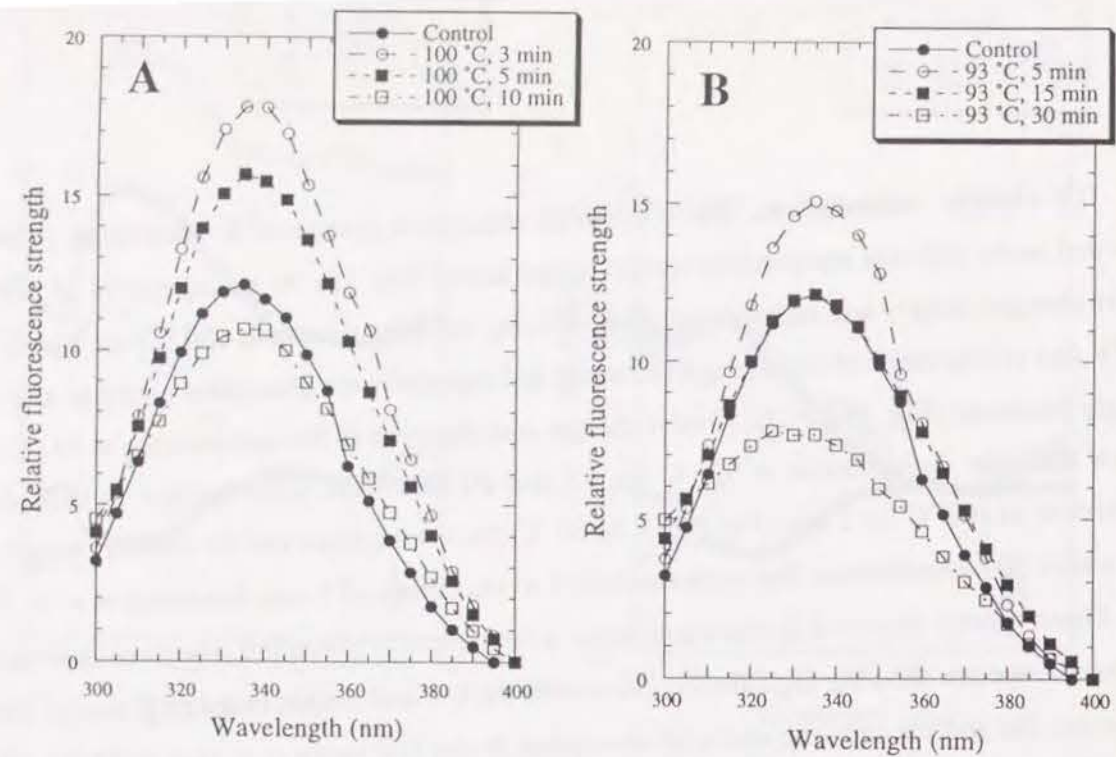


Fig. 16. The Trp fluorescence emission spectra of the enzyme denatured at 100 °C (A), 93 °C (B) and 80 °C (C). The enzyme (9 µgPEPC/ml) in the Tris-HCl (pH 8.0) containing 10% (wt/vol) glycerol was incubated for several periods of time at each temperature, and cooled on ice. Then the spectrum of the sample was measured at room temperature with the spectrofluorophotometer. In an attempt to examine the effect of the extrinsic thermostabilization factors, the spectra were measured under the denaturation at 93 °C for 30 min in the presence or absence of the factors (D). No apparent change was found in the spectra with each factor but the spectrum with all factors was unsettled at every experiment. All the spectra were contracted with the spectra of the incubation solution without the enzyme.

Fig. 17. The ANS fluorescence emission spectra of the enzyme denatured at 100 °C (A), 93 °C (B) and 80 °C (C). The enzyme (9 µgPEPC/ml) in the Tris-HCl (pH 8.0) containing 10% (wt/vol) glycerol was incubated for several periods of time at each temperature, and cooled on ice. Then ANS was added to the incubation solution at a final concentration of 0.1 µM. After 4 h of incubation at 4 °C, the spectrum of the solution with ANS was measured at room temperature with the spectrofluorophotometer. In an attempt to examine the effect of the extrinsic thermostabilization factors, the spectra were measured under the denaturation at 93 °C for 30 min in the presence or absence of the factors (D). No apparent change was found in the spectra with the factors between before and after the thermodenaturation. All the spectra were contracted with the spectra of the incubation solution without the enzyme.

unsettled.

ANS binding. ANS is a polycyclic aromatic fluorescence probe that interacts with proteins whose hydrophobic sites are, to some extent, solvent-exposed [97] and has been used to probe the molten globular states [98] of proteins and the overall foldings of proteins at some extreme conditions [99]. I applied this approach to *R. obamensis* PEPC to probe the structural changes during the thermodenaturation at different temperatures. Figure 16 demonstrates that the quantum yield for the ANS fluorescence emission dramatically increased in proportion as the denaturation of the enzyme developed. These enhancement were dependent of the denaturation temperatures and strongly related to the change of the UV-visible absorption (Fig. 17A, B, C). In accompany with three thermostabilization factors, the ANS-fluorescence spectra were not affected after 30 min denaturation at 93 °C but only PEP had an effect to suppress the increase of the quantum yield (Fig. 17D).

Renaturation analysis. The capability of renaturation from various states of thermodenaturation was tested. In the absence of the extrinsic thermostabilization factors, the enzyme demonstrated no renaturation at 5, 25, 45 and 65 °C from each denaturation state. However, the enzyme which was denatured for 15 or 30 h at 80 °C, or for 5 min at 93 °C dramatically recovered its activity when it was incubated with all of the factors at 45 °C (Fig. 18A, B). These denaturation states of the enzyme, capable of renaturation, maintained more than 40% of the residual activity and the denatured enzyme with no or little residual activity lost the renaturation capability. The optimum temperature for the final renaturation yield was found to be 45 °C. A higher temperature of 65 °C provided a higher renaturation rate but a smaller yield and lower temperatures of 5 and 25 °C gave lower renaturation rates and smaller yields. In order to determine which factor had a renaturation effect, the renaturation of the enzyme denatured at 93 °C for 5 min was performed with each of the factors at 45 °C (Fig. 18C). Of these factors, only PEP revealed the renaturation effectiveness and the renaturation yield by PEP was approximately equal to that by all factors.

4. Discussion

As described above, a number of thermophilic proteins have been extensively studied due to their unusual thermostability [2-4, 10-12]. The central interest is how the thermophilic proteins maintain their active foldings or structures at high temperature and hence their intrinsic mechanisms of thermostability have been probed by the comparison of amino acid sequences between thermophilic and mesophilic homologous proteins [28, 29], the analyses of protein foldings [30, 99], the

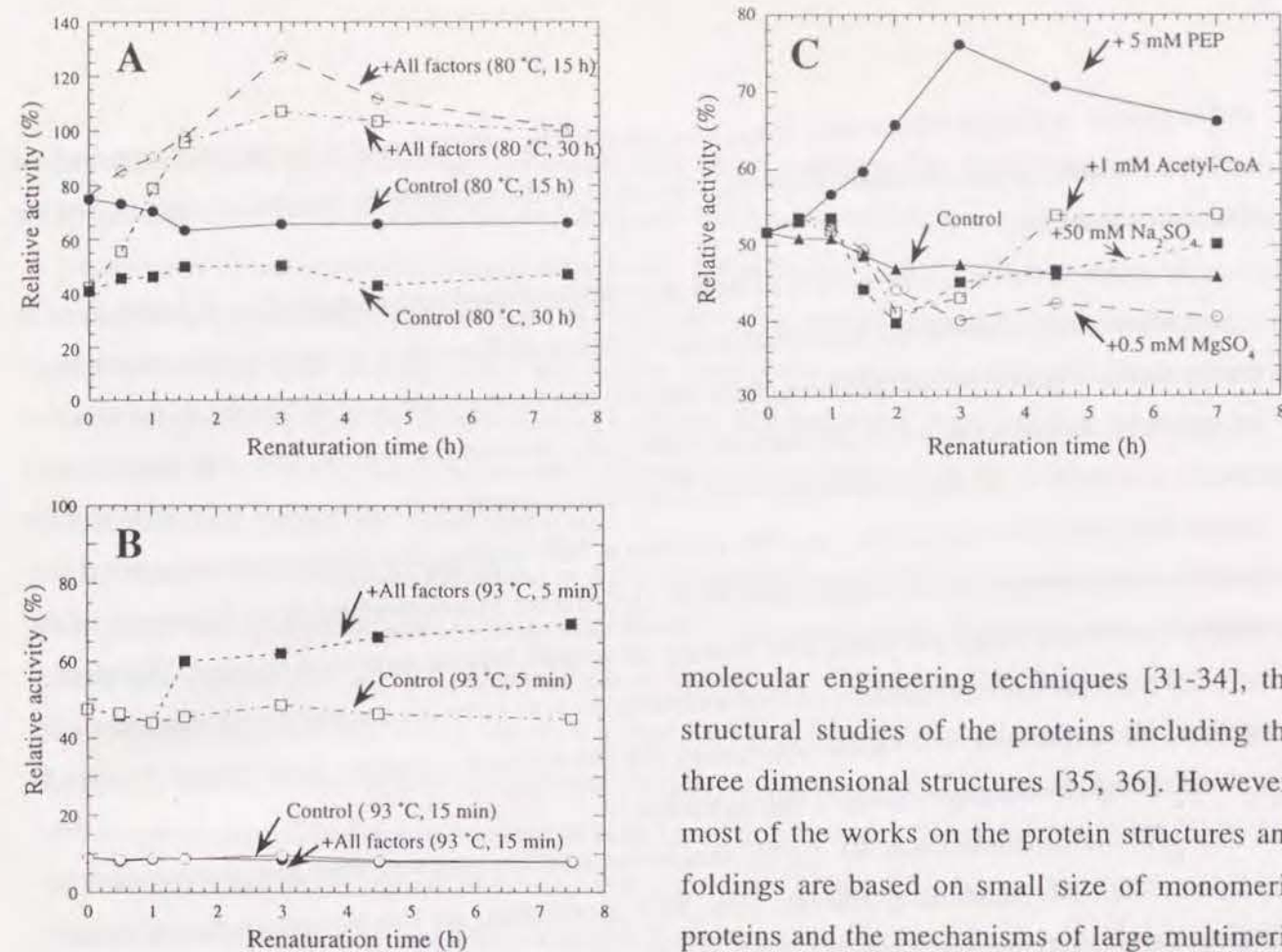


Fig. 18. The renaturation analysis from the different states of denaturation and the effect of extrinsic factor on the renaturation. The renaturation capability of the enzyme denatured at 80 °C for 15 and 30 h (A), or at 93 °C for 5 and 15 min (B) was examined in the presence or absence of the factors. The enzyme (9 µgPEPC/ml) in the incubation buffer (50 mM Tris-Tris-HCl, pH 8.0 containing 10% glycerol) was incubated at 80 °C for 15 and 30 h, or at 93 °C for 5 and 15 min, and cooled on ice. Then all the factors were added to the enzyme solution at a final concentration of 5 mM for PEP, 0.5 mM for MgSO₄, 50 mM for Na₂SO₄ and 1 mM for acetyl-CoA. After the incubation at 45 °C for different periods of time, the enzyme activity was measured at 75 °C under the standard assay condition. (C) The effect of each factor on the renaturation was tested. The enzyme (9 µgPEPC/ml) in the incubation buffer (50 mM Tris-HCl, pH 8.0 containing 10% glycerol) was incubated for 5 min at 93 °C, and cooled on ice. Each of the factors was added to the solution at a final concentration of 5 mM for PEP, 0.5 mM for MgSO₄, 50 mM for Na₂SO₄ or 1 mM for acetyl-CoA, respectively. After the incubation at 45 °C for different periods of time, the enzyme activity was measured at 75 °C under the standard assay condition.

molecular engineering techniques [31-34], the structural studies of the proteins including the three dimensional structures [35, 36]. However, most of the works on the protein structures and foldings are based on small size of monomeric proteins and the mechanisms of large multimeric proteins are poorly understood due to their quaternary structures.

In addition, the extrinsic mechanisms for the protein thermostability have been paid less attention to than the intrinsic ones. In Chapter 3, I found the extrinsic thermostabilization system in the extremely thermostable phosphoenolpyruvate carboxylase (PEPC) from the recently isolated *Rhodothermus obamensis* [78, 96, Chapters 2, 3]. The intrinsic thermostability of *R. obamensis* PEPC was notable but it was significantly enhanced in the presence of the substrate, cofactor, salts and allosteric effectors [96, Chapter 3]. These substances were assumed to be the extrinsic thermostabilization factors to the enzyme

and to play an important role *in vivo*. Here, I focused on the interaction of these factors to the enzyme and their function in the thermostabilization, especially on the relationship between the factors and the thermodenaturation.

In general, thermostability of a protein was demonstrated and compared as the half lives at supraoptimal temperatures. At such temperatures, thermodenaturation is likely to take place more rapidly than in optimal temperature range for activity and to be accelerated according to the elevated temperature. In the case of *R. obamensis* PEPC, the thermoinactivation rate was dramatically enhanced around 90 °C (Fig. 12). Below 90 °C, the thermoinactivation proceeded very slow and the enzyme completely lost its activity in a few minutes at 100 °C (Fig. 12). These results suggested that the thermodenaturation of the enzyme developed in different manners which were dependent of the denaturation temperatures and that it was strongly associated with the structural changes. Therefore, I analyzed the representative patterns of thermodenaturation at different denaturation temperatures by means of electrophoresis, UV-visible absorption, Trp fluorescence emission, 1-anilinonaphthalene-8-sulfonate (ANS) binding and renaturation capability.

Under the denaturation at 80 °C, the thermoinactivation rate was very low and the enzyme possessed 40% of the residual activity after 30 h incubation. At this temperature, the enzyme displayed the tetrameric and dimeric bands after 30 h incubation in the native-PAGE (Fig. 13) and exhibited small change of the UV-visible absorption spectra as compared to the non-denatured spectrum (Fig. 15C). It is assumed that the change of UV-visible absorption spectrum reflects, to some extent, the change of the global structure; the change in the UV range is related with the change in the main chain of proteins and the generation of the aggregate might increase the signal in the visible range. The results from the native-PAGE and UV-visible absorption showed that the quaternary structure of the enzyme was largely maintained after the denaturation for 30 h at 80 °C. This was supported by the results from the Trp fluorescence emission and ANS binding experiment. Contrary to the UV-visible absorption spectra, Trp fluorescence emission is thought to represent the change of the local structure such as the change of the side chain of proteins to some extent. The Trp fluorescence emission signal somewhat increased after 15 h incubation but restored in 30 h (Fig. 16C). In addition, the ANS fluorescence emission was stable during the denaturation at 80 °C (Fig. 17C). On the basis of these results, the enzyme showed no significant change in the global and local structure except for the inactivation. Although the enzyme activity decreased to 40% of activity after the denaturation for 30 h at 80 °C, the enzyme activity was successfully recovered by the renaturation at 45 °C with the extrinsic thermostabilization factors (Fig. 18B). It was demonstrated that the

hyperthermophilic glyceraldehyde-3-phosphate dehydrogenase from *Thermotoga maritima* denatured by guanidinium chloride could be activated and refolded by dilution of the denaturant and the renaturation of the enzyme accompanied with the reassociation from the dissociated monomer and dimer to the active form of the tetramer [30, 100]. Moreover, it was suggested that several mesophilic PEPCs regulated their activity by the association-dissociation equilibrium [88, 89]. The recovery of the enzyme activity from the denaturation at 80 °C for 30 h suggested, therefore, that the denaturation states after 30 h at 80 °C was possible for the renaturation and persisted in the dissociation step of the tetrameric form, namely the dissociated state.

A similar phenomenon was found in the enzyme denatured at 93 °C for 5 min. The all features measured were almost the same to those after the 80 °C denaturation for 15 or 30 h. This implied that the 5 min denaturation at 93 °C was equivalent to a couple of 10 hours denaturation at 80 °C and appeared to lead the enzyme to the dissociated states of denaturation. However, this state was gradually shifted to the further denatured states at this temperature. After 15 and 30 min denaturation, the active tetrameric and dimeric structures were found to decrease in the native-PAGE (Fig. 13). The UV-visible absorption signal exhibited the increment in the UV range (Fig. 15B), the Trp fluorescence emission decreased from the high fluorescence strength of the enzyme denatured for 5 min (Fig. 16B) and the ANS fluorescence emission was significantly enhanced (Fig. 17B). In addition, the enzyme lost the renaturation capability (Fig. 18B). From these results, it was obvious that the further structural changes in addition to the dissociation, which were irreversible changes, occurred in the enzyme over 5 min at 93 °C. Furthermore, it was also obvious that most enzyme did not reach to the irreversibly aggregated state because there still remained some of the tetrameric form in the native-PAGE and the absorption signals within the visible range in the enzyme denatured for 15 and 30 min were stable as compared to those before the denaturation (Figs. 13 and 15B). It was assumed that the increment of the UV absorption of the enzyme denatured for 15 and 30 min indicated not only the dissociation of the multimeric form but also some changes of the lower level of structures such as secondary and super-secondary structures in the subunit, and the enhancement of the ANS fluorescence emission reflected to some extent the exposure of the internal hydrophobic regions to the surface of the protein. Hence, this denaturation state was likely to be the intermediate process between the dissociation and the irreversible aggregation that resulted in the incorrectly folded and enzymatically inactivated state of the enzyme, so called "the scrambled state" [101]. Another important change seen in the scrambled state was that the amount of the monomeric subunit was reduced after the denaturation at 93 °C for 30 min in the SDS-PAGE (Fig. 14A, B). The result

suggested that the subunit of the enzyme was hydrolyzed at Asp and Glu residues by the heat effect and that the covalent process also took place. However, the deamidation from Asn or Gln residues, which was known as a major covalent process by heat [101], was thought to have little effect in the denaturation of the enzyme because there were observed no apparent change in the isoelectric point of the monomeric subunit during the denaturation at all temperatures tested. Therefore, the thermodenaturation at 93 °C might be subjected to the structural transition from the dissociated state to the scrambled state and the covalent process, mainly the hydrolysis of the monomeric form.

The putative scrambled state of the enzyme was also found under the denaturation at 100 °C. The thermoinactivation rapidly occurred and the enzyme completely lost its activity only in 3 min at 100 °C (Fig. 10). The enzyme with no residual activity after 3 min denaturation at that temperature showed the structural change similar to the change seen in the denaturation at 93 °C for 30 min. In the native-PAGE, the tetrameric form of the enzyme almost disappeared after 3 min denaturation at 100 °C (Fig. 13), and the UV-visible absorption spectrum and the ANS fluorescence emission spectrum overlapped those after 30 min denaturation at 93 °C (Figs. 15A, B, 17A, B). These results indicated that the global structure of the enzyme denatured for 3 min at 100 °C was similar to that of the enzyme denatured for 30 min at 93 °C. From these results, this denaturation state was thought to be the scrambled state of the enzyme accompanied with the dissociation. However, the denaturation process was not identical between them. For instance, the Trp fluorescence emission spectrum after 3 min denaturation at 100 °C differed markedly from the spectrum after 30 min denaturation at 93 °C (Fig. 16A, B), and the hydrolysis of the subunit was not found in the enzyme denatured for 3 min at 100 °C (Fig. 14). Further denaturation at 100 °C led the enzyme to the irreversibly aggregated state. The all forms of enzyme disappeared in the native-PAGE (Fig. 13) and the absorption signal in the both UV and visible range and the ANS fluorescence emission signal dramatically increased according to the denaturation time at 100 °C (Figs. 15A, 17A). The hydrolysis of the subunit also occurred after 10 min denaturation (Fig. 14B). Based on these results, it was concluded that the enzyme immediately reached the irreversibly aggregated state by the dissociated and scrambled states, and the covalent process also participated in the transition under the denaturation at 100 °C.






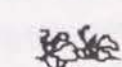


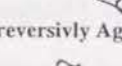
As described herein, the thermodenaturation of *R. obamensis* PEPC was dependent on temperature at which the enzyme was exposed, and subjected to the structural and covalent processes (Table 7). Of the several structural changes, the multimeric structures, the folding patterns and the exposurement of the hydrophobic regions that were to some extent expected from the native-PAGE, the UV-visible absorption and the ANS fluorescence emission, respectively, were cooperative

and consistent with the thermoinactivation during the thermodenaturation of the enzyme (Table 7). These changes might be correlated with each other and be reflected as the change of global structure. Although it remained obscure in this study how the change of the local structure and the covalent process were involved in the thermoinactivation and thermodenaturation of the enzyme, it was accepted that the thermodenaturation of *R. obamensis* PEPC comprised, to large extent, the transition of the global structure.

The extrinsic thermostabilization factors were strongly associated with the thermodenaturation of the enzyme. These factors had significant effect on the maintenance of the global structure, specifically on the maintenance of the quaternary structure (Fig. 13). In the presence of the factors, the enzyme could maintain the active multimeric (tetrameric or dimeric) forms under the denaturation at 93 °C where the enzyme was completely inactivated and denatured to the scrambled state without the factors (Fig. 13). These factors were discriminated into two types from their effects on the UV-visible absorption of the enzyme during the denaturation (Fig. 15D); one type contained the cofactor and salt (e.g. MgSO₄ and Na₂SO₄), and was able to protect the native folding or conformation of the non-denatured enzyme from the denaturation. The other contained the substrate and allosteric effector (PEP and acetyl-CoA), and appeared to improve the folding or conformation by the interaction with the enzyme rather than to protect the native one. These results also suggested that the thermostabilization effect of these factors primarily worked on the dissociation step of the thermodenaturation and the mechanism was to maintain the active multimeric structure despite different ways to function. The most notable feature in the extrinsic thermostabilization mechanism was the function of PEP. Of all factors, only PEP could suppress the exposurement of the internal hydrophobic region to the solvent and reassociate the dissociated subunit to the active multimeric structure in addition to the maintenance of the active enzyme (Figs. 17D, 18C). In Chapter 3, it was demonstrated that PEP had the relatively weak effect to prevent the thermoinactivation of the enzyme in all the factors (Table 5). Nevertheless the function of PEP was most effective on the structural changes during the thermodenaturation and on the renaturation process. It was supposed, therefore, that PEP played an important role *in vivo* as the substrate for the enzyme, the thermostabilization factor and the renaturation factor to the enzyme.

As a conclusion, it was concluded that the maintenance of the quaternary structure was important to the thermostability of *R. obamensis* PEPC and that the extrinsic thermostabilization factors also worked to maintain the active multimeric structure. The importance of the quaternary structure in the protein thermostability has been pointed out in several multimeric enzymes from

Table 7. The summary of the thermodenaturation at different temperatures in *R. obamensis* PEPC.

	Residual activity	Global structure	Covalent process	Local structure	Increment of hydrophobic regions	Renaturation by factors
Control	100%	 tetrameric form		Normal	+	
80 °C						
15 h	~70%			Weakly lax	+	Possible
30 h	~50%	 Dissociated		Normal	+	Possible
93 °C						
5 min	~50%	 Dissociated		Weakly lax	+	Possible
15 min	~10%	 Dissociated and Scrambled		Normal	++	Impossible
30 min	0%	 Dissociated and Scrambled	Hydrolysis	Strongly packed	+++	Impossible
100 °C						
3 min	0%	 Dissociated and Scrambled		Strongly lax	+++	Impossible
5 min	0%	 Irreversibly Aggregated		Weakly lax	++++	Impossible
10 min	0%	 Irreversibly Aggregated	Hydrolysis	Weakly packed	+++++	Impossible

thermophilic organisms [30, 39, 102-104]. It was also pointed out that the subunit-subunit bindings of multimeric proteins were significantly dependent on the hydrophobic interaction between the subunits and the enhanced hydrophobic interaction was one of the possible strategies for the thermostability of the proteins from thermophilic organisms [102, 103]. In Chapter 3, various ions in the buffer significantly enhanced the thermostability and the effectiveness was consistent with the water-structuring effectiveness of ions [78]. According to the solvophobic theory [92-95], it was suggested that the stabilization effect was attributed to the promotion of the intersubunit hydrophobic interaction due to water-structuring effects of the ions and the intersubunit hydrophobic interaction was strongly involved in the thermostability of this enzyme [78, Chapter 3]. Based on the results in Chapter 3 and 4, one of possible mechanisms for thermostabilization by the extrinsic factors is the promotion of the intersubunit hydrophobic interaction. It is still unclear how the extrinsic factors of PEP, MgSO₄ or acetyl-CoA to interact with the enzyme and provide the promotion of the intersubunit hydrophobic interaction. However, it is understandable that the interaction of substrates or allosteric effectors with enzymes lead the enzymes to some conformational changes and reduce the activation free energy of the enzymes that are essential for the enzyme activities or their regulations. Similarly, the substrate PEP and the allosteric effector acetyl-CoA are thought to interact with the PEPC and to induce some conformational change of the enzyme. Perhaps, the conformational change influences not only the active center domain but also the subunit-subunit binding domains and gives rise to the increased intersubunit hydrophobic interaction, resulting in the enhanced thermostability of the enzyme. For the inspection of this speculation, the further structural analysis including three dimensional structure and the structure-dependent molecular engineering of the enzyme are inevitable. Moreover, the intrinsic thermostabilization mechanism of *R. obamensis* PEPC remains unresolved. As the first step, the cloning and sequencing of the *R. obamensis* PEPC gene, and the overexpression in *E. coli* will be described in the next chapter. The intrinsic mechanisms for the thermostability of *R. obamensis* PEPC will be discussed based on the primary structure and the novel molecular evolution of PEPC will also be discussed.

Chapter 5

Cloning, Sequencing and Overexpression in *Escherichia coli* of Gene for Phosphoenolpyruvate Carboxylase (PEPC) from an Extreme Thermophile *Rhodothermus obamensis* OKD7

1. Introduction

In the previous chapters, I have studied the extrinsic thermostabilization mechanism of phosphoenolpyruvate carboxylase (PEPC) from the recently isolated extreme thermophile *Rhodothermus obamensis* [78, Chapter 2]. Most of PEPC that have been isolated and purified to date are homotetramer of about 400 kDa molecular mass consisting of about 100 kDa of subunits but only archaeal PEPCs from hyperthermophilic methanogen *Methanothermobacter sociabilis* and thermoacidophilic archaea *Sulfolobus* species are about 240 kDa of homotetramer with 60 kDa of subunits [52, 53, Sako, Y. *et al.* unpublished]. The PEPC purified from *R. obamensis* exhibited homotetrameric structure with 400 kDa of molecular mass and typical enzymological properties in bacterial entities except for its extreme thermophilicity and thermostability [96, Chapter 3].

I also found that the thermostability of the enzyme was strongly enhanced by the substrate, cofactor, salts and positive allosteric effectors, and these substances were possible extrinsic thermostabilization factors for the enzyme [96, Chapter 3]. Moreover, it was shown and suggested in Chapter 4 that the thermodenaturation of the enzyme globally resulted from the temperature-dependent shift of three structurally different states (dissociated, scrambled, and aggregated states) and that the extrinsic thermostabilization factors acted to large extent on the maintenance of quaternary structure [105]. However, the molecular basis of the interaction and function between the factors and enzyme, and the more detail view for the structural change induced by the extrinsic factors are still unknown. In order to resolve these problems and to determine the three dimensional structure of the enzyme, the cloning, sequencing and expression of the gene for *R. obamensis* PEPC are important and essential.

In addition, the intrinsic thermostabilization mechanisms of *R. obamensis* PEPC have not been

analyzed yet. Although the detail inspections of the intrinsic mechanisms as well as the extrinsic ones require the structural data including three dimensional structure of the enzyme, some successful approaches to the intrinsic mechanisms based on the comparison of primary and secondary structures of proteins have been reported in several thermophilic and extremely thermophilic proteins [32, 106, 107, 108]. I describe in this chapter, therefore, the cloning, sequencing and overexpression in *Escherichia coli* of the gene for *R. obamensis* PEPC (*ppc* gene). The amino acid sequence of the enzyme was compared with those of other thermophilic and mesophilic counterparts. Some preferences of the amino acid compositions and substitutions were found in the thermophilic enzymes. The possible contribution of these preferences to the thermostability will be discussed. Based on the phylogenetic analysis of the enzyme, the evolution of this enzyme is also discussed.

2. Materials and Methods

Bacterial strains and growth conditions. The bacterial strain used was *Rhodothermus obamensis* OKD7 (JCM 9785) which was isolated from a shallow marine hydrothermal vent at Tachibana Bay, Nagasaki Prefecture, Japan [78, Chapter 2]. For cultivation of *R. obamensis*, Jx medium was used [78, Chapter 2]. *R. obamensis* was grown at 76 °C and collected in the late exponential growth phase. Cell pellet was freeze-dried at -90 °C prior to genomic DNA extraction.

Genomic DNA extraction and direct sequencing of *ppc* gene. The genomic DNA was prepared as described in Chapter 2. The purified DNA was used for the southern analysis and the direct sequencing of the *ppc* gene. The partial fragment of the *ppc* gene was amplified by polymerase chain reaction (PCR). The primers used for amplification had the sequences 5'-TSACTGCYCAAYCC AACSGA-3' (TAHPT primer) and 5'-GTCCAGGCSATSACCCASGGGATGGC-3' (SLRAIP primer), corresponding to the highly conserved amino acid sequences among bacterial PEPCs reported to date and the positions 136-142 and 712-718 respectively in the amino acid sequence of *Escherichia coli* PEPC [109] (Fig. 19). This 1.9 kb of fragment was directly sequenced on both strand by the dideoxynucleotide chain termination method using DNA sequencer Model 373As (Applied Biosystem Inc., USA). Based on the partial sequence of the *ppc* gene, the thermal asymmetric interlaced (TAIL) PCR was carried out to determine the sequence of the unknown regions adjacent to the known sequence of the gene [110]. The long specific primers had the sequences 5'-CAGCAGGGTCTCCTGCTCCT-3' (LS1), 5'-CGACTTCGTCGCGAACGGTG-3' (LS2) and 5'-

ACCGCGACGGCAACCGGTAC-3' (LS3) for the 5'-end of region, and 5'-GGCCACGCGCAACCGTCTGA-3' (LS4), 5'-CGGCGCCTGATCGATGCGCC-3' (LS5) and 5'-TCAGCCGCCTACCCA TCGCC-3' (LS6) for the 3'-end of region, indicated in Fig. 19. For the TAIL PCR on the both regions, a short arbitrary degenerate primer was used and the sequence was 5'-GTCGASWGANAW GAAN-3' (AD1). The amplified fragments containing 5'- and 3'-flanking regions of the *ppc* gene were directly sequenced on both strand by the dideoxynucleotide chain termination method using DNA sequencer (Fig. 19).

Southern analysis. The same amount of genomic DNA (15 µg/lane) was digested with restriction endonucleases, electrophoresed in 1.0% (wt/vol) agarose gel and transferred to the positively charged nylon membrane (Boehringer Mannheim, Germany). As a hybridization probe, a 1.3 kb of RNA probe labeled by digoxigenin (DIG)-11-UTP was used. For the labeling, a 1.3 kb of DNA fragment was amplified by PCR using the primers with the sequences, 5'-CTTTGCAGATCGA AATCGAAGGC-3' (INIT primer) and 5'-CCCGGTAGTCGTTCTCGACA-3' (SPR2) indicated in Fig. 19, and subcloned into a site adjacent to the T7 RNA polymerase promoter in the pCRTMII vector (Invitrogen). The subcloned vector containing the 1.3 kb of fragment was linearized by a restriction enzyme of *Hind*III and used as a template for the *in vitro* transcription of the RNA probe. The DIG RNA labeling kit (Boehringer Mannheim) was used for the labeling and the procedure was described in the manufacturer's manual. Hybridization was carried out overnight in 50% (vol/vol) formamide, 5 x SSC (1 x SSC is 150 mM NaCl, 15 mM sodium citrate, pH 7.0), 0.02% (wt/vol) sodium dodecylsulfate (SDS), 0.1% (wt/vol) sodium-lauroylsarcosine and 2% (wt/vol) blocking reagent (Boehringer Mannheim) at 60 °C and the filter was washed twice with 2 x SSC, 0.1 % SDS at room temperature for 5 min and then washed twice with 0.1 x SSC, 0.1 % SDS at 68 °C for 30 min. The detection of DIG-labeled RNA hybridized with homologous DNA sequence was carried out by DIG luminescent detection kit for nucleic acids (Boehringer Mannheim).

Alignment of amino acid sequences and Data analysis of the sequences. A multiple alignment of amino acid sequences from various organisms was constructed by a software package, ODEN version 1.1.1 (National Institute of Genetics, Mishima, Japan). Then, the sequence identity and similarity for each aligned pair were calculated based on the alignment. Continuous gaps were regarded as a single substitution in the calculation and the sequence similarity was defined as the percentage of the sites occupied by the residues sharing the same physicochemical properties in the aligned pair. The molecular mass inferred from the sequence, codon usage in *R. obamensis ppc* gene and amino acid compositions of various PEPCs were calculated by DNASIS software ver. 3.6

(Hitachi Software, Tokyo, Japan). Based on the multiple alignment, the evolutionary distances among various PEPCs known to date were calculated by the method of Kimura and the phylogenetic tree was constructed by the neighbor-joining method [67] using the software of ODEN. The secondary structures of three PEPCs from *R. obamensis*, *Corynebacterium glutamicum* and *Thermus sp.* were inferred from the amino acid sequences by the method of Chou, Fasman and Rose [111] using the DNASIS software and compared to each other with respect to the location of the amino acid substitutions.

The cloning and overexpression of the *ppc* gene. The complete *ppc* gene of *R. obamensis* was amplified by PCR using the INIT primer described above and the END primer with the sequence, 5'-CTATCCGGTGCTCTGCATGGCGG-3' indicated in Fig. 19. The amplified gene was subcloned into the pCRTMII vector (Invitrogen) and this plasmid was designated as pCRP2.8 (Fig. 20). A 2.9 kb of fragment containing the *ppc* gene was cut out of pCRP2.8 and ligated in-frame into the open reading frame of glutathione S-transferase (GST) in the pGEX-5X-3 expression vector (Pharmacia). The resulting plasmid was designated as pPEP3.0 and contained about 3.5 kb of open reading frame for GST-PEPC fusion protein (Fig. 20). The cells of *Escherichia coli* INV α with pPEP3.0 or pGEX-5X-3 were cultivated at 37 °C in the LB medium (10 g of tryptone, 5 g of peptone, 10 g of NaCl per liter) containing 50 µg/ml of ampicillin. In the mid-exponential growth phase, 0.2 mM of isopropyl-1-thio- β -D-galactoside (IPTG) was added to the medium. The cells were grown at 37 °C for 5 h in the presence of IPTG and harvested by centrifugation (8000 x g, 20 min) at 4 °C. The cells were washed twice with 50 mM Tris-HCl (pH 7.5) at 4 °C and frozen at -90 °C prior to preparation of crude extracts.

Preparation of crude extracts and enzyme assay condition. The thawed cell paste was suspended with 50 mM Tris-HCl (pH 7.5) or 50 mM Tris-HCl (pH7.5) containing 9 M urea, 2% (vol/vol) triton X-100 and 2% (vol/vol) 2-mercaptoethanol. Both cells were broken by sonication and centrifuged at 24000 x g for 20 min. The supernatants were used as crude extracts. These crude extracts were applied not only to the electrophoresis but also to the enzyme assay for PEPC activity at high temperatures. The PEPC activity of the crude extracts was routinely coupled to the malate dehydrogenase (MDH) reaction and assayed by the above-mentioned method in Chapter 3 [96, 105].

Partial purification and characterization of recombinant GST-PEPC fusion protein. The cells of *E. coli* INV α /pPEP3.0 were grown and harvested as described above. The cell paste was suspended with 50 mM Tris-HCl (pH 7.5) and broken by sonication. The crude extract

CTG GAG ACC TTC GCG GTC ATC CGC GAG CTG GTG CAG CTC GAC CCC CGC CTC GTG	1512
L E T F A V I R E L V Q L D P R L V	500
GGC AGC TAC ATC GTG AGC ATG ACG CAC ACC GTC AGC GAC CTG CTC GAG CCC ATG	1566
G S Y I V S M T H T V S D L L E P M	518
CTG CTG GCC AAA GAA GTC GGG CTC TGG CAT TAC GAG CGC GAC CCC CGC ACC GGC	1620
L L A K E V G L W H Y E R D P R T G	536
AAG CCG GGC CAC GTG CGC TGC CCC ATC GAT TTT GTG CCG CTT TTC GAA ACG ATC	1674
K P G H V R C P I D F V P L F E T I	554
GAA GAC CTG GAG GCG GCC GCC AGC CGC ATG GAA GCC ATC CTG AGC CAT CCC GTC	1728
E D L E A A A S R M E A I L S H P V	572
TAC CGG ATG CAG GTG GCT GCC CGC GGT GGC TTT CAG GAA ATC ATG CTG GGC TAC	1782
Y R M Q V A A R G G F Q E I M L G Y	590
TCC GAC AGC ACG AAA GAC GGT GGC TAC TGG ATG GCC AAC TGG GCG CTG CAC CGG	1836
S D S T K D G G Y W M A N W A L H R	608
GCC CAG GAG CAG CTG GCC GAA GTA TGT CTT CGC CAT GGC GTG GAC TTC CGG CTG	1890
A Q E Q L A E V C L R H G V D F R L	626
TTT CAC GGG CGC GGC GGT ACT GTG GGA CGT GGG GGC GGC CGC GCC AAC CAG GCC	1944
F H G R G G T V G R G G G R A N Q A	644
ATC CTG GCC ATG CCG CCG GTG GTC CAC AAC GGT CGC ATT CGC TTC ACC GAG CAG	1998
I L A M P P V V H N G R I R F T E Q	662
GGC GAG GTG ATC TCG TTC CGC TAT GCC CTG CCC GAG ATC GCC CAT CGC CAC CTG	2052
G E V I S F R Y A L P E I A H R H L	680
GAG CAG ATC GTC AAT GCC ATG CTC CGC GTG GTC GGC CTC CCG GCC GCT TCC GGC	2106
E Q I V N A M L R V V G L P A A S G	698
ACC GAT GGC ACC GAT CCG GCC ACG CGC AAC CGT CTG ATG GAC GAG CTG GCT GCG	2160
T D G T D P A T R N R L M D E L A A	716
CGC TCT ATG CCG GCC TAC CGG CGC CTG ATC GAT GCG CCT GAC TTC TGG TCG TGG	2214
R S M R A Y R R L I D A P D F W S W	734
TAC ACG CGC ATC ACT CCG ATC GAC CAG ATC AGC CGC CTA CCC ATC GCC TCG CGG	2268
Y T R I T P I D Q I S R L P I A S R	752
CCG GTC TCG CGC AGC AGC GCC CGT GAG GTA GAT TTC GAA AGC CTG CGG GCC ATC	2322
P V S R S S A R E V D F E S L R A I	770
CCC TGG GTC TTC GCC TGG ACC CAG GTC CGC TAC CTG ATT CCG GGC TGG TTC GGG	2376
P W V F A W T Q V R Y L I P G W F G	788
ATC GGC CAG GCC CTC GAC GAG TTG CTC CAG ACG TCG CCC GAG CAT CTG GAG ACG	2430
I G Q A L D E L L Q T S P E H L E T	806
CTT CGC ACC TGG TAT CGA TCC TGG CCG TTT TTC CGC ACC GTG CTG CAG AAC GCC	2484
L R T W Y R S W P F F R T V L Q N A	824
CAG CGC GAG ATG GTC CGC GCC CGC CTG GAA ATT GCC GCC TAC TAC GAC CGG CTA	2538
Q R E M V R A R L E I A A Y Y D R L	842
CTG GGC GAC GGC CCG ACG GCA TTC CAT CAG ATG ATC GAG GAA GAC TAT CAT CGA	2592
L G D G P T A F H Q M I E E D Y H R	860
GCC CGG ACG GCC ATC CTA CGC ATC ACC GAT CAG GAG TCG TTG CTC GAC CAC GAT	2646
A R T A I L R I T D Q E S L L D H D	878
CCG ATC ATC CGC AAA TCC GTG CAG CTC CGC AAC CCG TAC ACC GAT GTG CTG AAC	2700
P I I R K S V Q L R N P Y T D V L N	896
CTG GTG CAG CTC GAG CTG ATG CCG CGC ATC CGA TCA GGC GCC GAG GCC GAT CGG	2754
L V Q L E L M R R I R S G A E A D R	914
GAG CCG CTC CGG CGC GCT CTG TTC CTG AGC ATC AAC GGG ATC GCC GCC ATG	2808
E P L R R A L F L S I N G I A A A M	932
CAG AGC ACC GGA TAG	2862
Q S T G *	936
gtg ttg cac cgc gag gct att gcc gga gcg gcg gct cct gct ttg 3'	2907

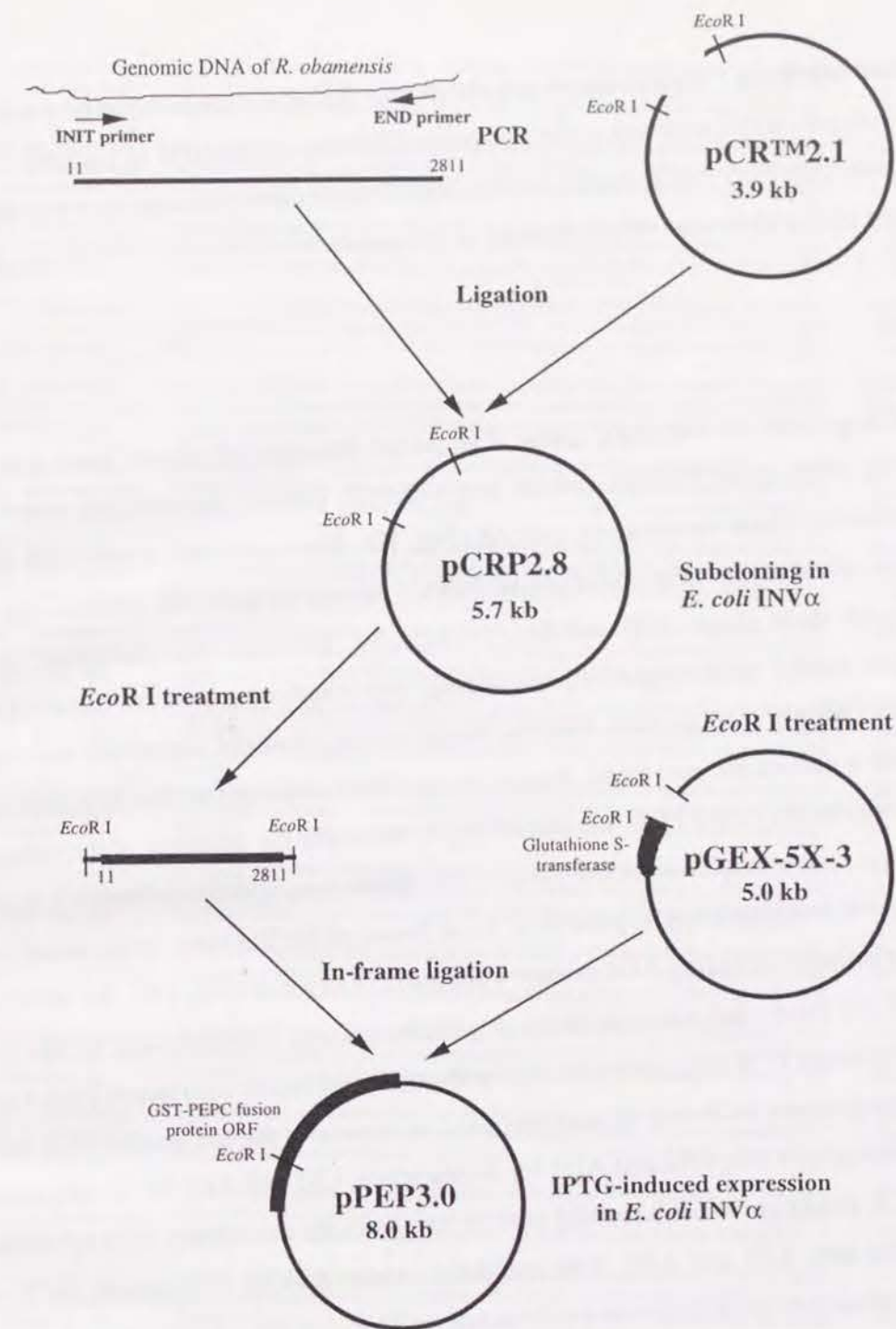


Fig. 20. The scheme for the cloning and expression in *E. coli* of the *ppc* gene from *R. obamensis*. The complete *ppc* gene of *R. obamensis* was amplified by PCR using the INIT primer and the END primer with the sequences described in Materials and Methods. The amplified gene was subcloned into the pCRTMII vector (Invitrogen) and this 5.7 kb of plasmid was designated as pCRP2.8. A 2.9 kb of fragment containing the *ppc* gene was cut out of pCRP2.8 by a restriction enzyme *EcoR* I and ligated in-frame into the open reading frame of glutathione S-transferase (GST) in the pGEX-5X-3 expression vector (Pharmacia) at the *EcoR* I site. The resulting 8.0 kb of plasmid was designated as pPEP3.0 and contained about 3.5 kb of open reading frame for GST-PEPC fusion protein.

Other Methods. Polyacrylamide gel electrophoresis of the crude extracts was performed with 10% (wt/vol) polyacrylamide gel in the presence of SDS by the method of Laemmli [79]. Molecular weight markers for SDS-PAGE were from Bio-Rad. Protein concentrations were routinely estimated by Bradford [80] with bovine serum albumin as the standard.

3. Results

The sequence of the *ppc* gene. The partial fragment of the *ppc* gene was successfully amplified by PCR using TAHPT primer and SLRAIP primer, and directly sequenced by the dideoxynucleotide chain termination method (Fig. 19). The translated amino acid sequence was compared to other amino acid sequence of PEPCs known to date and showed significant high similarity with them (Figs. 19B and 21). In addition, the sequence contained several highly conservative amino acid sequences including the putative substrate binding site motif, FHGRGGXXGRGG, seen in most PEPCs. These results strongly supported that the amplified fragment was a part of the *ppc* gene. Based on the DNA sequence of the fragment, the thermal asymmetric interlaced (TAIL) PCR was carried out to determine the sequence of the unknown regions adjacent to the known sequence of the gene [110]. Three long specific primers (LS1-3 or LS4-6) were constructed from the DNA sequences at 5'- or 3'-end of the fragment, respectively, and several short random primers including AD1 primer were also constructed (Fig. 19A, B). With the primers LS3 and AD1 for the 5'- unknown sequence or with the primers LS4 and AD1 for the 3'- unknown sequence, the primary PCR was carried out by the thermal asymmetric interlaced (TAIL) cycling. The products of the primary PCR was diluted and used as templates for the second PCR by the TAIL cycling with the primer sets, LS2 and AD1 for 5'- sequence, LS5 and AD1 for 3'- sequence. Finally, the second PCR products were diluted and used as templates for the tertiary PCR by normal cycling with the primer sets, LS1 and AD1, LS6 and AD1. About 600 bp of fragment for 5'- unknown sequence and about 800 bp of fragment for 3'- unknown sequence were predominantly amplified and then, these fragments were directly sequenced by the dideoxynucleotide chain termination method. As the result, both DNA sequences were successfully connected with the known sequence and the translated amino acid sequences revealed significantly high similarity with other amino acid sequences of PEPCs (Figs. 19B and 21). In the sequence, the termination codon TAG and the possible initiation codon GTG, which is often seen in genes from thermophiles [112] were found (Fig. 19B). This position of the initiation codon was quite similar to the initiation positions of

R._obamensis	MLPPLQIEIEGTGISRPLSEHVNLGGLLGQVITQEMAGPEMELVETLRLRCKQAAQENR	60
C. glutamicum	-----MTDFLRDDIRFLGQILGEVIAEQEGQEVYELVEQARLTSFDIAK--G	45
Thermus sp.	-----MSDPFEALKAEDVLLGRLLGEAIRKVSGERFFALVEEVRLLSKARRQ--GD	49
R._obamensis	PEFREQAYTRHSATYDELLWLLRAYTAFHVLVNAEQEIEIRINRERAQOSTPERPRPE	120
C. glutamicum	NAEMDSLQVDFDITPAKATPIARAFSHFALLANLAED---LYDEELREQALDAGDTPFD	102
Thermus sp.	GAAAEVLSQRVERMPVEEMALVRAFTHYFHLVNLAEERHRVRVNRRLRTEGETLENRPE	109
R._obamensis	-SIDEAILALKQQGRTLDVLTLLERLDIQPTVTAHPTAARRRSILYKQQHIAQMLSQQR	179
C. glutamicum	STLDATWKLNEGNVGAEAVDVLRNAEVAPVLTAHPTETRRRTVFDQKRWITTHMRERH	162
Thermus sp.	-GFLALAKALKERGLSLEEAHLNRLALLLTTAHTPTERRRTRRHHLERLQEELEGGD	168
R._obamensis	RCQ-----LTPEQETLLLDLHNQITLLLGTAEVREERPTVRDEVEQGLYFIQSTIWEA	233
C. glutamicum	ALQSAEPTARTQSKLDEIEKNIRRRITILWQTALIRVARPRIEDEIEVGLRYKLSLLEE	222
Thermus sp.	R-----ER-----LLARVLLYATEEVRKARPSVEDEIKGGLYLPTTLWRA	210
R._obamensis	VPRIYEDVRRALRRYYGADVDFRPFRLYRSWIGSDRDGNPYVTPETITRWALTQRRALQ	293
C. glutamicum	IPRINRDVAVELRERFEGEVPKPVVKPGSWIGDHDGNPYVTAETVEYSTHRAAETVLK	282
Thermus sp.	IPKVEGLEAALERVYGRPHLRSPVFRSWMGDRDGNPYVTPVTAFAFRAGYAREVAKG	270
R._obamensis	RYMEELRQLRRRLSLSDRYVAPPEELRRSLARDAREVSLPPLVLRQFRHESFRKISYIM	353
C. glutamicum	YYARQLHSLHEHLSLSDRMNKVTPQLLA-----LADAGHNDVPSRVDEPYRRAVHGV	335
Thermus sp.	RYLEELALVRDLSEARIPVPKEVRE-----GGEG---VERFFGEPYRYYFAALY	319
R._obamensis	GRLHGLLQALDDPTQPA-----PDYDADFVEDLRLRQCLACGLERIAHDDQLTR	405
C. glutamicum	GRIIATTAELIGEDAVEGVWFKVFTPYASPEEFLNDALTDHSLRES-KDVLIADDRSLV	394
Thermus sp.	RALEG-----EALSTEGLARALKVAEKLEGVLAQVAQAFLRP-	358
R._obamensis	LLVLAQTGFPHLVTLDVRQHSVHEAAVAELRLLAGVENDYRALPESRRQELLAELSNP	465
C. glutamicum	LISAIESFGFNLYALDLRQNSSEYEDVLTTELPERAQVTANYRELSAEKLEVLKELRSP	454
Thermus sp.	LEARLSAFGLLAPLDLREESGKLEAAAEELRLGGVHPDFLALSPEEKEALLTEELKTA	418
R._obamensis	RPLLPGAR-VSEATRQVLETFVAVIRELVQLDP-RLVGSYIVSMHTVSDLEPMLLAKE	523
C. glutamicum	RPLIPHGSDSEYSEVTDRELGI FRTASEAVKFKGPRMVPKCIISMASSVTDLVLEPMLLKE	514
Thermus sp.	RPLLP-----VGEVPOGEALRVALGALRAWGD---KGAHVSMTHHPADLLAVFLLARE	469
R._obamensis	VGLWHYERDPRTGKPGHVRCPIDFVPLFETIEDLEAAASRMEAILSHPVYRMQVAARGGF	583
C. glutamicum	FGLIAAN---GDNP---RGTVDVPLFETIEDLQAGAGILDELWKIDLYRNYLLQDNDV	567
Thermus sp.	VGLYRP-----GKP---LPPDVVPLFETLEDLERAPEVLRLLANPVFRAHAQGRGG-	518
R._obamensis	QEIMLGYSDSTKGGYWMANWALHRAEQLEAEVCLRHGVDFRIFHGRGGTVGRGGGRANQ	643
C. glutamicum	QEVMLGYSDSNKGGYFSANWALYDAELQLVELCRSAGVKLRIFHGRGGTVGRGGGPSYD	627
Thermus sp.	VEVMI GYSDSNK DAGFLMANLALYQAQEAALHAGVGEAQGIPVFFHGRGTSARGGSPAGR	578
R._obamensis	AIALMPVHNGRIRFTBQGEVIFRYALPEIAHRHLEQIVNAMLRVVGLPAASGTDTGTD	703
C. glutamicum	AIALQPRGAVQGSVRITBQGEIISAKYGNPETARRNLEALVS-----ATLEASLLDVSE	681
Thermus sp.	ATAGLPPKSVGHRLRLTEQGEALADRYAHPDLAVRHLEQLL-----YHFAQAALGDGVE	632
R._obamensis	PATRNRLMD---ELAARSMRAYRRLIDAP-DFWSWYTRITPIDQISRLPIASRPVSRSSA	759
C. glutamicum	LTDHQRAYDIMSEISELSLKKYASLVHEDQGFIDYFTQSTPLQEIIGSLNIGSRFSSR--K	739
Thermus sp.	PKAHWREALG--EAGERSMARYRALLSQE-GFFPFPEAFTPIREIGELPIASRPVYR-HG	688
R._obamensis	REVDFESLRAIPWVFAWTQVRYLIPGWFGIGQALDELL--QTSPEHLETLRWYRSWPF	816
C. glutamicum	QTSVVEDLRAIPWVLSWSQSRVMLPGWFGVGTALQWIGEGEQATQRIAEQLTNESWPF	799
Thermus sp.	RVRDIRDLRAIPWVMAWTQVRLLLPGWYGLS-----ALEGLPMPLLREMYREWPF	738
R._obamensis	FRTVLQNAQREMVRARLEIAAYDRLLGD--GPTAFHQMI EEDYHRARTAILRITDQESL	874
C. glutamicum	FTSVLNDMAQVMSKAELRLAKLYADLPDTEVAERVYSVIREEYFLTKKMFCVITGSDDL	859
Thermus sp.	FATTLESAAMALAKADLGAERYLKLVP--GLQGFYHHLAEYRRRTVALLEAIFAP-L	795
R._obamensis	LDHDPIIRKSVQLRNPYTDVNLVQLELMRRIRSGAEADREPLRRALFSLINGIAAAMQS	934
C. glutamicum	LDDNPLLARSVQRRYPYLLPLNVIQVEMMRRYRKG--DQSEQVSRNIQLTMNGLSTALRN	917
Thermus sp.	LHNQKTLERQIALRNPYVDPINFVQVELLARYRAPGGREDEGVRRALLLSLLGVAAGLRN	855
R._obamensis	TG	936
C. glutamicum	SG	919
Thermus sp.	AG	857

Fig. 21. The alignment of PEPCs from *R. obamensis*, *Corynebacterium glutamicum*, and *Thermus sp.* Amino acids that are identical in three PEPCs are indicated by asterisks below the alignment and amino acids that are physicochemically similar in three PEPCs are indicated by dots below the alignment. The bars in the alignment reveal the gaps in the sequences. The boxed sequence indicated the putative substrate binding site of PEPC.

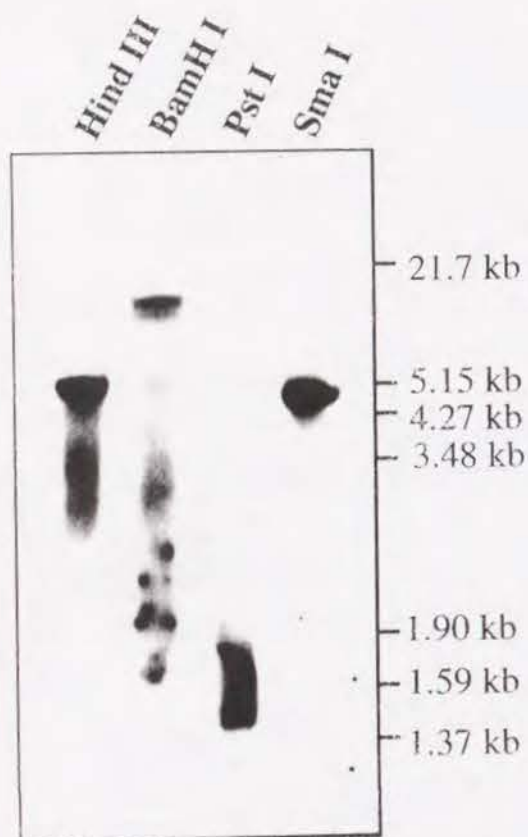


Fig. 22. The southern blot analysis of *R. obamensis* genomic DNA. *R. obamensis* genomic DNA was digested to completion with *Hind* III, *Bam*H I, *Pst* I or *Sma* I, size-fractionated on an 1.0% agarose gel, transferred to the positively charged nylon membrane and hybridized with a 1.3 kb of RNA probe labeled by digoxigenin (DIG)-11-UTP. DNA size marker was from indicated on the left.

All restriction digests showed a single fragment that hybridized to the probe, indicating that PEPC is encoded by a single copy of gene (Fig. 22). This result also strengthened that the sequence directly determined by the PCR-mediated method was the gene for *R. obamensis* PEPC.

The alignment of PEPCs and phylogenetic analysis. The deduced amino acid sequence of *R. obamensis* PEPC was aligned with those of 16 PEPCs from various bacteria and plants. The alignment indicated that the amino acid sequence of *R. obamensis* PEPC was closely related with those of PEPCs from thermophile *Thermus* sp. or mesophile *C. glutamicum*, with a

other PEPCs (Fig. 21) and was preceded by the putative ribosomal RNA binding site (Shine-Dalgarno sequence) (Fig. 19B). These results suggested that this GTG codon was the proper initiation codon of the *ppc* gene.

The open reading frame consisted of 2,811 bp, encoding a polypeptide of 937 amino acid residues with calculated molecular mass of 107,808 Da. This value matched the apparent molecular mass of the purified *R. obamensis* PEPC estimated by SDS-PAGE [96]. The GC content of *R. obamensis ppc* coding region was high (66.2%) and the extreme bias for G or C was found in the third position of the codons (85.0%).

The nucleotide sequence of the *ppc* gene for *R. obamensis* PEPC was deposited in EMBL Nucleotide Sequence Database under accession number X99379.

Southern analysis. To estimate the number of *R. obamensis ppc* gene, a 1.3 kb of RNA probe labeled by digoxigenin (DIG)-11-UTP, corresponding to 5'-half of the *ppc* gene (Fig. 19A), was hybridized with *R. obamensis* genomic DNA digested with various restriction endonucleases (Fig. 22).

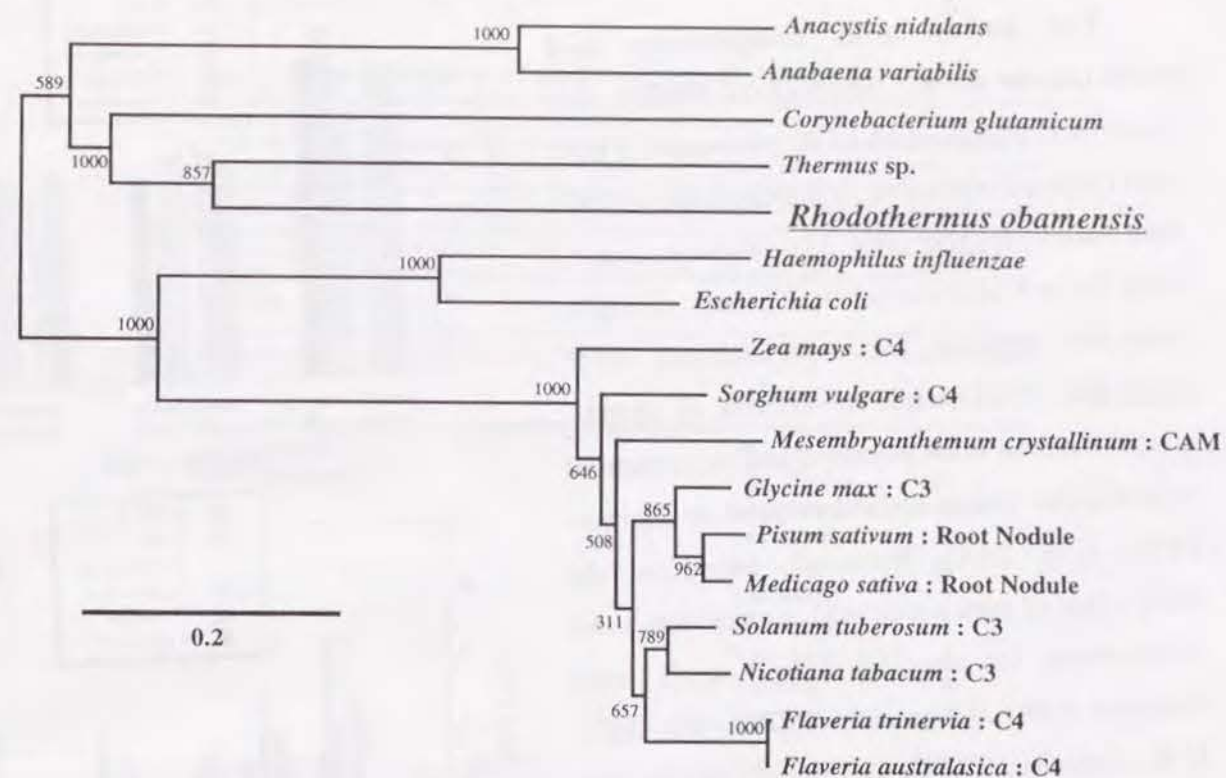


Fig. 23. The unrooted phylogenetic tree of representative bacterial and eucaryal PEPCs. Each number shows the bootstrap value on the branching (1000 replicates). Scale bar indicates substitutions per residue. The PEPC sequences in this figure are from GenBank under accession numbers: *Anabaena variabilis*, M80541; *Anacystis nidulans*, M11198; *Corynebacterium glutamicum*, M25819; *Thermus* sp., D42166; *Rhodothermus obamensis*, X99379; *Escherichia coli*, X05903; *Haemophilus influenzae*, L46266; *Zea mays* C4, X03613; *Sorghum vulgare* C4, X55664; *Mesembryanthemum crystallinum* CAM, X13660; *Pisum sativum* Root Nodule, D64037; *Medicago sativa* Root Nodule, M83086; *Glycine max* C3, D13998; *Solanum tuberosum* C3, X67053; *Nicotiana tabacum* C3, X59016; *Flaveria trinervia* C4, X61304; *Flaveria australasica* C4, Z25853.

45.3% or 37.7% of identity and a 61.5% or 56.5% of similarity, respectively. The alignment of amino acid sequences from three closely related PEPCs was shown in Fig. 21.

Based on the multiple alignment of 17 PEPCs including *R. obamensis* PEPC, the unrooted phylogenetic tree was constructed by the neighbor-joining method [67] (Fig. 23). From the topology of the tree, it was indicated that *R. obamensis* PEPC was most closely related with *Thermus* PEPC and it was suggested that these extremely thermophilic PEPCs were derived from the mesophilic type of enzyme (Fig. 23). In addition, the phylogenetic tree showed the close phylogenetic relationship in PEPCs between proteobacteria and plants (Fig. 23). The branching pattern between them represented significant robustness by the bootstrap examination (1000/1000), indicating that the eucaryal PEPC was descendent of the bacterial entities.

The amino acid composition and substitution of *R. obamensis* PEPC. The amino acid composition of *R. obamensis* PEPC was compared with those of representative PEPCs from various sources (Fig. 24). In comparison of three distinct physicochemical groups of amino acids, no apparent feature was found in *R. obamensis* PEPC while the content of neutral-nonpolar amino acids increased and the content of neutral-polar amino acids decreased in *Thermus* PEPC (Fig. 24A). However, based on the comparison of each amino acid composition, some preferences for specific amino acids were observed in two thermophilic PEPCs (Fig. 24B). In *R. obamensis* PEPC, the contents of Gly, Ser, Asn and Lys decreased and the contents of Gln, His and Arg increased (Fig. 24B). Among them, the amino acid composition changes in Asn, Ser, Lys, His and Arg were common to the changes in *Thermus* PEPC. However, lower content of Gly and higher content of Gln were peculiar to *R. obamensis* PEPC.

In addition, the amino acid substitutions were examined among the closely related PEPCs from *R. obamensis*, *Thermus* sp., *C. glutamicum* to examine whether some bias for the specific amino acid substitutions existed between the mesophilic and thermophilic PEPCs (Table 8).

As the result, three types of substitutions (*R. obamensis*-specific, *Thermus*-specific or universal substitution) were found to be dominant in the thermophilic PEPCs (Table 8). Most of the dominant substitutions in two thermophilic PEPCs were in good agreement with those previously observed with other thermophilic proteins [32, 108] but the substitutions from Leu to Ile, Val to Ile and Ala to

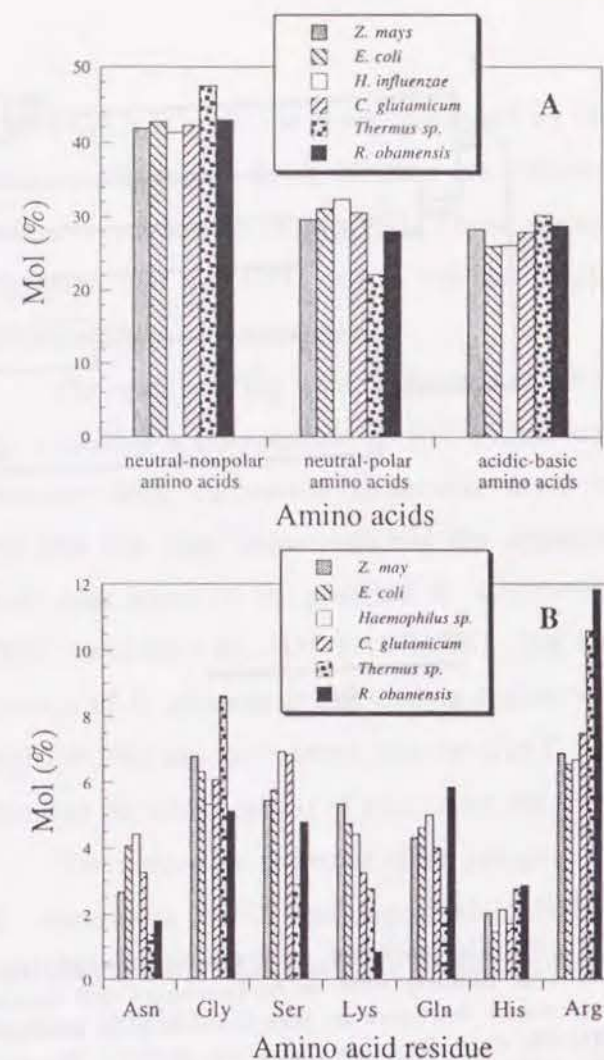


Fig. 24. The amino acid compositions of representative bacterial and eucaly PEPCs. (A) The comparison of three distinct physicochemical groups of amino acids. The neutral-nonpolar amino acids contain Ala, Ile, Leu, Met, Phe, Pro and Val, the neutral-polar amino acids contain Asn, Cys, Gln, Gly, Ser, Thr, Trp and Tyr, and the acidic or basic amino acids include Arg, Asp, Glu, His and Lys. (B) The comparison of some amino acid compositions that demonstrate relatively high or low contents in *R. obamensis* PEPC. The amino acid compositions in this figure were found to be different between *R. obamensis* PEPC and all other mesophilic PEPCs. Hence, some amino acid compositions were similar between *R. obamensis* PEPC and *Thermus* PEPC.

Table 8. The preferred residue changes in PEPCs from *C. glutamicum*, *Thermus* sp. and *R. obamensis*. Analysis was carried out over the region of the sequence alignment, as shown in Fig. 3. The comparison between *C. glutamicum* and both extreme thermophiles implies the amino acid replacements from residues in *C. glutamicum* PEPC to the identical residues in both thermophilic PEPCs. (U) means the frequent substitutions universally seen in *Thermus* sp. and *R. obamensis* (universal substitutions), and (R) or (T) means the frequent substitutions specifically seen in *R. obamensis* or *Thermus* sp. (*R. obamensis* specific substitutions or *Thermus* specific substitutions). * shows the frequent substitutions in the comparison between *C. glutamicum* and both extreme thermophiles and the substitutions written in bold line represent the possible thermophilic substitutions previously proposed or observed [32, 106, 107, 108].

Comparison	Total amino acid changes	Most frequent amino acid change			
		substitution	changes		
<i>C. glutamicum</i> and <i>R. obamensis</i>	506	Ile→Leu*(U)	13		
		Glu→Ala(U)	12		
		Ala→Leu(U)	11		
		Leu→Ile(R)	11		
		Ser→Thr*	10		
		Val→Ile(R)	9		
		Ala→Gln(R)	8		
		Val→Leu*(U)	8		
		Val→Arg	8		
		Thr→Leu	8		
<i>C. glutamicum</i> and <i>Thermus</i> sp.	496	Val→Leu*(U)	14		
		Ser→Ala(T)	14		
		Ile→Leu*(U)	13		
		Asp→Glu(T)	10		
		Ala→Arg*	9		
		Ala→Glu(T)	9		
		Ala→Leu(U)	8		
		Glu→Ala(U)	8		
		Leu→Val	7		
		Val→Ala	7		
		Met→Leu*	7		
		Gln→Glu*	7		
		<i>C. glutamicum</i> and both extreme thermophiles	104	Ile→Leu*(U)	7
Ile→Val*	4				
Ser→Thr*	4				
Ala→Arg*	4				
Val→Leu*(U)	3				
Met→Leu*	3				
Gly→Ala*	3				
Gln→Glu*	3				
<i>Thermus</i> sp. and <i>R. obamensis</i>	448			Leu→Ile(R)	19
				Ala→Glu(T)	11
				Val→Ile(R)	11
				Gly→Ala*	11
				Glu→Arg	10
		Glu→Asp	10		
		Ala→Val	9		
		Ala→Arg*	9		
		Val→Leu*(U)	8		
		Glu→Gln	8		
		Ala→Gln(R)	7		
		Arg→Gln	7		

Gln dominant in *R. obamensis* PEPC were not consistent with such general rule for thermophilic proteins. In relation to the secondary structure of *R. obamensis* PEPC, most of the substitutions from Leu to Ile and Val to Ile occurred in the β -sheet structures. On the contrary, most of the *Thermus*-specific substitutions were found in the α -helices structures of the secondary structure.

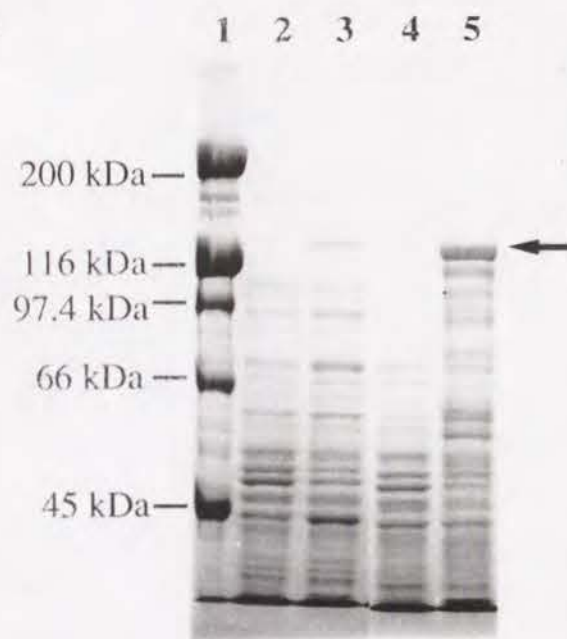


Fig. 25. The SDS-PAGE of the recombinant GST-PEPC fusion protein expressed in *E. coli* INV α . Approximately 20 μ g of protein were applied to each lane. After electrophoresis, the gel was stained by 40% (vol/vol) methanol-10% (vol/vol) acetate containing 0.2% (wt/vol) coomassie brilliant blue (CBB) R250. Lane 1 contains the molecular weight marker from Bio-Rad, lane 2, 3; crude extracts from INV α /pGEX-5X-3 and INV α /pPEP3.0 with 50 mM Tris -HCl (pH 7.5), respectively, lane 4, 5; crude extracts from INV α /pGEX-5X-3 and INV α /pPEP3.0 with 50 mM Tris-HCl (pH7.5) containing 9 M urea, 2% (vol/vol) triton X-100 and 2% (vol/vol) mercaptoethanol, respectively. A 126 kDa of protein, corresponding to the recombinant GST-PEPC fusion protein, is indicated by an arrow on the right.

The expression of *R. obamensis* ppc gene in *E. coli* and the characterization of the recombinant GST-PEPC fusion protein.

E. coli INV α cells were transformed with the recombinant plasmid pPEP3.0 to express the cloned gene as a GST-PEPC fusion protein (Fig. 20). The specific activities of PEPC in crude extracts from INV α /pPEP3.0 was 0.601 μ molNADH/min/mg protein at 65 °C. Fig. 25 shows the SDS-PAGE of crude extracts from INV α /pPEP3.0 and INV α /pGEX-5X-3 with 50 mM Tris -HCl (pH 7.5) or 50 mM Tris-HCl (pH7.5) containing 9 M urea, 2% (vol/vol) triton X-100 and 2% (vol/vol) 2-mercaptoethanol. A 126 kDa of protein could be observed in the extracts from INV α /pPEP3.0 (lane 3 and 5 in Fig. 25). In the SDS-PAGE, the extract with 50 mM Tris-HCl (pH7.5) containing 9 M urea, 2% (vol/vol) triton X-100 and 2% (vol/vol) mercaptoethanol apparently contained a larger amount of 126 kDa protein than the extract with 50 mM Tris -HCl (pH 7.5). This result suggested that a significant amount of recombinant GST-PEPC fusion protein was expressed in *E. coli* as an insoluble body.

However, when the transformant was grown not at 37 °C but at 25 °C, the soluble fraction of the fusion protein was significantly increased (data not shown). These results indicated that a thermophilic PEPC of *R. obamensis* was successfully expressed in *E. coli*.

The recombinant GST-PEPC fusion protein was partially purified by the column of glutathione Sepharose 4B (Pharmacia) and characterized with respect to its enzymological properties and thermostability (Fig. 26 and Table 9). The fusion protein was purified 30.5 fold by the affinity chromatography. The partially purified fusion protein was digested with a restriction protease, Factor Xa, which recognizes an amino acid sequence of -Ile-Glu-Gly-Arg- in proteins and hydrolyzes a C-terminal side of peptide bond at Arg residue in the sequence, in order to separate the recombinant PEPC from the GST at the junction of fusion protein. However, two different size of proteins (100 kDa and 80 kDa) were generated as the recombinant *R. obamensis* PEPC after 3 h digestion at 37 °C and the mixture of these proteins revealed a significantly lower optimum temperature for activity at 55 °C (Fig. 26).

In contrast, the recombinant GST-PEPC fusion protein had similar optimum temperature for activity (80 °C) to that of the wild type of *R. obamensis* PEPC (Fig. 26). The result implied that the digestion by the restriction protease gave rise to the thermolabile enzyme and the fusion protein was better for the comparison. On this account, the GST-PEPC fusion protein was characterized and compared with the wild type of PEPC. The enzymological properties of the recombinant GST-PEPC were basically similar to those of the wild type (Table 9). The apparent differences were the shift of the optimum temperature (from 75 °C to 80 °C) and pH (from 8.0 to 9.5) for activity and the weaker sensitivity to a negative allosteric effector of L-malate. In addition, the recombinant GST-PEPC was less thermostable than the wild PEPC and the half life at 90 °C was decreased from 240 min for the wild type to 3 min for the recombinant GST-PEPC (Table 9). However, the extrinsic thermostabilization

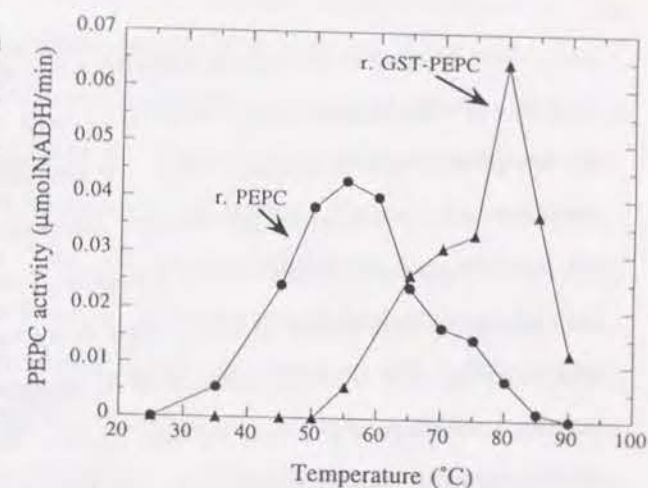


Fig. 26. The effect of temperature on PEPC activity in the partially purified GST-PEPC (r. GST-PEPC) and the protein sample treated with the restriction protease Factor Xa (r. PEPC). The activity was measured at various temperature at an enzyme concentration of 3.6 μ g protein/ml under standard assay condition [30] except for the pH of the reaction mixture at 9.5.

systems were effective in the recombinant GST-PEPC fusion protein and the effectiveness of the extrinsic thermostabilization factors in the fusion protein was the identical order to that in the wild *R. obamensis* PEPC (Table 9).

4. Discussion

The gene for phosphoenolpyruvate carboxylase (PEPC) from an extremely thermophilic bacterium *Rhodothermus obamensis* was successfully cloned, sequenced and expressed in *Escherichia coli* in this study (Figs. 19 and 20). The DNA sequence containing the *ppc* gene was determined by the thermal asymmetric interlaced (TAIL) PCR (Fig. 19). The gene consisted of 2,811 bp, encoding a polypeptide of 937 amino acid residues with the calculated molecular mass of 107,808 Da. The gene was found to be a single copy in the genomic DNA of the organism by the southern analysis (Fig. 22). The GC content of *R. obamensis ppc* coding region was 66.2% and the content in the third position of the codons was 85.0%. The GC content of the genomic DNA and 16S rRNA gene (accession number X95071), the firstly sequenced gene in *R. obamensis*, were 66.6% and 60.2% [78, Chapter 2]. The high GC contents in the genomic DNA and the *ppc* gene were observed in the genus of *Thermus* [14, 47]. Therefore, it was expected that the extreme bias for G or C was strongly associated with the thermophily of the organisms.

The thermophily was also thought to be associated with the amino acid composition of the enzyme. The amino acid composition of *R. obamensis* PEPC was compared with those of other PEPCs from various bacteria and plants (Fig. 24). Although there was no apparent change of the composition in comparison of three distinct physicochemical groups of amino acids, some preferences for specific amino acids were observed in thermophilic PEPCs based on the comparison of each amino acid composition (Fig. 24B). In *R. obamensis* PEPC, the contents of Gly, Ser, Asn and Lys were decreased and the contents of Gln, His and Arg increased (Fig. 24B). Among them, the amino acid composition changes in Asn, Ser, Lys, His and Arg were consistent with the changes in *Thermus* PEPC. The composition changes in these amino acids were also consistent with the "traffic rules", previously proposed by Argos et al. [108] and Menendez-Arias and Argos [32] for the preferential alterations of the amino acid composition in the proteins from thermophiles. However, lower content of Gly and higher content of Gln were peculiar to *R. obamensis* PEPC and especially, the increased Gln content was opposed to such rules for the thermophilic adaptation. In addition, the amino acid substitutions were examined among the closely related PEPCs from *R. obamensis*,

Thermus sp., *Corynebacterium glutamicum* (Fig. 21) to examine whether some bias for the specific amino acid substitutions existed between the mesophilic and thermophilic PEPCs (Table 8). From the phylogenetic analysis of PEPC described below, it was suggested that two thermophilic PEPCs of *R. obamensis* and *Thermus* sp. were derived from the mesophilic enzyme from *C. glutamicum*. Hence, the substitutions of amino acids from *C. glutamicum* to each thermophile were likely to reflect the strategy for the intrinsic thermal adaptation of these thermophilic PEPCs (Table 8). As the results, three types of substitutions (*R. obamensis*-specific, *Thermus*-specific or universal substitution) were found to be dominant in the thermophilic PEPCs (Table 8). The universal substitutions were the frequent substitutions both from *C. glutamicum* to *R. obamensis* and from *C. glutamicum* to *Thermus* and contained the replacements of Ile by Leu, Val by Leu, Ala by Leu and Ala by Arg. Most of them were also the frequent simultaneous substitutions from *C. glutamicum* to both thermophile and consistent with the possible thermophilic substitutions previously proposed or observed [32, 106, 107, 108]. Moreover, most of the *Thermus*-specific substitutions, which were the frequent substitutions only from *C. glutamicum* to *Thermus*, were also in good agreement with the possible thermophilic substitutions. However, the replacements of Leu by Ile, Val by Ile and Ala by Gln were peculiar to the substitutions from *C. glutamicum* to *R. obamensis* and these replacements did not agree with the possible thermophilic substitutions for the proteins of thermophilic and extremely thermophilic bacteria [32, 108] but were similar to the frequent amino acid substitutions seen in hyperthermophilic bacteria and archaea [28, 29]. In comparison of amino acid compositions of D-glyceraldehyde-3-phosphate dehydrogenase (GAPDH) from mesophilic and thermophilic sources, it was shown that the Ile content was significantly increased and the Leu content was decreased in the GAPDH of an hyperthermophilic archaeon *Pyrococcus furiosus* and the increased content of Ile was also observed in the GAPDH of an hyperthermophilic bacterium *Thermotoga maritima* [28]. In addition, Britton *et al.* indicated that the replacements of Leu by Ile and of Val by Ile were the most frequent substitutions from the mesophilic bacterium *Clostridium symbiosum* to the hyperthermophilic archaea *Thermococcus litoralis* and *P. furiosus* based on the comparison of the glutamate dehydrogenase [29]. It was suggested from the inferred three dimensional structures of these hyperthermophilic enzymes that these exchanges of amino acids involved the addition of an extra methyl group to the enzymes and the increased packing density by these exchanges were associated with the thermostability of the thermococcal enzymes [29]. From the inferred secondary structures of the thermophilic PEPCs, most of the *R. obamensis*-specific substitutions were occupied in the β -sheet structure while most of the *Thermus*-specific substitutions were in the α -helices. The

increased hydrophobicity from the exchange from Leu to Ile or from Val to Ile was expected to have effect on stabilizing the β -sheet structure in *R. obamensis* PEPC. However in the higher levels of structures, as suggested in the thermococcal glutamate dehydrogenases, these exchanges might be involved in the increased packing density at the molecular cavity or hydrophobic core in the enzyme. The more detail inspection of the specific amino acid composition and substitutions for *R. obamensis* PEPC will require the structural data including the three dimensional structure of the enzyme and the structure-dependent molecular engineering of the thermostability. For the first step of them, I sought to establish the overexpression of the *ppc* gene in *E. coli*.

The cloned *ppc* gene was successfully expressed in *E. coli* using glutathione S-transferase (GST) gene fusion vector system (Fig. 20). The recombinant GST-PEPC fusion protein was a 126 kDa of protein and had the specific activity for PEPC at high temperatures although a significant amount of the protein was insolubilized in the mesophilic host of cells (Fig. 25). When the *E. coli* cells with the expression plasmid pPEP3.0 were grown not at 37 °C but at 25 °C, the soluble fraction of the fusion protein was considerably increased. These results indicated that the high yield of expression was possible in this system. The recombinant GST-PEPC fusion protein was partially purified 30.5 fold by the column of glutathione Sepharose 4B (Pharmacia). To separate the recombinant PEPC from the GST at the junction of fusion, the fusion protein was digested with a restriction protease, Factor Xa, which recognizes an amino acid sequence of -Ile-Glu-Gly-Arg- in proteins and hydrolyzes a C-terminal side of peptide bond at Arg residue in the sequence. The amino acid sequence of *R. obamensis* PEPC did not contain the restriction sequence but two different size of proteins (100 kDa and 80 kDa) were generated after 3 h digestion at 37 °C. A 100 kDa of protein corresponded to the intact *R. obamensis* PEPC. Since the longer digestion with Factor Xa gave rise to the increasing amount of 80 kDa protein, this peptide was thought to be the extra-digested peptide of *R. obamensis* PEPC. In addition, the mixture of these proteins revealed a significantly lower optimum temperature for activity at 55 °C than those of the wild type enzyme (75 °C) and the GST-PEPC fusion protein (80 °C) (Fig. 26). It was obscure that the decreased optimum temperature for activity was due to the inactivation or less thermostability of the extra-digested peptide, or the less thermostability of the intact recombinant *R. obamensis* PEPC separated from the fusion protein, or both. On this account, in an attempt to examine the enzymological properties and thermostability of the expressed enzyme, the GST-PEPC fusion protein was used. The enzymological

Table 9. The comparison of enzymological properties and thermostability between the wild type of PEPC from *R. obamensis* and recombinant GST-PEPC fusion protein expressed in *E. coli* INV α . The enzymological properties of the fusion protein were determined on the same conditions as those of the wild type [30] except for the assay temperature at 80 °C and pH at 9.5 in case of the fusion protein. In the experiment for thermostability of the fusion protein, the thermoinactivation was performed under a concentration of 36 μ g GST-PEPC/ml as described previously [30]. $K_{Mg^{2+}}$, $S_{Acetyl-CoA}$ and $S_{F-1,6 PP}$ imply the concentrations, which provided 50% of maximum activity or of maximum effectiveness, and S_{L-Asp} and $S_{L-Malate}$ show the concentrations, which provided 50% of inhibition on the enzyme activity. Italic letters show the properties which were found to be different between the wild type and the recombinant GST-PEPC.

Properties	wild type of PEPC from <i>R. obamensis</i>	recombinant GST-PEPC from <i>E. coli</i> INV α
T_{opt}	~75 °C	~80 °C
pH_{opt}	8.0	9.5
$K_{Mg^{2+}}$	~0.5 mM	~0.6 mM
K_{PEP}	20.9 mM	18.6 mM
V_{max}	378 μ molNADH/min·mig	420 μ molNADH/min·mig
$S_{Acetyl-CoA}$	~0.35 mM	~0.35 mM
$S_{F-1,6 PP}$	~1.2 mM	~1.6 mM
S_{L-Asp}	~0.7 mM	~0.6 mM
$S_{L-Malate}$	~0.3 mM	~1.2 mM
Thermostability		
half lives	240 min at 90 °C 60 min at 91 °C 10 min at 93 °C (under 9 μ gPEPC/ml)	120 min at 75 °C 15 min at 80 °C 3 min at 90 °C (under 36 μ gPEPC/ml)
Effects of extrinsic factors	3.14 by PEP 4.37 by MgSO ₄ 8.81 by Acetyl-CoA (under 9 μ gPEPC/ml, at 95 °C)	11.0 by PEP 13.1 by MgSO ₄ 17.3 by Acetyl-CoA (under 36 μ gPEPC/ml, at 80 °C)

properties of the recombinant GST-PEPC were basically similar to those of the wild type (Table 9). The apparent differences were the shifts of the optimum temperature (from 75 °C to 80 °C) and pH

(from 8.0 to 9.5) for activity and the weaker sensitivity to a negative allosteric effector of L-malate (Table 9). As compared to the differences in the enzymological properties, the thermostability of the fusion protein was strongly altered. The half life at 90 °C was decreased from 240 min for the wild type to 3 min for the recombinant GST-PEPC (Table 9). The sample containing 100 kDa and 80 kDa of proteins were much less thermostable and the activity was completely lost after 65 °C for 10 min. From the results, the effect of GST in the fusion protein on the enzymological properties was likely to be moderate and it was suggested that the reduced thermostability was accounted for by the less thermostability of *R. obamensis* PEPC expressed in the mesophilic organism rather than the negative effect of GST on the thermostability of the fusion protein. One of possible explanations for this reduced thermostability is that the intrinsic thermostability of *R. obamensis* PEPC is accomplished by some post-translational modification and processing of the enzyme in the cell of *R. obamensis*, and in the cell of the mesophilic host, the thermostability of enzyme is not maintained and sustained by such thermostabilization systems. Now, the establishment of the high efficiency expression system for the *R. obamensis* *ppc* gene without the fusion process is underway. If the thermostability of the expressed enzyme in the system is determined, the reduced thermostability will be well discussed.

The phylogenetic analysis of PEPCs from various bacteria and plants indicated the interesting molecular evolution of the enzyme (Fig. 23). The phylogenetic tree showed not only the close relationship between the extremely thermophilic PEPCs from *R. obamensis* and *Thermus* and the possible mesophilic origin of these extremely thermophilic enzymes but also the remarked relationship between the proteobacterial and eucaryal PEPCs and the possible bacterial origin of the eucaryal enzymes (Fig. 23). Recent phylogenetic studies widely among living organisms based on the molecules involved in the central dogma such as the ribosomal rRNAs [5, 6, 113], elongation factors [76, 114] and RNA polymerase [115] have suggested the thermophilic origin of life [57] and the closer relationship between the domain Archaea and Eucarya than to the domain Bacteria [5, 6]. On the other hand, the phylogenetic trees from the central metabolic enzymes such as malate dehydrogenase, enolase and phosphoglycerate kinase have shown the closer relationship between Bacteria and Eucarya than to Archaea [reviewed in 116]. PEPC is primarily a central metabolic enzyme catalyzing the reaction that fixes HCO₃⁻ on phosphoenolpyruvate (PEP) to form oxaloacetate (OAA) and inorganic phosphate and regulating the junction between the hexose metabolisms and citric acid cycle. Therefore, it was accepted that the close relationship between proteobacterial and eucaryal enzymes and the bacterial origin of the eucaryal PEPCs were consistent with the central metabolic enzyme type of molecular evolution. In the study on the phylogenetic position of *R. obamensis*, this

extremely thermophilic bacterium was placed close to the root of the *Flexibacter-Cytophaga-Bacteroid* (F-C-B) group and did not represent a deep branching within the domain Bacteria in the phylogenetic tree of 16S rRNA [78, Chapter 2]. From these results, I concluded that *R. obamensis* was an apparently modern lineage of extremely thermophile and speculated that extreme thermophily was not necessarily ancient characteristic but possibly had another modern origin within the Bacteria [78, Chapter 2]. The modern lineage of extreme thermophily was also postulated in the phylogenetic tree of PEPC (Fig. 23). However, since the tree in this study was unrooted and the placement of a root among bacterial and eucaryal PEPCs was unknown, the evolutionary direction of the enzyme was still obscure. The coworkers and I have studied several archaeal PEPCs from hyperthermophilic methanogen *Methanothermus sociabilis* and thermoacidophilic *Sulfolobus* species [52, 53, Sako Y. *et al.* unpublished]. Based on the comparison of the molecular and enzymological properties, archaeal PEPCs were significantly different from bacterial and eucaryal counterparts with respect to the small size and non- or incomplete-allosteric property. These results suggested that archaeal PEPCs were phylogenetically distant from the bacterial and eucaryal enzymes and were placed out of the bacterial-eucaryal cluster in the phylogenetic tree. The amino acid sequences of archaeal PEPCs are important clues for understanding the evolution of the enzyme. Not only the structural study and the structure-dependent molecular engineering of the thermostability in *R. obamensis* PEPC but also the cloning and sequencing of the gene for the archaeal PEPC are the foci of the future work. The structure-dependent intrinsic and extrinsic mechanisms for *R. obamensis* PEPC thermostability and the evolutionary relationship among various PEPCs could be discussed.

Chapter 6

Summary and Conclusion

In order to elucidate thermostability of proteins from extremely thermophiles and hyperthermophiles, phosphoenolpyruvate carboxylase (PEPC) from an extremely thermophilic bacterium *Rhodothermus obamensis* OKD7 was studied as a model protein with respect to its intrinsic and extrinsic thermostabilization systems.

In Chapter 2, the bacterial strain OKD7, which was isolated from a shallow marine hydrothermal vent, was characterized. The isolate was an extremely thermophilic bacterium with an optimum temperature for growth at 80 °C and capable of growth up to 85 °C. Based on the physiological, chemical and molecular characteristics, the isolate was a novel extremely thermophilic species of the genus *Rhodothermus*, designated *Rhodothermus obamensis* OKD7. The phylogenetic analysis of 16S rRNA gene indicated that this organism was an apparently modern lineage of extreme thermophile. The finding not only postulated the second possible origin of extreme thermophily but also suggested that the mechanisms for the thermostability of proteins in this organism were different from those of other ancient lineage of extreme thermophiles and hyperthermophiles. This presented another interest into the study on the mechanisms for the thermostability of *R. obamensis* PEPC. In Chapters 3, 4 and 5, *R. obamensis* PEPC was purified, characterized and probed with an focus on the extrinsic thermostabilization mechanisms of the enzyme.

The findings and possible mechanisms for intrinsic and extrinsic thermostabilizations in this study are summarized as follows.

(1) *R. obamensis* PEPC was a 400 kDa of homotetramer consisting of a 100 kDa of subunit and was an allosteric enzyme. Its molecular and enzymological properties were similar to those of bacterial entities except for the extreme thermophilicity and thermostability.

(2) *R. obamensis* PEPC was extremely thermostable with half lives at various temperatures of 26 h at 80 °C, 11 h at 85 °C, 240 min at 90 °C, 60 min at 91 °C and 10 min at 93 °C, respectively.

(3) The thermostability was affected by pH, enzyme concentration and presence of salts and the effects of them inferred the importance of the subunit-subunit hydrophobic interaction on the intrinsic

thermostability.

(4) The thermostability was also strongly enhanced by the presence of substrate, cofactor and allosteric effectors. These substances protected the enzyme from the thermoinactivation and thermodenaturation at supraoptimum temperatures for bacterial growth and enzyme activity. Therefore, these were the possible extrinsic thermostabilization factor.

(5) The effects of the extrinsic thermostabilization factors were non-competitive and additive. The result suggested that the way to function of each factor was expected to be different and independent each other.

(6) Based on structural analyses and renaturation test of the enzyme, it was indicated that the thermodenaturation was dependent on the denaturation temperature and was subjected to the structural transition of the three major states of denaturation; the dissociation of quaternary structure (dissociated state), the incorrect foldings or conformational changes of the subunit (scrambled state), the aggregation of the scrambled enzyme (aggregated state) and also subjected to the covalent degradation of the enzyme such as hydrolysis of the peptide under the severe thermodenaturation. Among these processes, the dissociation of the quaternary structure was the first step of thermodenaturation and thought to be the most important step for the intrinsic thermostability and the extrinsic thermostabilization.

(7) In addition, the effects of the extrinsic thermostabilization factors on the thermodenaturation were analyzed in relation to the structural change of the enzyme. All factors had effects on the dissociation step from the quaternary structure and the mechanism was to maintain the active multimeric forms of enzyme and protect them from the temperature-induced dissociation. However, the ways to function of the factors were distinguished into two types; the one type contained the cofactor and salt (e.g. MgSO₄ and Na₂SO₄), and was able to protect the native folding or conformation from the denaturation. The other contained the substrate and allosteric effector (PEP and acetyl-CoA), and appeared to improved the folding or conformation by the interaction with the enzyme rather than to protect the native one.

(8) For the inspection of the intrinsic thermostability and the preparation of the three dimensional structure of the enzyme, *R. obamensis* PEPC gene (*ppc* gene) was cloned, sequenced and expressed in *E. coli*. An open reading frame for a 937-amino-acid polypeptide was found in the gene. The *ppc* gene had a high G+C content (66.2%) and the third position of the codon exhibited strong preference of G or C usage (85.0%). By the southern analysis, the *ppc* gene was found to be a single copy in the genomic DNA of this organism.

(9) Based on the phylogenetic analysis of PEPCs from various kinds of organisms, *R. obamensis* PEPC was most closely related with *Thermus* PEPC and it was suggested that both thermophilic entities were derived from the mesophilic type of ancestor. It was also postulated from the phylogenetic tree of PEPC that the molecular evolution of this enzyme was quite different from ribosomal-RNA-type of evolution.

(10) In comparison of amino acid sequence between the thermophilic and mesophilic PEPC, there were observed distinct or common preferences of specific amino acid composition and substitution in the two thermophilic PEPC from *Thermus* sp. and *R. obamensis*.

(11) The cloned gene was expressed in *E. coli* as a fusion protein with glutathione S-transferase (GST) and the recombinant GST-PEPC fusion protein had similar enzymological properties and thermophilicity with the wild type of *R. obamensis* PEPC. However, the fusion protein was less thermostable than the wild type. The reduced thermostability was thought to result from mesophilic expression in *E. coli*. These results suggested that the intrinsic thermostability of PEPC was supported by some thermostabilization system such as post-translational modification or processing in *R. obamensis* cells.

In this study, I clarified the importance of the extrinsic thermostabilization system in the protein thermostability, the some mechanisms for the extrinsic thermostabilization and the relationship between the system and the thermodenaturation of the enzyme. I also discussed the some mechanisms for the intrinsic thermostability and the possible intrinsic factors from the comparison of primary structures. However, there are still lots of unresolved problems and lots of speculations to be verified such as improvement of expression system for recombinant enzyme, determination of three dimensional structure, more detail analysis for extrinsic thermostabilization mechanisms from three dimensional structure and examination of possible intrinsic factors by structure-dependent molecular engineering. Further analysis for the phylogeny of PEPC among all three domain of life is also required. These are important and essential for the final goal of this study and the foci of future work.

Acknowledgement

Above all, I would like to express my greatest thank to Dr. Yoshihiko Sako, Associate Professor, Dept. of Applied Bioscience, Kyoto University, for 6 years' his directions, advices, discussions and communications with me and this work. I would like to appreciate Dr. Yuzaburo Ishida, Dr. Aritsune Uchida, Last and Present Professor, Dept. of Applied Bioscience, Kyoto University, for their advices and suggestions. Mr. Takahiro Nishizaka, Mr. Kaneaki Kin, Mr. Takuro Nunoura, Dr. Yoko Katayama, Associate Professor, Tokyo University of Agriculture and Technology and Dr. Yoshizumi Ishino, Biomolecular Engineering Research Institute, are the persons who should be appreciated for their help and share to a part of this work. I also thank Mr. Norimichi Nomura and Mrs. Pamela Chavez very much as co-workers of "hyperthermophilic research group" for their useful and cordial advices and discussions.

I hope my sincere thanks will reach over the Pacific Ocean to Dr. John A. Baross, Professor, School of Oceanography, University of Washington, Dr. James F. Holden, University of Georgia, and the students in the Laboratory of Microbiology, School of Oceanography, University of Washington, who gave kindness and consideration, instructive suggestions and advices to me in Seattle. I want to tell my pleasure to Dr. Rainier Jaenicke, Professor, University of Regensburg, and Dr. Yigal Burnstain, Professor, Weizmann University, for very instructive suggestions to my work at the "Thermophiles '96" meeting.

I like to thank Dr. Ikuo Yoshinaga, Mr. Takeshi Yoshikawa, Mr. Hirotaka Kitaguchi, Mr. Takashi Yoshida, Mr. Masatoshi Yagi, Mr. Kiyotaka Takishita, Mr. Masatomo Rokushima and other members in Laboratory of Marine Microbiology for everything they have been given to me and my work since I started my research in this laboratory.

At last, I would like to let her know my pleasure and thanks beyond description with love, Miss Hiromi Saeki.

References

1. Stetter, K. O., Fiala, G., Huber, G., Huber, R. and Segere, G. (1990) Hyperthermophilic organisms, *FEMS Microbiol. Rev.* 75, 117-124.
2. Adams, M. W. W. (1993) Enzymes and proteins from organisms that grow near and above 100 °C, *Ann. Rev. Microbiol.* 47, 627-658.
3. Adams, M. W. W., Perler, F. B. and Kelly, R. M. (1995) Extremozyme: expanding the limits of biocatalysis, *Bio/technology* 13, 662-668.
4. Adams, M. W. W. (1994) Biochemical diversity among sulfur-dependent, hyperthermophilic microorganisms, *FEMS Microbiol. Rev.* 15, 261-277.
5. Woese, C. R., Kandler, O. and Wheelis, M. L. (1990) Towards a natural system of organisms: proposal for the domains Archaea, Bacteria, and Eucarya, *Proc. Natl. Acad. Sci. USA* 87, 4576-4579.
6. Olsen, G. J., Woese, C. R. and Overbeck, R. (1994) The winds of (evolutionary) change: breathing new life into microbiology, *J. Bacteriol.* 176, 1-6.
7. Holden, J. F., Takai, K., Zyskowski, J. A. and Baross, J. A. (1996) Diversity among deep-sea hyperthermophilic sulfur-reducing *Thermococcus* and *Pyrococcus* species, *FEMS Microbiol. Eco.* submitted.
8. Ravot, G., Magot, M., Ferdeau, M.-L., Patel, B. K. C., Prensier, G., Egan, A., Garcia, J.-L. and Ollivier, B. (1995) *Thermotoga elfii* sp. nov., a novel thermophilic bacterium from an african oil-producing well, *Int. J. Syst. Bacteriol.* 45, 308-314.
9. Jeanthon, C., Reysenbach, A.-L., L'Haridon, S., Gambacorta, A., Pace, N. R., Glenat, P. G. and Prieur, D. (1995) *Thermotoga subterranea* sp. nov., a new thermophilic bacterium isolated from a continental oil reservoir, *Arch. Microbiol.* 164, 91-97.
10. Cowan, D. A. (1995) Protein stability at high temperatures, *Essays in Biochem.* 29, 193-207.
11. Jaenicke, R. (1996) Stability and folding of ultrastable proteins: eye lens crystallins and enzymes from thermophiles, *FASEB J.* 10, 84-92.
12. Daniel, R. M. (1996) The upper limits of enzyme thermal stability, *Enzyme Microb. Technol.* 19, 74-79.
13. Brock, T. D. (1986) Introduction: an overview of the thermophiles, In *Thermophiles* (Brock, T. D. ed.) pp. 1-16, Wiley-interscience, New York.
14. Brock, T. D. and Brock, M. L. (1984) Genus *Thermus*, In *Bergey's Manual of Systematic Bacteriology* (Krieg, N. R. ed.) vol. 1, pp. 333-337, Williams and Wilkins, Baltimore.
15. Sanangelantoni, A. M., Bocchetta, M., Cammarano, P. and Tiboni, O. (1994) Phylogenetic depth of S10 and spc operons: cloning and sequencing of a ribosomal protein gene cluster from extremely thermophilic bacterium *Thermotoga maritima*, *J. Bacteriol.* 176, 7703-7710.
16. Huber, R., Wilharm, T., Huber, D., Trincone, A., Burggraf, S., König, H., Rachel, R., Rockinger, I., Fricke, H. and Stetter, K. O. (1992) *Aquifex pyrophilus* gen. nov. sp. nov. represents a novel group of marine hyperthermophilic hydrogen-oxidizing bacteria, *System. Appl. Microbiol.* 15, 340-351.
17. Grayling, R. A., Bechtel, W. J. and Reeves, J. N. (1995) Structure and stability of histone Hmf from hyperthermophilic archaeon *Methanothermus fervidus*, *Biochemistry* 34, 8441-8448.
18. Starich, M. R., Sandman, K., Reeves, J. N. and Summers, M. F. (1995) NMR structure of HmfB from the hyperthermophile, *Methanothermus fervidus*, confirms that this archaeal protein is a histone, *J. Mol. Biol.* 255, 187-203.
19. Forterre, P., Confalonieri, F., Charbonnier, F. and Dugnet, M. (1995) Speculations on the origin of life and thermophily: review of available information on reverse gyrase suggests that hyperthermophilic prokaryotes are not so primitive, *Origin of Life and Evolution of the Biosphere* 25, 235-249.
20. Forterre, P., Bergerat, A. and L-Garcia, P. (1996) The unique DNA topology and DNA topoisomerases of hyperthermophilic archaea, *FEMS Microbiol. Rev.* 18, 237-248.
21. Kumagai, I., Watanabe, K. and Oshima, T. (1982) A thermostable tRNA (guanosine-2'-)-methyltransferase from *Thermus thermophilus* HB27 and the effect of ribose methylation on the conformational stability of tRNA, *J. Biol. Chem.* 257, 7388-7395.
22. Edmonds, C. G., Crain, P. F., Gupta, R., Hashizume, T., Hocart, G. H., Kowalak, J. A., Pomerantz, S. C., Stetter, K. O. and McCloskey, J. A. (1991) Posttranslational modification of tRNA in thermophilic archaea (archaeobacteria), *J. Bacteriol.* 173, 3138-3148.
23. Kates, M. (1992) Archaeobacterial lipids: structure, biosynthesis and function, In *Archaeobacteria: biochemistry and biotechnology* (Danson, M. J., Hough, D. W. and Lunt, G. G. eds.) pp. 51-72, Portland Press, London.
24. De Rosa, M., Gambacorta, A. and Gliozzi, A. (1986) Structure, biosynthesis, and physicochemical properties of archaeobacterial lipids, *Microbiol. Rev.* 50, 70-80.

25. De Rosa, M., Esposito, E., Gambacorta, A., Nicolaus, G. and Bu'Lock, J. D. (1980) Regularity of isoprenoid biosynthesis in the ether lipid of archaeobacteria, *Phytochemistry* 19, 827-831.
26. Hasegawa, Y., Kawada, N. And Nosoh, Y. (1980) Change in chemical composition of the membrane of *Bacillus caldotenax* after shifting growth temperature, *Arch. Microbiol.* 126, 103-108.
27. Da Costa, M. S. (1995) The cell walls and lipids of *Thermus*, In *Thermus species* (Sharp, R., Williams, R. eds.) pp. 143-156, Plenum Press, New York and London.
28. Böhm, G. and Jaenicke, R. (1994) Relevance of sequence statistics for the properties of extremophilic proteins, *Int. J. Protein Res.* 43, 97-106.
29. Britton, K. L., Baker, P. J., Borges, K. M. M., Engel, P. C., Pasquo, A., Rice, D. W., Robb, F. T., Scandurra, R., Stillman, T. J. and Yip, K. S. P. (1995) Insight into thermal stability from a comparison of the glutamate dehydrogenases from *Pyrococcus furiosus* and *Thermococcus litoralis*, *Eur. J. Biochem.* 229, 688-695.
30. Schultes, V. and Jaenicke, R. (1991) Folding intermediates of hyperthermophilic D-glyceraldehyde-3-phosphate dehydrogenase from *Thermotoga maritima* are trapped at low temperature, *FEBS Lett.* 290, 235-238.
31. Cannio, R., Rossi, M. and Bartolucci, S. (1994) A few amino acid substitutions are responsible for the higher thermostability of a novel NAD⁺-dependent bacillar alcohol dehydrogenase, *Eur. J. Biochem.* 222, 345-352.
32. Arias, L. M. and Argos, P. (1989) Engineering protein thermal stability: sequence statistics point to residue substitutions in α -helices, *J. Mol. Biol.* 206, 397-406.
33. Tamakoshi, M., Yamagishi, A. and Oshima, T. (1995) Screening of stable proteins in an extreme thermophile, *Thermus thermophilus*, *Mol. Microbiol.* 16, 1031-1036.
34. Kotsuka, T., Akamura, S., Tomuro, M., Yamagishi, A. and Oshima, T. (1996) Further stabilization of 3-isopropylmalate dehydrogenase of an extreme thermophile, *Thermus thermophilus*, by a suppressor mutation method, *J. Bacteriol.* 178, 723-727.
35. Chan, M. K., Mukund, S., Kletzin, A., Adams, M. W. W. and Rees, D. C. (1995) Structure of a hyperthermophilic tungstopterin enzyme, aldehyde ferredoxin oxidoreductase, *Science* 267, 1463-1469.
36. Day, M. W., Hsu, B. T., Joshuaor, L., Park, J. B., Zhou, Z. H., Adams, M. W. W. and Rees, D. C. (1992) X-ray crystal structures of the oxidized and reduced forms of the rubredoxin from the marine hyperthermophilic archaeobacterium *Pyrococcus furiosus*, *Protein Science* 1, 1494-1507.
37. Hensel, R., Laumann, S., Lang, J., Heumann, H. and Lottspeich, H. (1987) Characterization of two glyceraldehyde-3-phosphate dehydrogenases from the extremely thermophilic archaeobacterium *Thermoproteus tenax*, *Eur. J. Biochem.* 170, 325-333.
38. Scholz, S., Sonnenbichler, J., Schäfer, W. and Hensel, R. (1992) Di-myo-inositol-1,1'-phosphate: a new inositol phosphate isolated from *Pyrococcus woesei*, *FEBS Lett.* 306, 239-242.
39. Taguchi, H., Yamashita, M., Matsuzawa, H. and Ohta, T. (1982) Heat-stable and fructose 1,6-bisphosphate-activated L-lactate dehydrogenase from an extremely thermophilic bacterium, *J. Biochem.* 91, 1343-1348.
40. Huber, R., Kurr, M., Jannasch, H. and Stetter, K. O. (1989) A novel group of abyssal methanogenic archaeobacteria (*Methanopyrus*) growing at 110 °C, *Nature* 342, 833-834.
41. Jaenicke, R. (1987) Folding and association of proteins, *Progr. Biophys. Mol. Biol.* 49, 117-237.
42. Risse, B., Stempfer, G., Rudolph, R. and Jaenicke, R. (1992) Stability and characterization of the stabilizing effect of point mutations of pyruvate oxidase from *Lact. Plantarum*, *Protein Sci.* 1, 1699-1718.
43. Holden, J. F. and Baross, J. A. (1993) Enhanced thermotolerance and temperature-induced changes in protein composition in the hyperthermophilic archaeon ES4, *J. Bacteriol.* 175, 2839-2843.
44. Hartl, F. U. (1996) Molecular chaperons in cellular protein folding, *Nature* 381, 571-580.
45. Utter, M. F. and Kolenbrander, H. M. (1972) Formation of oxaloacetate by CO₂ fixation on phosphoenolpyruvate, in *The enzymes* (Boyer, P. D., ed) pp. 117-168, Academic Press, New York.
46. Terada, K. and Izui, K. (1991) Site-directed mutagenesis of the conserved histidine residue of phosphoenolpyruvate carboxylase, *Eur. J. Biochem.* 202, 797-803.
47. Nakamura, T., Yoshida, I., Takahashi, M., Toh, H. and Izui, K. (1995) Cloning and sequence analysis of the gene for phosphoenolpyruvate carboxylase from extreme thermophile, *Thermus* sp., *J. Biochem.* 118, 319-324.
48. Owttrim, G. W., and Coleman, J. R. (1986) Purification and characterization of phosphoenolpyruvate carboxylase from a cyanobacterium, *J. Bacteriol.* 168, 207-212.

49. Höfner, R., Vazquez-Moreno, L., Abou-Mandour, A. A., Bohnert, H. J. and Schmitt, J. M. (1989) Two isoforms of phosphoenolpyruvate carboxylase in facultative CAM plant *Mesembryanthemum crystallinum*, *Plant Physiol. Biochem.* 27, 803-810.
50. Janc, J. W., O'Leary, M. H. and Cleland, W. W. (1992) A kinetic investigation of phosphoenolpyruvate carboxylase from *Zea mays*, *Biochemistry* 31, 6421-6426.
51. Morikawa, M., Izui, K., Taguchi, M., and Katsuki, H. (1980) Regulation of *Escherichia coli* phosphoenolpyruvate carboxylase by multiple effectors in vivo. I. Estimation of the activities of the cells grown on various compounds, *J. Biochem.* 87, 441-449.
52. Sako, Y., Takai, K., Uchida, A. and Ishida, Y. (1996) Purification and characterization of phosphoenolpyruvate carboxylase from hyperthermophilic archaeon *Methanothermus sociabilis*, *FEBS Lett.* 392, 148-152.
53. Sako, Y., Takai, K., Nishisaka, T., Uchida, A. and Ishida, Y. (1996) Biochemical relationship of phosphoenolpyruvate carboxylases (PEPCs) from hyperthermophilic and extremely thermophilic archaea, *FEBS Lett.* submitted.
54. Alfredsson, G. A., Kristjansson, J. K., Hjörleifsdóttir, S. and Stetter, K. O. (1988) *Rhodothermus marinus*, gen. nov., sp. nov., a thermophilic, halophilic bacterium from submarine hot springs in Iceland, *J. Gen. Microbiol.* 134, 49-68.
55. Nunes, O. C., Donato, M. M. and Da Costa, M. S. (1992) Isolation and characterization of *Rhodothermus* strains from S. Miguel, Azores, *System. Appl. Microbiol.* 15, 92-97.
56. Thorbjarnardóttir, S. H., Jónsson, Z. O., Andrésson, Ó. S., Kristjánsson, J. K., Eggertsson, G. and Palsdóttir, A. (1995) Cloning and sequence analysis of the DNA ligase-encoding gene of *Rhodothermus marinus*, and overproduction, purification and characterization of two thermophilic DNA ligases, *Gene* 161, 1-6.
57. Achenbach-Richter, L., Gupta, R., Stetter, K. O. and Woese, C. R. (1987) Were the original eubacteria thermophiles? *System. Appl. Microbiol.* 9, 34-39.
58. Burggraf, S., Olsen, G. J., Stetter, K. O. and Woese, C. R. (1992) A phylogenetic analysis of *Aquifex pyrophilus*, *System. Appl. Microbiol.* 15, 352-356.
59. Shima, S., Yanagi, M. and Saiki, H. (1994) The phylogenetic position of *Hydrogenobacter acidophilus* based on 16S rRNA sequence analysis, *FEMS Microbiol. Lett.* 119, 119-122.
60. Andrésson Ó. S. and Fridjónsson, Ó. H. (1994) The sequence of the single 16S rRNA gene of the thermophilic eubacterium *Rhodothermus marinus* reveals a distant relationship to group containing *Flexibacter*, *Bacteroides*, and *Cytophaga* species, *J. Bacteriol.* 176, 6165-6169.
61. Kawasumi, T., Igarashi, Y., Kodama, T. and Minoda, Y. (1984) *Hydrogenobacter thermophilus* gen. nov. and sp. nov., an extremely thermophilic, aerobic, hydrogen-oxidizing bacterium, *Int. J. Syst. Bacteriol.* 34, 5-10.
62. Kristjánsson, J. K., Ingason, A. and Alfredsson, G. A. (1985) Isolation of thermophilic obligately autotrophic hydrogen-oxidizing bacteria, similar to *Hydrogenobacter thermophilus* from Icelandic hot springs, *Arch. Microbiol.* 140, 321-325.
63. Marmur, J. and Doty, P. (1962) Determination of the base composition of deoxyribonucleic acid from its thermal denaturation temperature, *J. Mol. Biol.* 5, 109-118.
64. Lauerer, G., Kristjánsson, J. K., Langworthy, T. A., König, H. and Stetter, K. O. (1986) *Methanothermus sociabilis* sp. nov., a second species within the *Methanothermaceae* growing at 97 °C, *System. Appl. Microbiol.* 8, 100-105.
65. Tamaoka, J. and Komagata, K. (1984) Determination of DNA base composition by reversed-phase high-performance liquid chromatography, *FEMS Microbiol. Lett.* 25, 125-128.
66. Brosius, J., Palmer, J. L., Kennedy, J. P. and Noller, H. F. (1978) Complete nucleotide sequence of a 16S ribosomal RNA gene from *Escherichia coli*, *Proc. Natl. Acad. Sci. USA* 75, 4801-4805.
67. Saitou, N. and Nei, M. (1987) The neighbor-joining method: a new method for reconstructing phylogenetic trees, *Mol. Biol. Evol.* 4, 406-425.
68. Huber, R., Langworthy, T. A., König, H., Thomm, M., Woese, C. R., Sleytr, U. B. and Stetter, K. O. (1986) *Thermotoga maritima* sp. nov. represents a new genus of unique extremely thermophilic eubacteria growing up to 90°C, *Arch. Microbiol.* 144, 324-333.
69. Jackson, T. J., Ramaley, R. F. and Meinschein, W. G. (1973) *Thermomicrobium*, a new genus of extremely thermophilic bacteria, *Int. J. Syst. Bacteriol.* 23, 28-36.
70. Collins, M. D. and Jones, D. (1981) Distribution of isoprenoid quinone structural types in bacteria and their taxonomic implication, *Microbiol. Rev.* 45, 316-354.
71. Kristjánsson, J. K. and Alfredsson, G. A. (1986) Life in Icelandic hot springs, *Naturufraedingurinn* 56, 49-68.
72. Kristjánsson, J. K., Hreggisson, G. O. and Fredsson, G. A. (1986) Isolation of halotolerant *Thermus* spp. from submarine hot springs in Iceland, *Appl. Environ. Microbiol.* 52, 1313-1316.
73. Reysenbach, A-L., Wickham, G. S. and Pace, N. R. (1994) Phylogenetic analysis of the hyperthermophilic pink filament community in Octopus Spring, Yellowstone National Park,

- Appl. Environ. Microbiol.* 60, 2113-2119.
74. Völkl, P., Huber, R., Drobner, E., Rachel, R., Burggraf, S., Trincone, A. and Stetter, K. O. (1993) *Pyrobaculum aerophilus* sp. nov., a novel nitrate-reducing hyperthermophilic archaeum, *Appl. Environ. Microbiol.* 59, 2918-2926.
 75. Woese, C. R. (1987) Bacterial evolution, *Microbiol. Rev.* 51, 221-271.
 76. Rivera, M. C. and Lake, J. A. (1992) Evidence that eukaryotes and eocyte prokaryotes are, immediate relatives, *Science* 257, 74-76.
 77. Duffield, M. L. and Cossar, D. (1995) Enzymes of *Thermus* and their properties, *Biotechnology handbooks: Thermus species* (Sharp, R. and Williams, R., eds) pp. 93-143, Plenum Press, New York and London.
 78. Sako, Y., Takai, K., Uchida, A., Ishida, Y. and Katayama, Y. (1996) *Rhodothermus obamensis* sp. nov., a modern lineage of extremely thermophilic marine bacterium, *Int. J. Syst. Bacteriol.* 46, 1099-1104.
 79. Laemli, V. K. (1970) Cleavage of structural proteins during the assembly of the head of bacteriophage T4, *Nature* 227, 680-685.
 80. Bradford, M. M. (1976) A rapid and sensitive method for the quantitation of microgram quantities of protein utilizing the principle of protein-dye binding, *Anal. Biochem.* 72, 248-254.
 81. Burgess, J. (1988) Basic principles of chemical interactions, in *Ions in solution* (Langer, P., Packer, L. and Vasilescu, V., eds) p. 45, J. Burgess/Ellis Horwood, London.
 82. Von Hippel, P. H. and Schleich, T. (1969) Ion effects on the solution structure of biological macromolecules, in *Structure and Stability of Biological Macromolecules* (Fasman, G. D. and Timasheff, S. N., eds) p. 417, Marcel Dekker, New York.
 83. Mori, M. and Shiio, I. (1985) Purification and some properties of phosphoenolpyruvate carboxylase from *Brevibacterium flavum* and its aspartate-overproducing mutant, *J. Biochem.* 97, 1119-1128.
 84. Mukerji, S. K. (1977) Corn leaf phosphoenolpyruvate carboxylases: Purification and properties of two isoenzymes, *Arch. Biochem. Biophys.* 182, 343-351.
 85. Ishijima, S., Katagiri, F., Kodaki, T., Izui, K., Katsuki, H., Nishikawa, K., Nakashima, H. and Ooi, T. (1985) Comparison of amino acid sequences between phosphoenolpyruvate carboxylases from *Escherichia coli* (allosteric) and *Anacystis nidulans* (non-allosteric): identification of conserved and variable regions, *Biochem. Biophys. Res. Com.* 133, 436-441.
 86. Whol, R. C. and Markus, G. (1972) Phosphoenolpyruvate carboxylase of *Escherichia coli*: purification and some properties, *J. Biol. Chem.* 247, 5785-5792.
 87. Weigend, M. and Hinch, D. K. (1992) Quaternary structure of phosphoenolpyruvate carboxylase from CAM-C₄- and C₃-plants: no evidence for diurnal changes in oligomeric state, *J. Plant Physiol.* 140, 653-660.
 88. Willeford, K. O. and Wedding, R. T. (1992) Oligomerization and regulation of higher plant phosphoenolpyruvate carboxylase, *Plant Physiol.* 99, 755-758.
 89. Wu, M. X., Meyer, C. R., Willeford, K. O. and Wedding, R. T. (1990) Regulation of the aggregation state of Maize phosphoenolpyruvate carboxylase: evidence from dynamic light-scattering measurements, *Arch. Biochem. Biophys.* 281, 324-329.
 90. Taguchi, H., Yamashita, M., Matsuzawa, H. and Ohta, T. (1982) Heat-stable and fructose 1,6-bisphosphate-activated L-lactate dehydrogenase from an extremely thermophilic bacterium, *J. Biochem.* 91, 1343-1348.
 91. Iwata, S., Kamata, K., Yoshida, S., Minowa, T. and Ohta, T. (1994) T and R states in the crystals of bacterial L-lactate dehydrogenase reveal the mechanism for allosteric control, *Nat. Struct. Biol.* 1, 176-185.
 92. Jansen, W. A., Armstrong, J. M., Giorgio, J. D. and Hearn, M. T. W. (1995) Stability studies on Maize leaf phosphoenolpyruvate carboxylase: the effect of salts, *Biochemistry* 34, 472-480.
 93. Halicioglu, T. and Sinanoglu, O. (1969) Solvent effects on cis-trans azobenzene isomerization: a detailed application of a theory of solvent effects on molecular association, *Ann. N.Y. Acad. Sci.* 158, 308-317.
 94. Sinanoglu, O. and Abdunur, S. (1965) Effect of water and other solvents on the structure of biopolymers, *Fed. Proc.* 24, S12-S23.
 95. Sinanoglu, O. (1980) The solvophobic theory for the prediction of molecular conformations and biopolymer bindings in solutions with recent direct experimental tests, *Int. J. Quantum Chem.* 18, 381-388.
 96. Takai, K., Sako, Y., Uchida, A. and Ishida, Y. (1996) Purification and characterization of an extremely thermostable phosphoenolpyruvate carboxylase from *Rhodothermus obamensis*, *Eur. J. Biochem.* submitted.
 97. Semisotnov, G. V., Rodionova, N. A., Razgulyaev, O. I., Uversky, V. N., Gripas, A. F. and Gilmanishin, R. I. (1991) Study of the "molten globule" intermediate state in protein folding by a hydrophobic fluorescent probe, *Biopolymers* 31, 119-128.
 98. Kuwajima, K., Garvey, E. P., Finn, B. E., Matthews, C. R. and Sugai, S. (1989) Transient

- intermediate in the folding of dihydrofolate reductase as detected by far UV circular dichroism spectroscopy, *Biochemistry* 30, 7693-7703.
99. Cavagnero, S., Zhou, Z. H., Adams, M. W. W. and Chan, S. I. (1995) Response of rubredoxin from *Pyrococcus furiosus* to environmental changes: implications for the origin of hyperthermostability, *Biochemistry* 34, 9865-9873.
 100. Alexander W., Schweiger, A., Schultes, V. and Jaenicke, R. (1990) Extremely thermostable D- glyceraldehyde-3-phosphate dehydrogenase from the eubacterium *Thermotoga maritima*, *Biochemistry* 29, 7584-7592.
 101. Ahern, T. J. and Klibanov, A. M. (1985) The mechanism of irreversible enzyme inactivation at 100 °C, *Science* 228, 1280-1284.
 102. Imada, K., Sato, M., Tanaka, N., Katsube, Y., Matsuura, Y. and Oshima, T. (1991) Three-dimensional structure of a highly thermostable enzyme, 3-isopropylmalate dehydrogenase gene of *Thermus thermophilus* at 2.2 Å resolution, *J. Mol. Biol.* 222, 725-738.
 103. Kurino, H., Aoki, M., Aoshima, M., Hayashi, Y., Ohba, M., Yamagishi, A., Wakagi, T., and Oshima, T. (1994) Hydrophobic interaction at the subunit interface contributes to the thermostability of 3-isopropylmalate dehydrogenase from an extreme thermophile, *Thermus thermophilus*, *Eur. J. Biochem.* 220, 275-281.
 104. Rehder, V. and Jaenicke, R. (1992) Stability and reconstitution of D-glyceraldehyde-3-phosphate dehydrogenase from the hyperthermophilic eubacterium *Thermotoga maritima*, *J. Biol. Chem.* 267, 10999-11006.
 105. Takai, K., Sako, Y., Uchida, A. and Ishida, Y. (1996) Extrinsic thermostabilization factors and thermodenaturation mechanism of phosphoenolpyruvate carboxylase (PEPC) from an extremely thermophilic bacterium *Rhodothermus obamensis*, *Eur. J. Biochem.* submitted.
 106. Privalov, P. L. and Gill, S. J. (1988) Stability of protein structure and hydrophobic interaction, *Adv. Protein Chem.* 39, 191-234.
 107. Zuber, H. (1988) Temperature adaptation of lactate dehydrogenase: structural, functional and genetic aspects, *Biophys. Chem.* 29, 171-179.
 108. Argos, P., Rosmann, M. G., Grau, U. M., Zuber, H., Frank, G. and Tratschin, J. D. (1979) Thermal stability and protein structure, *Biochemistry* 18, 5698-5703.
 109. Fujita, N., Miwa, T., Ishijima, S., Izui, K. and Katsuki, H. (1984) The primary structure of phosphoenolpyruvate carboxylase of *Escherichia coli*. Nucleotide sequence of the *ppc* gene and deduced amino acid sequence, *J. Biochem.* 95, 909-916.

110. Liu, Y. G. and Whittier, R. F. (1995) Thermal asymmetric interlaced PCR: automable amplification and sequencing of insert end fragments from P1 and YAC clones for chromosome walking, *Genomics* 25, 674-681.
111. Chou, P. Y. and Fasman, G. D. (1978) Prediction of the secondary structure of proteins from their amino acid sequences, *Adv. Enzymol.* 47, 45-148.
112. Itaya, M. and K. Kondo. (1991) Molecular cloning of a ribonuclease H (RNase HI) gene from an extreme thermophile *Thermus thermophilus* HB8: a thermostable RNase H can functionally replace the *Escherichia coli* enzyme in vivo, *Nucleic Acids Res.* 19, 4443-4449.
113. Rijk, P. D., Peer, Y. V., Broeck, I. V. and Wachter, R. D. (1995) Evolution according to large ribosomal subunit RNA, *J. Mol. Evol.* 41, 366-375.
114. Creti, R., Ceccarelli, E., Bocchetta, M., Sanangelantoni, A. M., Tiboni, O., Palm, P. and Cammarano, P. (1994) Evolution of translational elongation factor (EF) sequences: reliability of global phylogenies inferred from EF-1 α (Tu) and EF-2 (G) proteins, *Proc. Natl. Acad. Sci. USA* 91, 3255-3259.
115. Klenk, H.-P. and Zillig, W. (1994) DNA-dependent RNA polymerase subunit B as a tool for phylogenetic reconstructions: branching topology of archaeal domain, *J. Mol. Evol.* 38, 420-432.
116. Doolittle, W. F. and J. R. Brown. (1994) Tempo, mode, the progenote, and the universal root, *Proc. Natl. Acad. Sci. USA* 91, 6721-6728.

Research papers related to the author

1. Sako, Y., Takai, K., Uchida, A., Ishida, Y. and Katayama, Y. (1996) *Rhodothermus obamensis* sp. nov., a modern lineage of extremely thermophilic marine bacterium, *Int. J. Syst. Bacteriol.* 46, 1099-1104.
2. Sako, Y., Takai, K., Uchida, A. and Ishida, Y. (1996) Purification and characterization of phosphoenolpyruvate carboxylase from hyperthermophilic archaeon *Methanothermus sociabilis*, *FEBS Lett.* 392, 148-152.
3. Takai, K., Sako, Y., Uchida, A. and Ishida, Y. (1996) Purification and characterization of an extremely thermostable phosphoenolpyruvate carboxylase from *Rhodothermus obamensis*, *Eur.*

J. Biochem. submitted.

4. Takai, K., Sako, Y., Uchida, A. and Ishida, Y. (1996) Extrinsic thermostabilization factors and thermodenaturation mechanism of phosphoenolpyruvate carboxylase (PEPC) from an extremely thermophilic bacterium *Rhodothermus obamensis*, *Eur. J. Biochem.* submitted.
5. Takai, K., Sako, Y., Uchida, A. and Ishida, Y. (1996) Cloning, sequencing and overexpression in *Escherichia coli* of gene for phosphoenolpyruvate carboxylase (PEPC) from an extreme thermophile *Rhodothermus obamensis*, *Eur. J. Biochem.* submitted.
6. Sako, Y., Takai, K., Nishisaka, T., Uchida, A. and Ishida, Y. (1996) Biochemical relationship of phosphoenolpyruvate carboxylases (PEPCs) from hyperthermophilic and extremely thermophilic archaea, *FEBS Lett.* submitted.
7. Holden, J. F., Takai, K., Zyskowski, J. A. and Baross, J. A. (1996) Diversity among deep-sea hyperthermophilic sulfur-reducing *Thermococcus* and *Pyrococcus* species, *FEMS Microbiol. Eco.* submitted.